A viral non-coding RNA induces an inflammatory response to promote virus production in infected cells

2018

Zhe Li

Heidelberg, Germany

Dissertation

submitted to the

Combined Faculties for the Natural Sciences and for Mathematics of the

Ruperto-Carola University of Heidelberg, Germany

for the degree of

Doctor of Natural Sciences

presented by

Zhe Li, M.Sc.

born in: Qingdao, China

Oral-examination: 13th Augest 2018

Title:

A viral non-coding RNA induces an inflammatory response to promote virus production in infected cells

Referees: Prof. Dr. Dr. Henri-Jacques Delecluse

Prof. Dr. Martin Müller

Table of Contents

Summary

The Epstein-Barr virus (EBV) infects the majority of the population. The EBV M81 strain isolated from a nasopharyngeal carcinoma (NPC) efficiently infects and transforms primary B cells, but it also induces potent virus lytic replication in a minority of these cells. We used recombinant viruses to reveal the function of the EBER RNAs. We found that the number of cells in which lytic replication takes place is increased both *in vitro* and *in vivo* by the non-coding RNA EBER2, but not by its homolog in the genome of the B95-8 strain. M81 and B95-8 EBER2 homologs displayed a limited number of polymorphisms, some of which influence their half-life and expression levels. M81 EBER2 modified the expression of a large number of cellular genes including CXCL8. This chemokine was able to compensate the absence of EBER2, suggesting that it represents the main target of this non-coding RNA. We found that the exosomal fraction of B cells infected with wild type M81 carries the EBER molecules, are able to increase CXCL8 and BZLF1 production. The effect of EBER2 on EBV lytic replication required a functional TLR7, a sensor of viral single-stranded RNA (ssRNA). Therefore, we propose a model in which EBERs are vehicled into the exosomal fraction of infected B cells to initiate lytic replication in a paracrine manner through CXCL8 secretion induced by TLR7 stimulation. These results indicate that EBERs NPC-derived virus variant contribute to lytic replication in B cells and activate production of a chemokine involved in carcinogenesis.

Zusammenfassung

Ein Großteil der Bevölkerung ist mit dem Epstein-Barr-Virus (EBV) infiziert. Der aus Nasopharyngealkarzinomen isolierte Virusstamm M81 infiziert und transformiert primäre B-Zellen, kann aber auch in einem kleinen Teil dieser Zellen eine lytische Replikation induzieren. Wir nutzten rekombinante Viren um die Funktion der EBER RNAs zu untersuchen. Wir konnten zeigen, dass die Anzahl der Zellen, in welchen lytische Replikation stattfand, durch die nicht-kodierende RNA EBER2 sowohl *in vitro* als auch *in vivo* erhöht wird. Dies war allerdings nicht bei dem Homolog aus dem 95-8 Genom der Fall. Die M81 und B95-8 EBER2 Homologe haben eine bestimmte Zahl ein Polymorphismen, teilweise können diese ihre Halbwertszeit und Expressionslevel beeinflussen. M81 EBER2 hatte Auswirkungen auf die Expression vieler zellulärer Gene, darunter auch CXCL8. Dieses Chemokin konnte ein Fehlen von EBER2 kompensieren, was ein Zeichen dafür sein könnte, dass CXCL8 das Hauptziel von EBER2 ist. Wir fanden heraus, dass Exosomen von M81-infizierten B-Zellen EBER-Moleküle enthalten, welche die CXCL8 und BZLF1-Produktion erhöhen können. Die Wirkung von EBER2 auf die lytische Replikation von EBV benötigte einen funktionalen TLR7, welcher ein Sensor für virale einzelsträngige RNA (ssRNA) ist. Deswegen schlagen wir ein Modell vor, in welchem EBER in Exosomen von infizierten B-Zellen gebracht werden, um so eine lytische Replikation durch TLR7-induzierte CXCL8 Sekretion zu induzieren. Diese Resultate weisen darauf hin, dass EBER aus NPC-abgeleiteten Virusstämmen zur lytischen Replikation in B-Zellen beitragen und die Produktion eines Chemokins aktivieren, welches in der Karzinogenese involviert ist.

List of Abbreviations

Δ	knockout; deletion
Ab	Antibody
Amp	Ampicillin
BAC	Bacterial artificial chromosome
BL	Burkitt's lymphoma
Cam	Chloramphenicol
DNA	Deoxyribonucleic acid
DTT	Dithiothreitol
E.coli	*Escherichia coli*
EBER	Epstein-Barr virus encoded RNA
EBNA	Epstein-Barr virus nuclear antigen
EBVaGC	Epstein-Barr virus-associated gastric carcinoma
EDTA	Ethylenediaminetetraacetic acid
FBS	Fetal bovine serum
GC	Gastric carcinoma
GFP	Green fluorescence protein
gp	Glycoprotein
HL	Hodgkin's lymphoma
HRP	Horseradish peroxidase
IFN	Interferon
IL	Interleukin
IM	Infectious mononucleosis
Kan	Kanamycin
Kb	Kilobase pair
kDa	Kilodalton
LB	Luria-Bertani
LCL	Lymphoblastoid cell line

moi	Multiplicity of infection
NF-kB	Nuclear factor kappa-light-chain-enhancer of activated B-cells
NPC	Nasopharyngeal carcinoma
OriLyt	Lytic Origin of replication
OriP	Latent Origin of replication
PAGE	Polyacrylamide gel
PBS	Phosphate buffered saline
PCR	Polymerase chain reaction
PKC	Protein kinase C
Pol	Polymerase
PTLD	Post-transplant lymphoproliferative disorder
qPCR	Quantitative polymerase chain reaction
rB95-8	Recombinant B95-8 EBV strain
rEBV	Recombinant EBV
rM81	Recombinant M81 EBV strain
RNA	Ribonucleic acid
rpm	Round per minute
RPMI	Roswell Park Memorial Institute
SDS	Sodium dodecyl sulfate
Tet	Tetracycline
TPA	12-O-tetradecanoylphorbol-13-acetate
TR	Terminal repeat
Tris	Tris-Hydroxymethyl-Aminomethane
UV	Ultraviolet
Wt	wild type
miRNA	Micro-Ribonucleic acid

1 Introduction

1.1 EBV and its related diseases

Epstein-Barr Virus (EBV) is the first discovered human tumor virus. In March 1964, Anthony Epstein and other colleagues identified herpesvirus-like particles in cultured tumor cells derived from African Burkitt's lymphoma tissue (Epstein et al., 1964). At that time, the idea that a virus could cause human tumor was met with some skepticism because the theory that cancer was infectious had been dismissed in the previous century. The Epstein-Barr Virus (EBV) (Figure 1.1 A), also called human herpesvirus 4 (HHV-4) is a common human virus that can cause both infectious mononucleosis and lymphoproliferative disease. EBV infects more than 90% of the adult population between 35-40 years old in the U.S, usually without clinical consequences, particularly when people are infected during childhood (Liebowitz D, 1993).

Because EBV belongs to the member of the herpesvirus family, it is very efficient at establishing a long-term latent infection in B cells. Previous exposure to EBV can be detected by serology, and latent forms of EBV can be readily detected by molecular methods in a small percentage of B-lymphocytes from healthy individuals.

EBV is associated with the development of cancers such as Burkitt's lymphoma, Hodgkin's lymphoma, and nasopharyngeal carcinoma. The virus is able to infect host B-cells and epithelia, and induce proliferation of its host via a non-lytic mechanism. During this latent process, virus-encoded nuclear proteins (EBNAs) and latent membrane proteins (LMPs) are expressed in infected host cells (Young and Rickinson, 2004).

EBV genome: The Epstein-Barr virus is a Baltimore Class I virus of the family Herpesviridae. Researchers used electron microscopy to describe these viral particles and found that EBV was very similar in structure to Herpes simplex virions (Fig. 1.1 A) (Epstein et al., 1964). The EBV genome is made of double-stranded DNA and is around 180 kb long (Baer et al., 1984). Herpes viruses possess relatively big genomes; Herpes simplex has a 152-kilobase genome (Mahiet et al., 2012). The open reading frames (ORFs) of EBV are generally broken up into separate lytic and latent sections. While most of the viral genes encode proteins, some of the latent genes remain noncoding (EBERs and microRNAs). During latent infection, the EBV genome exists in a circularized form localized in the host cell nucleus (Young and Rickinson, 2004). The open reading frames for the LMPs and EBNAs are clustered separately within the episomes (Fig. 1.1 B).

(A)

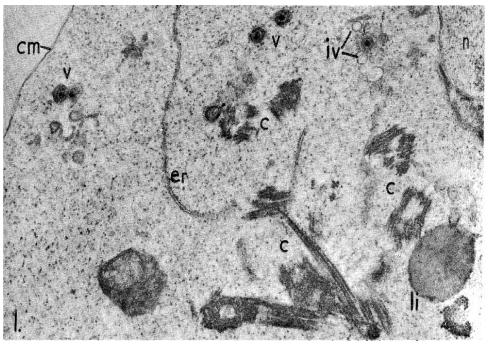

(C)

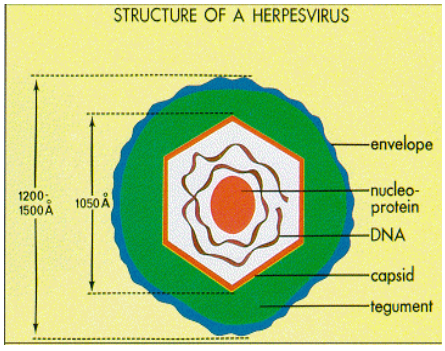

(B)

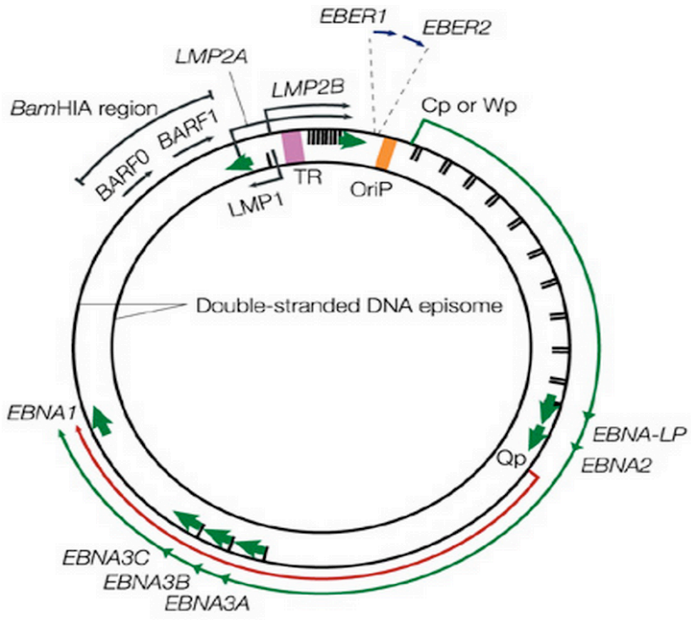

Fig. 1.1 (A) Original micrographs (EM) of cultured Burkitt's Lymphoma tissue published by Epstein and Barr in 1964. V indicates the presence of EBV virions. (B) A general diagram of an Epstein-Barr Virus dsDNA episome. Note the clustering of open reading frames for EBNA and LMP genes and the location of the origin of replication, oriP. The green arrows show the direction of transcription initiation during latency III (Young and Rickinson, 2004). (C) A general diagram of the structure of a herpesvirus virion (Wikipedia). The dsDNA genome is wrapped around a central nucleo-protein. Spike glycoproteins (not labeled) on the surface play a role in host cell entry.

EBV virion structure: Epstein and Barr observed that this lymphoma-associated virus was around 20% smaller in size than those typical Herpes simplex virions (Epstein et al., 1964). Similar to other Herpesviruses, the innermost part of the EBV virion consists of a copy of linearized viral DNA wrapped around a central nucleo-protein core (Fig. 1.1 C). The core of the virion is surrounded by a nucleocapsid, a layer of protein tegument, and an outer envelope with spike glycoproteins (Liebowitz

D, 1993). This nucleocapsid consists of a polymer of viral capsid proteins that play a key role in wrapping the viral genome into the core of the nucleocapsid layer and the delivery of the viral DNA at the nuclear membrane (Kieff et al., 1982). The tegument proteins display multiple enzymatic activities that are not only important for the infection but also for the maturation of the virus (Kalejta, 2008). Many of these glycoproteins are important for host-cell entry and fusion mechanisms. Infected host cells release EBV virus particles exclusively during the lytic cycle.

EBV-related diseases: EBV is transmitted orally and is often acquired during childhood. Primary EBV infection is usually clinically silent or not different from the usual minor respiratory infections that occur in children. In developed countries, infection with EBV is often delayed until adolescence. Infection with EBV may also develop unnoticed in this case, although some people develop infectious mononucleosis, which is described by symptoms of sore throat, lymphadenopathy, fever and fatigue (Balfour et al., 2013). In both cases, EBV infection is countered by a robust immune response, natural killer cells, CD8+ cytotoxic T-cells and CD4+ helper T-cells (Rickinson et al., 2014). This response can be very potent and the consequences of infectious mononucleosis are thought to come from an exuberant immune response to infection. Nevertheless, the immune system cannot clear the virus that establishes permanent infection in the host's B-lymphocytes, evading anti-viral immunity response by silencing viral protein expression. This strategy enables EBV to persist for the lifetime of the host as a latent infection. In order to be transmitted to new hosts, some of the B cells carrying EBV undergo reactivation, producing new progeny virus in the oropharynx for transmission to susceptible individuals (Taylor et al., 2015).

The co-existence between EBV and its host means that most people have no long-term health effects from this infection. Although relatively benign in most people, EBV has powerful growth transforming potential and is classified as a group I carcinogen by the World Health Organization. EBV is associated with several distinct lymphomas: Burkitt lymphoma, Hodgkin lymphoma, T/NK lymphoma and about 10% of diffuse large B cell lymphomas. EBV is also a problem in the transplant setting, where iatrogenic immunosuppression may result in post transplant lymphoproliferative disease (PTLD) (Rickinson et al., 2014). EBV has the ability to infect and transform epithelial cells *in vivo*. EBV is associated with 10% of gastric carcinomas and with almost all cases of the non-keratinizing subtype of nasopharyngeal carcinoma (NPC). This subtype represents most cases (>95%) of NPC in Southeast Asia where the disease is endemic. Taken together, EBV is related to an estimated 200,000 cases of cancer each year, representing 1% of all cancers worldwide (Parkin, 2006).

All EBV-associated malignancies express viral proteins but the viral protein expression pattern is different in different diseases (Table 1.1). Post-transplant lymphomas, particularly those that arise in the first year after transplantation when immunosuppression is greatest, express all nine EBV latent proteins. These comprise six Epstein-Barr Nuclear Antigens (EBNAs) and three Latent Membrane Proteins (LMPs). The EBNA 3A, 3B, and 3C proteins, which are good CD8+ T-cell targets, are expressed (Taylor et al., 2015). In contrast, a lower number of EBV proteins is expressed in the remaining EBV-associated malignancies, possibly reflecting their origin in people who are not overtly immunosuppressed.

Table. 1.1 EBV-associated malignancies and the viral proteins in the tumor cells

Tumour	EBV proteins expressed
Post-transplant lymphoproliferative disease	EBNA1, 2, 3A, 3B, 3C, LP, LMP1, LMP2
Hodgkin lymphoma	EBNA1, LMP1, LMP2
Diffuse large B lymphoma	EBNA1, LMP1, LMP2[a]
Burkitt lymphoma	EBNA1[b]
Extranodal T/NK lymphoma	EBNA1, LMP2[c]
Gastric carcinoma	EBNA1, LMP2[d]
Nasopharyngeal carcinoma	EBNA1, (LMP1[e]), LMP2[d]

[a], some DLBCL tumours express a wider range of latency proteins; [b], 10–15% of endemic Burkitt lymphomas express EBNA-1, -3A, -3B -3C, -LP and BHRF-1; [c], a shortened version of LMP2 is expressed in extranodal T/NK lymphoma; [d], BARF1 is reported to be expressed in a proportion of EBV-positive carcinomas; [e], LMP1 is expressed in a subset of NPC tumours at apparently low levels. EBNA, Epstein-Barr Nuclear Antigen; LMP, Latent Membrane Protein; EBV, Epstein-Barr virus; NPC, nasopharyngeal carcinoma.

1.2 The EBV infection modes

1.2.1 Lytic life cycle

Like all herpesviruses, EBV exhibits two life cycles: latency and lytic replication phase that leads to the generation of progeny viruses (Kieff and Rickinson, 2007). Although the EBV lytic life cycle is more rarely observed than the latent cycle, it is very important since it is the only way that the virus may produce virions and be transmitted horizontally between hosts or cells. Increased free virion levels are observed in immunosuppressive diseases like AIDS in the blood. While virions are often found in the saliva of infected hosts, little or no lytic-infected cells are typically detected in the body (Swaminathan S., 2009). Human cytotoxic T-cells are particularly good at recognizing and killing lytically infected cells expressing early stage lytic genes. Although lytic replication contributes to drive EBV spread in human populations, latent infection is more common in infected cells. Alpha and Beta herpesviruses have evolved elaborate mechanisms for lytic gene concealment from the host immune system; however, EBV has few mechanisms to evade immune-mediated destruction of lytic-infected cells. For example, Herpes simplex virus is able to inhibit host Major Histocombatibility Complex (MHC) expression, which reduces B-cell antigen presentation and recognized by cytotoxic T-cells. In contrast to other herpes viruses, EBV have a different mechanism to evade the host immune response. EBV mainly relies on a latent replication cycle in which it copies its genome within dividing host B-cells using the replication machinery of the host (Steven et al., 1997). Therefore, unlike other herpesviruses that rely on lytic replication for spread within a host, EBV relies more on its latent replication. Because latent mechanisms are

responsible for persistence in the host, EBV is not under significant selective pressure to develop elaborate lytic immune avoidance traits.

Latent infection plays a primary role in the development of lymphoproliferative disease (LPD) in EBV infected individuals. The role of lytic replication in EBV-associated malignancies is not well understood. Researches reported that EBV mutants (B95-8 strain) that cannot undergo lytic viral replication are defective in promoting EBV-mediated lymphoproliferative disease (LPD). In more detail, they found that early-passage lymphoblastoid cell lines (LCLs) derived from EBV mutants with a deletion of either viral immediate-early gene (*BZLF1*) grew similarly to wild-type (WT) virus LCLs *in vitro* but were deficient in producing LPD when inoculated into SCID mice. In addition, lytic infection contributes to stimulate the secretion of paracrine factors that may promote the growth of latently infected B-cell lines. While it may have a more diffuse effect than the latent mechanism, EBV lytic infection-mediated signaling may contributes to the development of lymphoproliferative disease (Hong et al., 2005).

The lytic cycle produces progeny viruses that can target host cells, such as B cells. To enter B cells, viral glycoprotein gp350 bind to cellular receptor CD21 (also known as CR2) (Nemerow et al., 1987). Then, viral glycoprotein gp42 interacts with cellular MHC class II molecules. Subsequently, fusion between the viral envelope and endocytotic membrane is mediated by gH/gL and gB (Kirschner et al., 2006). Following fusion, the viral capsid enters into the cytoplasm and is transported to the nuclear membrane by microtubule-mediated transport. The EBV viral genome is released into the nucleus through a nuclear pore. During the lytic replication cycle, the viral genome replicates in the nucleus (Daikoku et al., 2005). The viral genome is

replicated using an EBV DNA polymerase, which stimulates the production of viral structural proteins. Viral particles are assembled in the nucleus (Henson et al., 2009). After full particles are assembled, they bud out of the nuclear membrane, then through the Golgi membrane.

Two immediate-early lytic genes including BZLF1 (also known as Zta, associated with its product gene ZEBRA) and BRLF1 (associated with its product gene Rta) cooperate to promote most of the lytic genes transcription. Early lytic gene products perform functions such as replication, metabolism, and blockade of antigen processing. Finally, late lytic gene products tend to be proteins with structural roles, such as VCA, which forms the viral capsid. Other late lytic gene products, such as BCRF1, help EBV evade the immune system.

1.2.2 Latent infection

In most cases, once EBV virions accomplish primary infection of B-lymphocytes, the virus mainly replicates by a latent form (Jochum et al., 2012). This results in the transformation of B-cells into proliferating lymphoblastoid cell lines (LCLs) (Young and Rickinson, 2004). The latent replication cycle is defined in two aspects: 1) No production of virions, and 2) the production of few viral proteins and transcripts. These latent viral proteins activate the proliferation of host B-cells and contribute to lymphoproliferative disease (Cesarman, 2011).

EBV can exhibit three latency programs: Latency I, Latency II, and Latency III. In latency I, only EBNA1 is expressed (Cesarman, 2011), while in latency II EBNA1 is expressed along with the LMP proteins (Young and Rickinson, 2004). In Latency III, the six EBNAs and the three LMP proteins (LMP1, 2A, and 2B) are produced. The transcription of EBV genome initiates at either the Wp or Cp promoter. Differential

splicing of the same long transcript generates the different EBNA mRNA. *In vitro,* LCLs typically display latency III-like expression profiles (Cesarman, 2011). B-cells must have latency III expression profiles for successful generation of LCLs *in vitro* (Klein and Ernberg, 2007). In addition to these latent proteins, several non-coding RNAs (EBERs) and micro-RNAs are also expressed during all these latency types (Fok et al., 2006; Young and Rickinson, 2004).

1.2.3 Reactivation from latent phase to lytic phase

Latent EBV in B cells can be reactivated to switch to lytic replication. This is known to happen *in vivo*, but the precise mechanism why EBV is reactivated is unknown. *In vitro*, EBV latency in B cells can be reactivated by stimulating the B cell receptor, so reactivation *in vivo* probably happens when latently infected B cells respond to unrelated infections (Odumade et al., 2011). *In vitro*, EBV latency in B cells can also be reactivated by treating with sodium butyrate or TPA. In most EBV-positive cell lines, BZLF1 protein alone is sufficient to induce the switch from latency to lytic replication.

BZLF1 interacts directly with histone acetylating complexes, such as CBP and p300 and the general transcription factors TFIID and TFIIA. During viral reactivation (EBV genome is highly methylated in cells), BZLF1 initially activates the transcription of BRLF1 gene. BZLF1 and BRLF1 then promote the transcription of many of the early lytic viral genes that often contain binding sites for both (Wille et al., 2013). They are both needed for expression of many, but not all, of the early-lytic genes in the EBV genome (Feederle et al., 2000). BZLF1 also makes contributions to the lytic EBV DNA replication, binding directly to many of the essential ZRE sites located within the lytic origin of replication, oriLyt. The direct interactions between

BZLF1 and core EBV replication proteins likely promote the formation of replication complexes.

BRLF1 can also induce the switch from latency to lytic phase in some EBV-positive cell lines, especially in epithelial cells. BRLF1 directly binds to GC-rich motifs known as R-responsive elements (RREs) (consensus 5'-GNCCN9GGNG-3') located within the promoters of early lytic genes (Heilmann et al., 2012). R directly interacts with both the general cellular transcription factors, such as TBP and TFIIB and the histone acetylating complex CBP and p300. Previous published data from transient transfection reporter assays suggest that BRLF1 activates both its own promoter and the BZLF1 promoter by indirect mechanisms in which the Sp1, MCAF1 and Oct-1 transcription factors, and some cellular kinases are involved in this process (Adamson et al., 2000; Darr et al., 2001; Ragoczy and Miller, 2001; Robinson et al., 2011). However, given that the strong enhancer activity of BRLF1-bound RREs, it is speculated that BRLF1 directly activates the BZLF1/BRLF1 transcription in the context of the EBV genome (Heilmann et al., 2012). At least two EBV-encoded proteins are involved in the ability of BRLF1 to regulate viral latency. The early-lytic viral protein BRRF1 activates phosphorylation of c-Jun and cooperates with BRLF1 to induce BZLF1 promoter transcription in the context of the intact EBV genome (Hagemeier et al., 2011; Hong et al., 2004). In contrast, the early-lytic EBV protein LF2 directly inhibits the activity of BRLF1, therefore, it limits viral lytic replication (Calderwood et al., 2008). The opposite roles of BRRF1 and LF2 might help to fine-tune the transcriptional effects of BRLF1 during the various stages of EBV lytic replication.

1.3 EBV-encoded small RNAs (EBERs)

1.3.1 Generalities

Epstein-Barr virus (EBV) expresses two noncoding RNAs called EBER1 (EBV-encoded RNA 1) and EBER2, that are 167 and 173 nucleotides (nts) long, respectively. They are transcribed by RNA polymerase III (Howe and Shu 1989). The EBERs are expressed in all forms of EBV latency and also during lytic replication. They are the most abundant viral transcripts in latently EBV-infected cells. EBER1 accumulates to 10^6 and EBER2 to 2.5 x 10^5 copies per infected cell. Currently, EBERs are used as preferential target molecules in *in situ* hybridization (ISH) detection of EBV-infected cells in tissues (Chang et al., 1992) and are considered a good marker to detect the presence of EBV, as they are highly expressed in EBV-infected cells. Previous papers have shown that EBERs are oncogenic. Expression of these RNAs in B-lymphocytes can induce colony formation in soft agar and tumor formation in nude mice (Komano et al., 1999; Ruf et al., 2000). Furthermore, EBERs can induce resistance to interferon-alpha-induced apoptosis in BL cells (Nanbo and Takada, 2002). Previous studies have also demonstrated that EBERs can induce the transcription of various cytokines, such as interleukin-10 (IL-10) in BL cells, insulin-like growth factor-1 (IGF1) in epithelial cells and IL-9 in T cells. These cytokines can subsequently act as autocrine growth factors for EBV-infected cancer cells (Iwakiri et al., 2003; Iwakiri et al., 2005; Kitagawa et al., 2000; Yang et al., 2004). More recent studies have shown that EBER1 is sufficient to elicit these phenotypes, suggesting that EBER2 is redundant (Houmani et al., 2009). The EBERs were reported to promote the pathogenic consequence of EBV infection by modulating innate immune signals (Iwakiri et al., 2009; Samanta et al., 2006; Samanta et al., 2008).

1.3.2 Structure of EBERs

EBER1 and EBER2 are short, nuclear-enriched non-coding RNAs that are 166 and 172 nucleotides (nts) in length, respectively (Rosa et al., 1981). These two RNAs display 54% sequence homology. The EBER genes are separated by 161 base pairs and are transcribed from left to right on the EBV map. Although these two EBERs show only limited sequence identity (54%), they exhibit striking similarities in their secondary structures and form several short stem loops (Fig. 1.2, (Rosa et al., 1981). However, the secondary structures are not identical, suggesting that EBER1 and EBER2 might have distinct functions.

EBER1 is highly conserved in its primary sequence among multiple EBV strains with only 5 polymorphisms as shown in Table 1.2, suggesting that the EBERs are very important in the virus life cycle. EBER1's secondary structure is very stable, and is organized into five conserved hairpins (Fig. 1.2) radiating from two multi-branch loop structures. In addition to its hairpins, EBER1 possesses a 9 nt single-stranded tail at its 3′ end. This RNA structure provides a platform for binding of host proteins to form EBER1 ribonucleoprotein (RNP). EBER2 also displays some polymorphisms among multiple EBV strains (Table 1.3). The distribution of the different EBER2 polymorphisms in lymphoma and in EBV-associated gastric carcinoma (EBVaGC) is nearly identical, however, there are some polymorphisms that are seen more frequently in nasopharyngeal carcinoma (NPC) as shown in Table 1.3 and Fig. 1.2, suggesting that NPCs carry a specific type of EBER2 that might have unique functions.

Table. 1.2 EBER1 polymorphisms among 137 EBV strains

Strains	20	52	106	116	160
B95-8	A	T	T	C	C
Wewak 1	T	T	T	C	C
sLCL-TM1.16	A	C	T	C	C
HN4	A	T	G	C	C
SLCL1.19	A	T	T	T	C
HL05	A	T	T	C	G

In all other 130 EBV strains, EBER1 is identical to B95.8; HN4 is identical to VGO.
Communication from R. Poirey (DKFZ)

Table. 1.3 EBER2 polymorphisms among multiple EBV strains

Groups	44	46	57	61	93	168	Ratio
B95-8	T	A	A	A	A	A	7.0%
Akata	T	A	A	A	A	G	68.6%
M81	G	T	G	T	C	G	16.3%

B95-8 (derived from IM) is equal to BL36, sLCL-1.02, 11, sLCL-IS1.04, 18, X50-7. (7% of total EBV genomes)
Akata (derived from Burkitt's lymphoma) is equal to EBVaGC1to9, GC1 (SNU719), and to the majority of other EBV strains (about 70% of total EBV genomes).
M81 is identical to HKNPC1to9 (about 20% of total EBV genomes).
BL, Burkitt lymphomas; EBVaGC, EBV associated gastric carcinomas; NPC, Nasopharyngeal carcinoma; LCL, Lymphoblastoid cell lines;
Communication from R. Poirey (DKFZ)

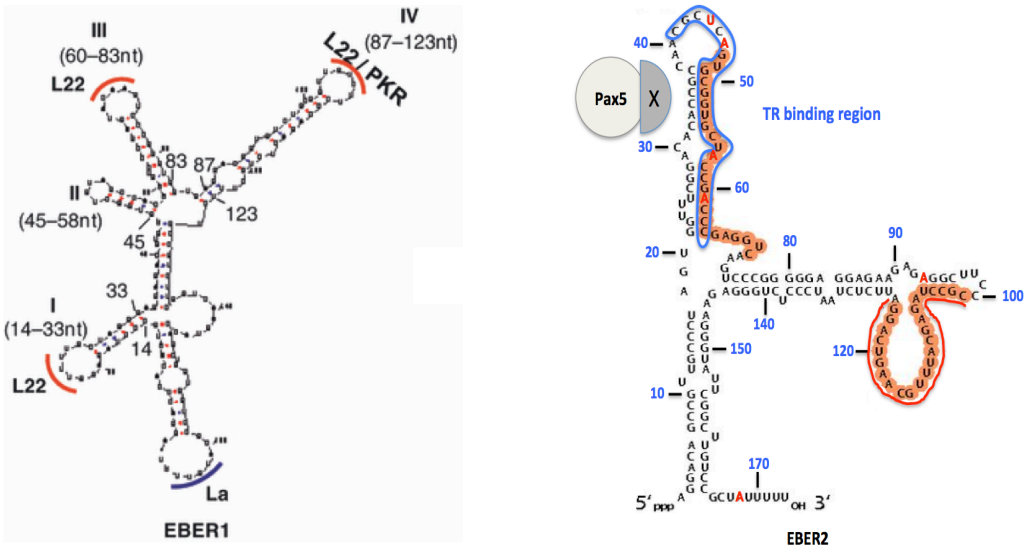

Fig. 1.2 Secondary structures of the EBER1, showing potential protein binding sites for L22, PKR, and La in red and blue. EBER1 structure is reproduced from Rosa *et al*. EBER2 structure is reproduced from Lee *et al*. The blue region (+41 to +64) can bind to the terminal repeat (TR) of the EBV genome. The red positions display polymorphism between B95-8 and M81 strains. In M81, at position 44 is G, position 46 is U, position 57 is G, position 61 is U, position 93 is C and position 168 is G. RNase H-sensitive regions are indicated in orange. The region hybridizing to the antisense oligonucleotides (ASOs) used in capture hybridization analysis of RNA targets (CHART) is in red. EBER, Epstein-Barr virus-encoded RNA.

1.3.3 Synthesis and expression of EBERs

EBERs are transcribed by RNA polymerase III. These genes show the typical intragenic Box A and Box B RNA Pol III promoter sequences. Furthermore, they contain three typical upstream promoter elements including a TATA box as well as ATF- and Sp1-like promoter elements as shown in Fig. 1.3. Sp1-like promoter element binds Sp1 protein or a related protein and ATF-like promoter element binds the activating transcription factor (ATF). These three upstream elements are typical of Pol II promoters and they together stimulate *in vivo* EBERs expression 50-fold. Both Pol II and Pol III promoter elements stimulate Pol III, but not Pol II-modulated transcription in EBV-transformed lymphocytes (Howe and Shu, 1989). A sequence

alignment between M81 and B95-8 shows that M81 and B95-8 carry the same Pol II promoter elements for EBER2 as shown in Fig. 1.4, however, they display one difference at position 57 in the polymerase III control regions as shown in Fig. 1.5.

The level of EBER expression appears to be correlated to the EBV DNA molecule copy number in infected cells (Arrand and Rymo, 1982). Upon EBV infection of primary B-lymphocytes, EBNA2 is expressed firstly at 6 h post infection, followed by other EBNA genes, latent membrane protein genes (LMPs) and by the EBERs. The non-transforming P3HR-1 strain that carries a deletion of the EBNA2 locus expresses only the EBNA-leader protein (EBNA-LP) and trace amounts of EBER1 in primary B lymphocytes, however, the same virus can express EBNA1, EBNA3(s), EBNA-LP and EBERs upon infection of EBV-negative BL cell lines (Rooney et al., 1989). These findings indicate that EBERs expression depends on the host cell, perhaps through products specific for the cell cycle or the state of B-cell differentiation induced by EBNA2.

EBER expression seems to be also influenced by the stage of viral life cycle. An early paper demonstrated that EBER transcription was down regulated during the switch from latent infection to lytic EBV replication. In contrast, the expression of EBERs remains unaltered within 72 h after the induction of lytic replication (Greifenegger et al., 1998). Although EBER1 and EBER2 are transcribed at approximately equal rates, EBER1 is present at about 10-fold higher levels compared to EBER2, probably due to the longer half-life of EBER1. Indeed, in the presence of actinomycin D, the half-lives of EBER1 and EBER2 are 8 to 9 h and 45 min, respectively (Clarke et al., 1992).

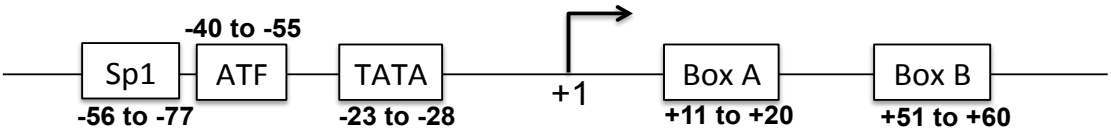

Fig. 1.3 Promoter structure of the Epstein–Barr virus-encoded small RNA (EBER)-2-gene, showing the upstream region containing TATA box (−23 to −28) and transcription factor ATF (−40 to −55), and Sp1 (−56 to −77) binding sites and the intragenic polymerase III control regions, box A (+11 to +20) and box B (+51 to +60). "+1" is the transcription start site (TSS) of the EBER2 transcript. Positive values are downstream location after the TSS of the EBER2 transcript. Negative values are upstream position before the TSS of the EBER2 transcript.

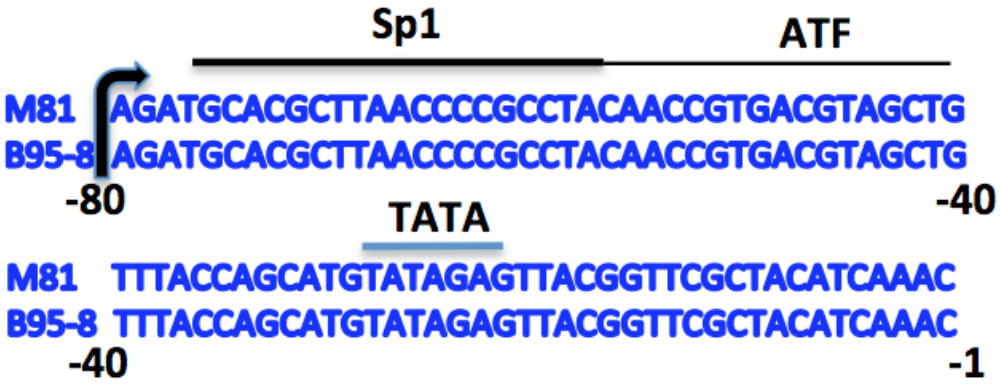

Fig. 1.4 A sequence alignment in Pol II promoter elements for EBER2 between M81 and B95-8.

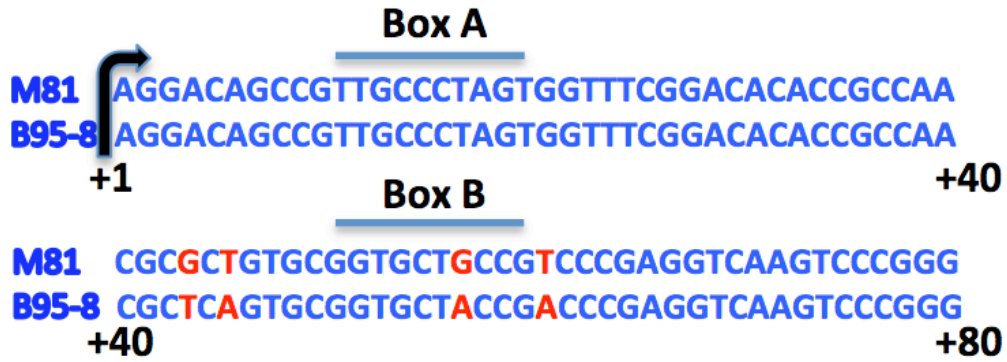

Fig. 1.5 A sequence alignment in Box A and Box B for EBER2 between M81 and B95-8.

1.3.4 Localization of EBERs

EBERs are found mainly in the nucleus and generate an intense nuclear signal after EBER ISH staining (Howe and Steitz, 1986). Fig. 1.6 shows an example of an EBER ISH staining. However, high-resolution ISH using confocal laser scanning microscopy has shown that EBERs are found in both the cytoplasm and nuclei of interphase cells (Schwemmle et al., 1992). Researchers previously reported that EBERs are found in a complex with the lupus antigen (La) protein (Iwakiri et al., 2009). As the EBERs can bind to types of proteins that are not only restricted to the nucleus but are also located in the cytoplasm, it was speculated that this is a reason why EBERs could also localize in the cytoplasm (Lee et al., 2012; Samanta et al., 2006).

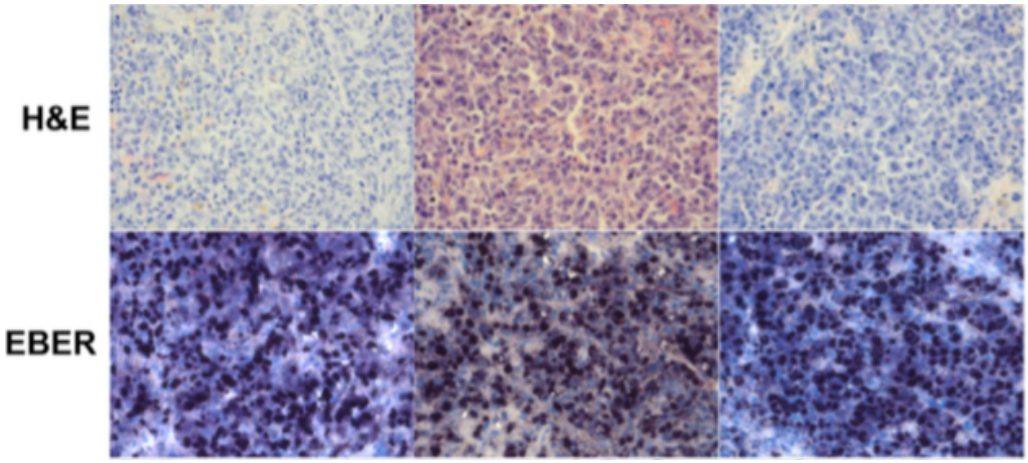

Fig. 1.6 This picture shows an example in situ hybridization with an EBER specific probe. We can see that EBERs can generate an intense nuclear signal after EBER ISH staining (Lin et al., 2015).

1.3.5 Proteins interacting with EBERs

La protein:

EBERs exist in the form of nuclear ribonucleoprotein (RNP) complexes that can be immunoprecipitated with anti-La antibodies (Lerner et al., 1981). The La protein binds the short oligouridylate stretch at the 3' ends of polymerase III transcripts, thereby facilitating the correct folding and maturation of RNA polymerase III transcripts (Gottlieb and Steitz, 1989). This binding is transient for most RNAs but stable for the EBERs (Howe and Shu, 1988). Abundantly expressed EBERs make stable complexes with La protein, and, therefore, the amount of free La protein is significantly reduced in EBV-infected cells (Glickman et al., 1988). Since the La protein plays an important role in the biogenesis of RNA polymerase III transcripts, the formation of stable complexes between La and EBERs is expected to affect the interaction between La and RNA polymerase III in EBV-infected cells.

La is mainly located in the nucleus, however, it can also be found in the cytoplasm under certain conditions (Bachmann et al., 1989; Meerovitch et al., 1993). The poliovirus-mediated cleavage of the La nuclear localization signals was reported to result in the shuttling of La from the nucleus to the cytoplasm. Their results suggest that La protein is involved in poliovirus internal initiation of translation and might function through a similar mechanism in the translation of cellular mRNAs (Meerovitch et al., 1993). A recent study indicated that the EBER-La interaction complex is making contributions to the secretion of EBER from EBV-infected cells into the extracellular medium, because EBER is primarily released when it forms a complex with the La protein (Iwakiri et al., 2009). The consequence of EBER-La interaction remains unknown, however, it seems likely that it plays some roles in

general replication, transcription, or RNA processing in EBV-infected cells.

PKR:

The adenovirus-encoded RNAs, VA1 and VA2, are small ncRNAs that are transcribed by RNA pol III and that are essential for adenovirus replication and that have been shown to inhibit PKR-mediated shutdown of translation (Shiroki et al., 1999). Although EBERs and VAs display no high sequence homology, they exhibit similarities in size, degree of secondary structure and genomic organization as shown in Fig. 1.7 (Akusjarvi et al., 1980). Intriguingly, the EBERs can functionally substitute for VAI/II and partly rescue replication of adenoviruses lacking VAI/II (Bhat and Thimmappaya, 1983). Similar to VA RNAs, EBERs can bind to the double-stranded RNA-dependent protein kinase (PKR), a serine/threonine kinase that can be induced by IFNα. PKR plays a role in mediating the antiviral effects of IFNα (Fok et al., 2006; Sharp et al., 1993). Previous study demonstrated that PKR could bind to the stem-loop IV of EBER1 as shown in Fig. 1.2 (Vuyisich et al., 2002). PKR phosphorylates the α-subunit of the protein synthesis initiation factor eIF2 and thus results in translational inhibition at the level of initiation. *In vitro* assays have demonstrated that EBERs can inhibit PKR activation and block the phosphorylation of eIF2α, thus blocking the eIF2α-mediated inhibition of protein synthesis (Katze et al., 1991; Sharp et al., 1993). In BL cells, EBERs were reported to confer resistance to IFN α induced apoptosis by directly binding to PKR and inhibiting its phosphorylation (Nanbo et al., 2002). A study also reported that EBERs/VAs preferentially bind to the latent dephosphorylated form of PKR, with a similar affinity to that of dsRNA activators. However, EBERs/VAs prevent PKR dimerization, which is required for efficient PKR trans-autophosphorylation. Consequently, the phosphorylation of the PKR substrate is blocked, and protein synthesis continues

unhindered (McKenna et al., 2007).

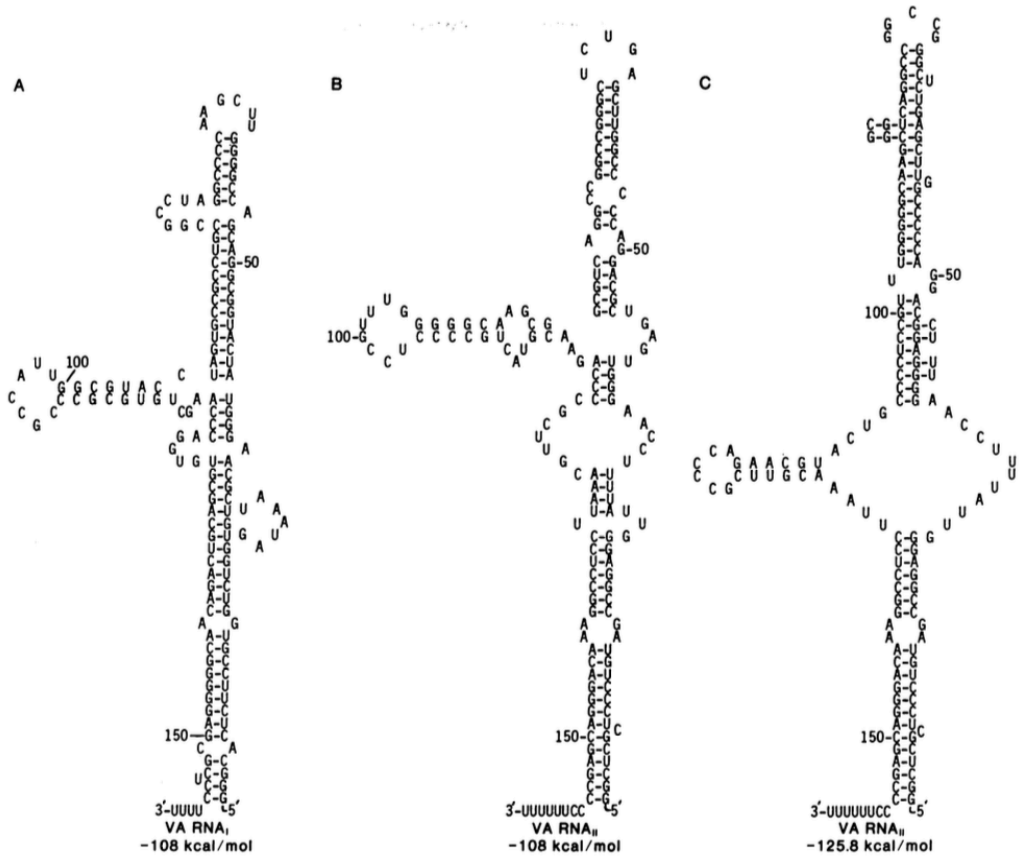

Fig. 1.7 The Secondary structure of VA RNAs. The structure of VA RNA1 (A) and two possible structures for VA RNAII (B and C) were derived by computer analysis. Reproduced from Akusjärvi *et al* (Akusjarvi et al., 1980).

L22:

EBERs exist in the form of nuclear ribonucleoprotein (RNP) complexes that can be immunoprecipitated with anti-La antibodies (Lerner et al., 1981). A second highly abundant EBER-associated protein (EAP) was also identified in La-containing RNP complexes (Toczyski and Steitz, 1991). EBER1 was reported to mainly bind to EAP and EAP was subsequently confirmed to be the ribosomal protein L22 (Toczyski et al., 1994; Toczyski and Steitz, 1993). Although its functions are not well known, L22 was identified as the target of chromosomal translocation in certain leukemia-

associated proteins (Nucifora et al., 1993), indicating that L22 expression levels might play an essential role in cell transformation. A study also suggested that the cellular functions of L22 might involve its association with the human telomerase (Le et al., 2000), and L22 has also been shown to interact with many other small viral RNAs (Leopardi et al., 1997; Wood et al., 2001).

L22 is located in the nucleolus and cytoplasm of primary uninfected human B-lymphocytes. However, in EBV-infected cells, probably 30%–50% of the L22 interacts with EBER1 and L22 relocalizes to the nucleoplasm (Toczyski et al., 1994). This suggests that the L22-EBER1 interaction can cause an abnormal cellular redistribution of L22 in EBV-infected cells. A recent study showed that the distribution of L22 was predominately located in the cytoplasm in EBV-transformed lymphoblastoid cell lines (LCLs), but that this process is independent of EBER1 (Gregorovic et al., 2011). Previous studies have reported that EBER1 contains multiple L22-binding sites, including stem-loop III (Toczyski and Steitz, 1993), stem-loop IV (Dobbelstein and Shenk, 1995), and stem-loop I (Fok et al., 2006). The existence of these multiple L22 binding domains suggest that most EBERs probably form complexes with L22 *in vivo* and that EBERs might modulate protein translation (Fok et al., 2006). A previous study reported that L22 and PKR compete for a common binding site on EBER1. L22 hampers the ability of EBERs to inhibit PKR activation by dsRNA through this competition. Transient introduction of EBER1 in murine embryonic fibroblasts causes reporter gene β-galactosidase activity upregulation and partially blocks the inhibitory effects of PKR. However, EBER1 is also stimulatory when transfected into PKR-null cells, suggesting a function that is PKR-independent. L22 expression prevents both the PKR-dependent and -independent effects of EBER1 *in vivo*. These findings suggest that the L22-EBER1

interaction can reduce the biological effect of viral ncRNA, including PKR inhibition and any other mechanism by which EBER1 induces gene expression (Elia et al., 2004).

Other interacting proteins:

Recent studies have reported that yet other cellular proteins can interact with EBERs. Pathogens infection can evoke the host innate immune responses that result in the elimination of invading pathogens. Cells express a limited number of germ-line encoded receptors known as pattern-recognition receptors (PRR) that specifically recognize pathogen-associated molecular patterns within microbes. The retinoic acid-inducible gene I (RIG-I) like receptor (RLR) family, which includes RIG-I (Yoneyama et al., 2004), melanoma differentiation-associated gene (Mda)-5 (Kang et al., 2002), and LGP2 (Yoneyama and Fujita, 2007), comprises cytoplasmic proteins that recognize viral RNA. RLRs are known to play a key role in IFN-inducible antiviral effects (Meylan and Tschopp, 2006). When RIG-I is activated by an interaction with viral dsRNA, it can initiate signaling pathways that result in the induction of protective cellular genes, including type I IFNs and inflammatory cytokines. RIG-I contains a C-terminal DExD/H-box RNA helicase domain and an N-terminal caspase recruitment domain (CARD). The helicase domain is responsible for dsRNA recognition, and the CARD domain activates downstream signaling cascades via the mitochondrial adaptor IFN-β promoter stimulator (IPS)-1, leading to activation of the transcription factors nuclear factor (NF)-κB and interferon regulatory factor 3 (IRF3) (Kang et al., 2002; Kawai et al., 2005). 5'-triphosphate RNAs are ligands for RIG-I. Therefore the EBERs, as 5'-triphosphate RNA molecules, could also interact with RIG-I (Hornung et al., 2006). Further studies found that EBER promotes BL cell growth by inducing expression of anti-inflammatory and growth-

promoting cytokine IL-10, which is dependent on RIG-I-mediated IRF3 signaling. These results suggested that EBER-mediated RIG-I activation contributes to EBV oncogenesis (Samanta et al., 2006; Samanta et al., 2008).

The AU-rich element-binding factor 1 (AUF1) has the ability to bind to AU-rich elements present in the 3'-untranslated regions of precursor RNA (Lu et al., 2006). The interaction between AUF1 and pre-mRNAs in the nucleus was reported to influence pre-mRNA processing, metabolism, and transport (Gratacos and Brewer, 2010), whereas AUF1 alone might contribute to stabilize certain transcripts (Lal et al., 2004). A recent paper demonstrated that AUF1 is a novel EBER1 binding protein as shown in Table 1.4. The EBER1/AUF1 interaction prevents AUF1 from binding to short-lived mRNAs (Lee et al., 2012). How this interaction might regulate the expression of EBV genes remains unclear. More recently, Lee et al demonstrated that EBER2 interacts with the B cell transcription factor PAX5 and is required for the localization of PAX5 to the terminal repeats (TRs) of the virus. Indeed, EBER2 and TR have partially complementary sequences that allow their interaction. EBER2 knockdown phenocopies a PAX5 depletion in upregulating the transcription of LMP2A/B and LMP1, the genes located nearest to the TRs. Knockdown of EBER2 also decreases EBV lytic replication, suggesting the essential role of the TRs in this process. Recruitment of the EBER2-PAX5 complex is mediated by base pairing between EBER2 and nascent transcripts from the TR locus. The interaction is evolutionarily conserved in the related primate herpesvirus CeHV15 despite great sequence divergence (Lee et al., 2015). To identify the interaction proteins between EBER2 and PAX5, the authors isolated EBER2-PAX5-containing complexes and analyzed the protein components by mass spectrometry. The top candidates include three host proteins splicing factor proline and glutamine rich (SFPQ), non-POU

domain-containing octamer-binding protein (NONO), and RNA binding motif protein 14 (RBM14), all reported to be components of nuclear bodies called paraspeckles. It remains unknown whether SFPQ, NONO, and RBM14 are likewise essential for viral lytic replication. Intriguingly, these proteins also play a role in the life cycle of HIV (Budhiraja et al., 2015; Kula et al., 2013; Zolotukhin et al., 2003), suggesting a more common involvement of these factors in viral regulation. Detailed studies of these RRM-containing proteins are complicated by the fact that all three proteins function in multiple cellular processes, including transcription regulation, paraspeckle formation, and notably alternative splicing (Amelio et al., 2007; Naganuma et al., 2012; Rosonina et al., 2005). In vivo RNA–protein crosslinking indicates that SFPQ and RBM14 contact EBER2 directly. Binding studies using recombinant proteins demonstrate that SFPQ and NONO associate with PAX5, potentially bridging its interaction with EBER2. Similar to EBER2 or PAX5 depletion, knockdown of any of the three host RNA-binding proteins results in the up-regulation of viral LMP2A mRNA levels, supporting a physiologically relevant interaction of these newly identified factors with EBER2 and PAX5 (Lee et al., 2016).

Table. 1.4 Summary of other interacting proteins with EBERs

Interaction Proteins	Interaction with EBER1 or EBER2	Interaction sites	Direct or indirect interaction	References
AUF1	EBER1	unknown	direct	Lee et al., 2012
hnRNP D	EBER1	unknown	direct	Lee et al., 2012
Pax5	EBER2	unknown	indirect	Lee et al., 2015
SFPQ	EBER2	unknown	direct	Lee et al., 2016
NONO	EBER2	unknown	indirect	Lee et al., 2016
RBM14	EBER2	unknown	direct	Lee et al., 2016

1.3.6 EBERs-mediated pathogenesis via modulation of innate immune signals

Interactions between EBERs and host dsRNA sensors have been demonstrated to play an important role in EBV-mediated pathogenesis (Fig. 1.8). Samanta *et al.* reported that EBER, which forms dsRNA structures, activates RIG-mediated signaling. The results suggest that in BL cells, RIG-I is activated by EBERs, resulting in the activation of NF-κB and IRF-3 pathways, and subsequent induction of type-I IFN. Although induction of IFN appears to be disadvantageous for the virus, EBV still can maintain a latent infection due to resistance to IFN, such as that provided by EBER-mediated PKR inhibition (Nanbo et al., 2002). EBER promotes BL cell growth by inducing expression of the anti-inflammatory and growth-promoting cytokine IL-10, which is dependent on RIG-I-mediated IRF3 signaling but independent of NF-κB (Samanta et al., 2008).

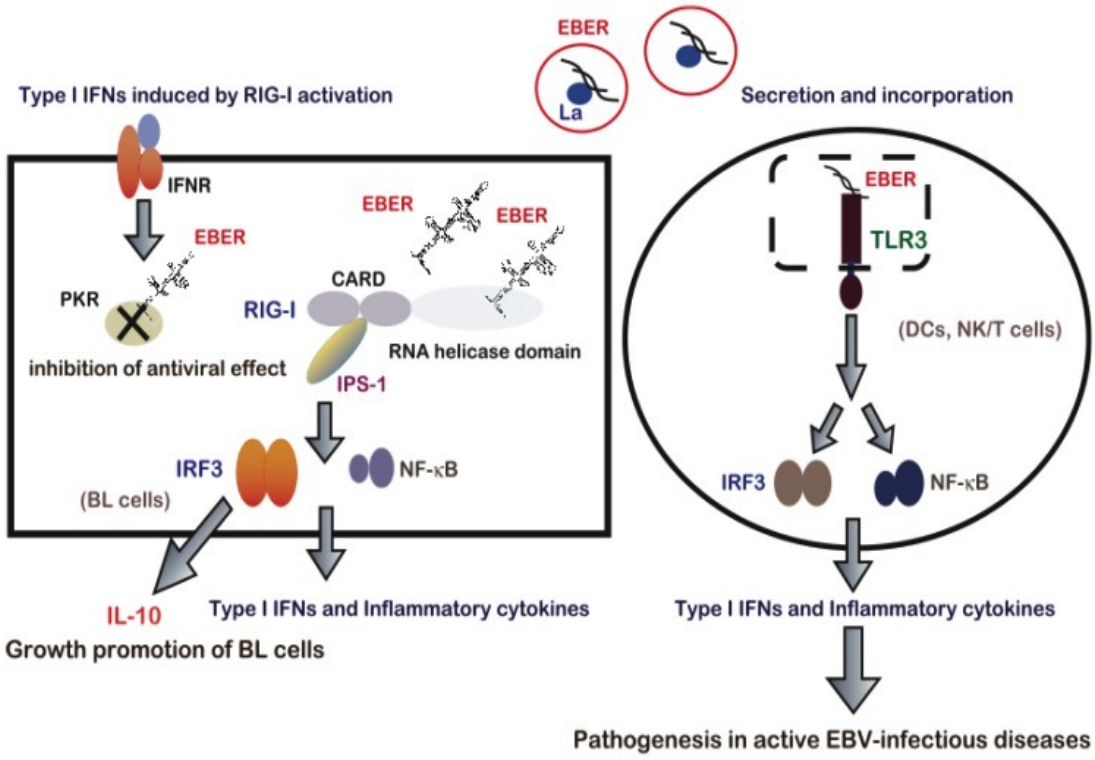

Figure. 1.8 EBER-mediated regulation of innate immune signaling contributes to EBV-mediated pathogenesis. Reproduced from Iwakiri *et al*. Left, in BL cells, EBERs are recognized by RIG-I via the RNA helicase domain of RIG-I. Following recognition, RIG-I associates with the adaptor IPS-1 protein via its CARD domain. IPS-1 initiates signaling that leads to the activation of IRF3 and NF-κB to induce type I IFNs and inflammatory cytokine expression. EBERs induce the expression of the growth-promoting cytokine IL-10 via RIG-I-mediated IRF3 activation and might support BL development. EBERs also bind to IFN-inducible PKR and block its activity, which is required for the IFN-mediated antiviral effect. Right, activation of innate immunity via TLR3 signaling in response to secreted EBER. During an active EBV-infection, EBER1 is released from EBV-infected lymphocytes mainly in a complex with La. Circulating EBER induces DC maturation via TLR3 signaling and induces type I IFN and inflammatory cytokine production by activating IRF3 and NF-κB. DC activation leads to T cell activation and systemic cytokine release. Furthermore, TLR3-expressing T and NK cells including EBV-infected T or NK cells could be activated by EBER1 through TLR3, thus leading to inflammatory cytokine production. Therefore, immunopathologic diseases caused by active EBV infections including T or NK cell activation and hypercytokinemia, could be attributed to EBER1-induced TLR3-mediated T cell activation and cytokinemia. IPS-1, interferon-β promoter stimulator-1; CARD, caspase recruitment domain; RIG-I, retinoic acid-inducible gene I; DC, dendritic cell; IFN, interferon; NK cell, natural killer cell; IL, interleukin; TLR, Toll-like receptor; PKR, RNA-dependent protein kinase; IRF 3, interferon regulatory factor 3.

Toll-like receptors (TLRs) comprise a distinct family of PRRs that sense virus-derived nucleic acids and trigger antiviral innate immune responses by activating signaling cascades via Toll/IL-1 receptor (TIR) domain-containing adaptors (Akira and Takeda, 2004). The role of TLR3 in the dsRNA recognition was demonstrated in a study of TLR3-deficient mice (Alexopoulou et al., 2001). DsRNA-induced signal transduction via TLR3 leads to the recruitment of TIR domain-containing adaptor inducing IFN-β (TRIF) and the subsequent phosphorylation of downstream molecules such as IRF3 and NF-κB (Meylan and Tschopp, 2006). Iwakiri *et al.* demonstrated

that EBERs are released in the extracellular environment and are recognized by TLR3, leading to the induction of type I IFN and inflammatory cytokines. The majority of the released EBER1 exists as a complex with La, suggesting that EBER1 is released from the cells via the active secretion of La. EBV causes infectious diseases such as infectious mononucleosis (IM), chronic active EBV infection (CAEBV) and EBV-associated hemophagocytic lymphohistiocytosis (EBV-HLH). IM is characterized by the expansion of reactive T-cells and is most likely an immunopathologic disease, in which the general symptoms are caused by inflammatory cytokines (Rickinson, 2007). CAEBV and EBV-HLH are active EBV infections with persistent or recurrent IM-like symptoms. EBV-HLH is characterized by an EBV infection of CD4-positive T cells or natural killer (NK) cells and the systemic release of inflammatory cytokines, leading to blood cell hemophagocytosis via activation of macrophages (Kasahara et al., 2001; Kikuta et al., 1993). On the other hand, in CAEBV, $CD8^+$-T cells are primary EBV infection targets (Kasahara et al., 2001). Iwakiri *et al.* demonstrated that sera from patients with IM, CAEBV and EBV-HLH contained EBER1. A further analysis revealed that serum EBER1 activates TLR3 signaling in immune cells, including dendritic cells, suggesting that EBER1, which is released from EBV-infected cells, is responsible for EBV-mediated immune activation, and induction of type I IFN and inflammatory cytokines (Iwakiri et al., 2009). Because $CD8^+$-T cells and NK cells express TLR3 and can be activated by TLR3 signaling (Schmidt et al., 2004; Tabiasco et al., 2006), TLR3-expressing T and NK cells could potentially be activated by EBER1 through TLR3 to produce inflammatory cytokines. Therefore, EBER1-induced activation of innate immunity would account for the immunopathologic diseases caused by an active EBV infection. A more recent study of a humanized mice model of an EBV-infectious disease

detected EBER1 in the serum, thus suggesting that EBER1 contribute to the disease pathology (Sato et al., 2011). In summary, EBERs contribute to EBV infection-related pathogenesis, including cancer and active infectious diseases, through interactions with RIG-I and TLR3 (Iwakiri and Takada, 2010).

1.3.7 Oncogenic role of EBERs

EBERs have been reported to contribute to the malignant phenotype of BL cells. Transfection of EBER genes into EBV-negative BL-derived Akata clones can restore the cell growth capacity in soft agar, promote tumor formation in severe combined immunodeficiency (SCID) mice, confer resistance to apoptotic inducers, and also upregulate the expression of anti-apoptotic bcl-2 protein that could protect Akata cells from c-Myc induced apoptosis (Komano et al., 1999; Ruf et al., 2000). Previous results have confirmed that EBERs can induce various cytokines expression. EBERs induce human IL-10 expression in BL cells (Kitagawa et al., 2000)(Kitagawa et al., 2000). Moreover, IL-10 is consistently expressed in EBV-positive but not in EBV-negative BL biopsies. Further analysis showed that IL-10 acts as an autocrine growth factor for BL cells, suggesting that EBERs play a role in BL development via IL-10 induction (Kitagawa et al., 2000). Additionally, EBERs were reported to contribute to the induction of IL-9, which also acts as an autocrine growth factor for T cell proliferation, suggesting that EBERs affect the development of EBV-associated T cell lymphoma (Yang et al., 2004). Furthermore, the EBERs have been demonstrated to contribute to the growth and proliferation of epithelial cell lines derived from NPC and GC. Iwakiri *et al.* demonstrated that EBERs could induce the expression of IGF1, which acts as an autocrine growth factor for NPC and GC cells. Further, IGF1 was expressed at high levels in EBV-positive but not in EBV-negative NPC or GC biopsies, indicating that EBERs promote epithelial carcinogenesis by the induction of

IGF1 expression (Iwakiri et al., 2003; Iwakiri et al., 2005). To determine the role of EBERs in the EBV-induced B cell growth program, recombinant EBV strains lacking EBERs have been engineered and introduced into host B-lymphocytes. However, conflicting observations regarding possible effects on B cell growth and transformation have been reported. An early study demonstrated that EBERs played no key role in infection with the EBV P3HR-1 strain, viral replication, or B-lymphocyte growth transformation (Swaminathan et al., 1991). However, another study reported that the 50% transforming dose of an EBER-deleted Akata virus was approximately 100-fold lower than that of the EBER-positive wild type EBV (Yajima et al., 2005); Subsequently, EBER2 was found to make positive contributions to an efficient LCL growth transformation via the induction of IL-6 expression (Wu et al., 2007). More recently, EBER deletion was reported to have no effect on LCL growth transformation efficiency of the B95-8 EBV strain (Gregorovic et al., 2011). It is important to note that all these results were obtained with different EBV strains. Thus, these discrepancies might be due to differences in the EBV strain background used in these experiments. We investigated the role of EBERs in the EBV strain M81 that was derived from NPC. Owing to the ability of M81 to induce spontaneous lytic virus replication, this model allows the study of the role of EBV-encoded small RNAs (EBERs) during this process.

The EBERs were previously shown to be dispensable for lytic replication (Swaminathan et al., 1991), suggesting that they exert their functions during latency. Furthermore, deletion of EBER1 or EBER2 individually in EBV B95-8 correlates with specific gene expression changes in LCLs. The EBER-related genes play important roles in membrane signaling, regulation of apoptosis, and interferon responses (Gregorovic et al., 2011). Consistent with these data, the EBERs can

protect EBV-infected BL cells from interferon alpha-induced apoptosis (Nanbo et al., 2002; Ruf et al., 2005).

Further insights into EBER function may come from the unique secondary structures adopted by these two RNAs, that can facilitate interactions with host proteins. A number of cellular proteins are known to interact with the EBERs to form ribonucleoprotein complexes as described above. EBER2 may provide additional structured RNA elements for binding to other as yet undefined host factors. Indeed, new studies demonstrate interactions between EBER2, the EBV terminal repeats, and the B cell transcription factor PAX5 that can mediate LMP expression (Lee et al., 2015). More recently, Zhao et al. analyzed a large number of samples from Northern China, a non-NPC endemic area and found that the distribution of EBER subtypes in lymphoma samples was similar to that in EBV-associated gastric carcinoma (EBVaGC) and throat washing (TW) from healthy donors, but was significantly different from that of NPC, suggesting that the NPC carry its unique EBERs which might have different functions. The distributions of EBER subtypes in samples used in this study are shown in Table. 1.5 and the location of EBER2 polymorphism is shown in Table. 1.6 **(**Zhao et al., 2017**)**.

Table. 1.5 Distribution of EBER subtypes in lymphoma, NPC, EBVaGC and TW

EBER subtype	Lymphoma (n = 101)	NPCs (n = 95)	EBVaGC (n = 50)	TWs (n = 92)
EB-6m	96 (95.0%)	56 (58.9%)	48 (96.0%)	89 (96.7%)
EB-8m	1 (1.0%)	32 (33.7%)	1 (2.0%)	1 (1.1%)
EB-10m	0	4 (4.2%)	0	0
UG	4 (4.0%)	3 (3.2%)	1 (2.0%)	2 (2.2%)

Data of NPC, EBVaGC and TW were cited from our previous study [26, 27]

NPC: nasopharyngeal carcinoma, EBVaGC: EBV-associated gastric carcinoma, TW: throat washings from healthy donor

Table. 1.6 Location of the EBERs polymorphism

		Intergenic region between EBER1 and EBER2						EBER2					
EBER subtype	position	-148	-90	-73	-71	-45	-12	44	46	57	61	93	168
B95-8		T	G	G	T	A	G	T	A	A	A	A	A
EB-6m		**A**	G	**A**	**G**	**G**	**A**	T	A	A	A	A	**G**
EB-8m		A	A	G	T	A	G	G	T	G	T	C	G

Numbers in the second row correspond to the nucleotide positions, under which the prototypic (B95-8) nucleotide sequence is listed. Here we use "+1" to represent the first nucleotide position of the EBER2 transcript. In the upstream of the EBER2 transcript, we use negative values to define the nucleotide position as shown before.

1.4 Animal study

EBV can only infect human and primates. EBV cannot infect commonly used rodent species at all. This makes the *in vivo* study of EBV very difficult. In this study, we inject virus infected fresh B cells intraperitoneally into NSG mice (*NOD.Cg-Prkdc*^{scid}*Il2rg*^{tm1Wjl}*/SzJ*; NSG). This mouse model simulates the post-transplant lymphoproliferative disease (PTLD) in patients infected with EBV. In most cases, PTLD is associated with Epstein-Barr virus (EBV) infection of B cells, either as a consequence of reactivation of the virus post-transplantation or from primary EBV infection. The majority of the PTLD patients display a deficiency in the immune system.

1.5 Aim of the thesis

The EBV EBERs have been shown to play an important role during the viral life cycle. However, the literature contains conflicting results about their functions and their contribution to tumorigenesis. These discrepancies could be due to the use of different EBV strains that carry polymorphism in the EBERs.

Therefore, the aim of my thesis was:

- To construct recombinant viruses from two different EBV strains B95-8 and M81 that lack the EBERs.
- To understand the contribution of the EBERs in these two different viruses.
- To unravel the role of polymorphisms in the function of EBERs.

2 Materials and Methods

2.1 Materials

2.1.1 Eukaryotic cells

Name	Description
HEK293	A specific cell line originally derived from human embryonic kidney cells
B lymphocytes	Primary B cells isolated from blood samples
WI38	Primary human lung embryonic fibroblasts

2.1.2 Primary cells

Name	Description
Peripheral blood CD19+ cells	Isolated from fresh buffy coats by Ficoll density gradient followed by selection with anti-CD19 PanB Dynabeads and detachment of the beads (Invitrogen)
Primary epithelial cells	Isolated from normal sphenoidal sinus biopsy material
License to use human primary cells	The Ethics Committee of the Universtiy of Heidelberg approved the study (approval 392/2005)

2.1.3 Cell culture media

Name	Source of supply
RPMI 1640	Invitrogen
DMEM	Life Technologies
Fetal calf serum (FCS)	Biochrom AG

2.1.4 Plasmids

2.1.4.1 Vector plasmid

Name	Source of supply, description
pcDNA3.1	This expression plasmid contains a CMV promoter.
pRK5	This expression plasmid also contains a CMV promoter.
B1249	B1249 (empty plasmid) contains a minimal CMV promoter controlled by a bidirectional Tet operator, a tetracycline transactivator protein (Tet-On) driven by a chicken beta-actin promoter with CMV enhancer (CAGp). One site of this bidirectional promoter contains the human neuron groewth factor receptor gene (NGFR) with a truncated cytoplasmic tail and GFP (Bornkamm et al., 2005). The other site is available for cloning. This plasmid also contains the latent EBV origin of replication (OriP) derived from B95-8 genome, and a rat CD2 gene derived by the hPGK promoter.

2.1.4.2 Expression plasmids

Name	Vector	Description
p509	pRK5	BZLF1 gene derived from B95-8 controled by a CMV promoter
pRA	pRK5	BALF4 (=gp110=gB) gene derived from B95-8, This plasmid will be co-transfected with BZLF1 to increase the B cells infectivity
B1460	B1249	Co-expression of NGFR gene and EBER1 and EBER2 (4 copies) derived from M81; controlled by a tetracycline inducible promoter
B1510	B1249	Co-expression of NGFR gene and EBER1 and EBER2 (4 copies) derived from B95-8; controlled by a tetracycline inducible promoter

2.1.5 Recombinant EBVs (rEBV; EBV-BAC)

Name	EBV strains/Backbone	Source of supply, description
B240	M81	M81 strain wild type
B996	M81/B240	M81 strain wild type EBER1 deletion
B997	M81/B240	M81 strain wild type EBER2 deletion
B963	M81/B240	M81 strain wild type both EBER1 and EBER2 deletion
B893	M81/B240	Revertant of M81 strain wild type both EBER1 and EBER2 deletion
B1468	M81/B240	M81 strain wild type that carry both EBER1 and EBER2 from B95-8
B95-8	B95-8/2089	B95-8 strain wild type
B222	B95-8/2089	B95-8 strain wild type both EBER1 and EBER2 deletion
B1465	B95-8/2089	B95-8 strain wild type that carry both EBER1 and EBER2 from M81

2.1.6 Plasmids used for constructing recombinant EBV

Name	Purpose	Description
pCP15	Template of kanamycin	This vector carries a region of homology with the EBV genome in which the kanamycin cassette can be inserted
pCP16	Template of tetracycline	This vector carries a region of homology with the EBV genome in which the tetracycline cassette can be inserted
pKD46	Red recombinase expression	This vector contains an Arabinose-inducible Red recombinase, which is used for homologous recombination in *E.coli*.
pCP20	Encoding the FLP recombinase	This plasmid shows temperature sensitive replication and thermal induction of FLP synthesis.

2.1.7 Antibodies

Name	Clone	Usage	Origin	Source of supply
Anti-alpha-actin	ACTN05, C4	WB	Mouse, momoclonal	Dianova
Anti-mouse lgG (HRP, secondary antibody)		WB	Goat	Promega
Anti-rabbit lgG (HRP, secondary antibody)		WB	Goat	Cell Signaling
Anti-rat lgG (HRP, secondary antibody)		WB	Goat	Dianova
EBNA1	IH4	WB	Rat	Hybridoma supernatant
EBNA2	PE2	WB, IHC	Mouse	Hybridoma supernatant
EBNA3A	4A5	WB	Rat	Hybridoma supernatant
EBNA3B	6C9	WB	Rat	Hybridoma supernatant
EBNA3C	A10	WB	Rat	Hybridoma supernatant
LMP1	CS1-4	WB, IHC	Mouse	Hybridoma supernatant
LMP2A	4E11	WB	Rat	2089 LCL
BZLF1	BZ.1	WB, IHC	Mouse	Hybridoma supernatant
gp350	72A1	IF	Mouse	Hybridoma supernatant
NGFR		IF, cell isolation	Mouse	
CD63	MX-49.129.5,	WB	Mouse	Santa Cruz

2.1.8 Enzymes

Name	Company	Usage
Phusion High-Fidelity DANN polymerase	Thermo Scienfitic	PCR for cloning

Restriction Enzymes	Fermentas, New England Biolabs	Check genomic interity of EBV-BAC
Alkaline Phosphatase	Roche	Cloning
Klenow Enzyme	Roche	Cloning
T4 DNA Polymerase	Fermentas	Cloning
RNase A	Roche	Mini/Midi-pepe
Lysozyme	Serva	mini-prep
DNaseI	Fermentas	qPCR
Proteinase K	Roche	Viral titer measurement
AMV Reverse Transcriptase	Roche	qPCR
RNAse inhibitor	Roche	qPCR
T4 DNA Ligase	Fermentas	Cloning
Taqman Universal Master Mix	Life technologies	qPCR

2.1.9 Commercial Kits

Name	Company	Usage in this study
Dneasy blood&Tissue kit	Qiagen	Isolation of total DANN from cells
Dynabeads CD19 PanB	Invitrogen	Human primary B cells isolation
Dynabeads Goat anti mouse lgG	Invitrogen	Cell isolation
Hygromycin B	Invitrogen	Stable cell selection
MicroRNA reverse transcript	Applied Biosystems	RT-PCR
RNU48	Applied Biosystems	Internal controls for miRNA RT-qPCR
Nucleobond BAC100	Macherer-Nagel	EBV-BAC preparation
Jestar 2.0 Plasmid Midi Kit	Genomed	High quality DNA Preparation
hGAPDH endogeous	Applied Biosystems	Internal controls for RT-

control		qPCR
Human IL-8 (CXCL8) ELISA development kit	Mabtech	CXCL8 measurement
Total Exosome Isolation (from cell culture media)	Invitrogen	Exosomes isolation

2.1.10 Equipment

Name	Source of supply
Amersham HyperfilmTM ECL	Stratagene
Amersham membrane HybondTM ECL	GE Healthcare Life Sciences
Applied Biosystems 7300 Real-time PCR	UVP
D-Tube Dialyzer Midi, cutoff 3.5kDa	Merck Millipore
G25 Microspin columns	Thermo Scientific
Magnetic rack	Applied Biosystems
Nanodrop	GE Healthcare Life Sciences

2.1.11 Chemicals and Reagents

Name	Source of supply
RNase inhibitor (RNasin)	Promega
Protease inhibitor cocktail	Roche
Acrylamide: 30% stock, with 0-8% bisacrylamide	Roche
Page Ruler Prestained Protein Ladder	Fermentas
1 kb DNA Ladder	Life Technologies
Taqman microRNA Reverse Transcription Kit	Applied Biosystems
TRIzol reagent	Life Technologies
Chloroform	Sigma aldrich
Phenol/Chloroform/Isoamylalcohol	Roth
Roti-Phenol	Roth

RNase free water	Invitrogen
3 M sodium acetate, pH 5.5, Rnase free	Invitrogen
GlycoBlue	Invitrogen
Isopropanol	Sigma aldrich
Ethidium bromide	Life Technologies
dNTP mix (10mM)	Invitrogen
Metafectene	Biontex Laboratories
6x DNA loading dye	Thermo Scientific

2.1.12 Buffers and solutions

Buffer	Composition
Antigen binding and washing	PBS+0.1% Tween 20
Citrate-phosphate buffer	4.7g/L citric acid, 9.2g/L Na2HPO4, pH 5.0
SDS loading buffer	100mM Tris-HCl pH=6.8, 4% (w/v) SDS (electrophoresis grade), 0.2% (w/v) bromphenol blue, 20% (v/v) glycerol, 200mM ß-merapto-Ethonal
5x RIPA lysis buffer	750mM NaCl, 2.5% NP40, 5% Sodium Deoxycholat, 0.5% SDS, 25mM EDTA, 100mM Tris HCl pH=7.5
DNA gel extraction buffer	300mM NaCl, 10mM Tris (pH 8.0), 1mM EDTA
Stacking gel buffer	2M Tris pH 6.8
Seperating gel buffer	2M Tris pH 8.9
10x SDS running buffer	250mM Tris, 1.92M glycine, 1% SDS, pH 8.5-8.8
2x SDS loading buffer	100mM Tris-HCl pH=6.8, 4% (w/v) SDS (electrophoresis grade), 0.2% (w/v) bromphenol blue, 20% (v/v) glycerol, 200mM ß-merapto-Ethonal
1x bloting buffer	25mM Tris, 150mM glycine, 10% MetOH
10x PBST	1.37M Nacl, 27mM KCl, 100mM Na2HPO4, 20mM KH2PO4, 1% Tween 20

3% low fat milk	3% low-fat milk power in 1xPBST
ECL reagents	Enhanced Luminol Reagent and Oxidizing Reagent, store at 4°C
PBS	137mM Nacl, 2.7mM KCl, 10mM Na2HPO4, 2mM KH2PO4, pH 7.4
PBS-T	0.1% Tween-20 in PBS
TAE	40mM Tris, 1mM EDTA, 19mM acetic acid
TBE	100mM Tris, 90mM boric acid, 1mM EDTA
Lysis buffer (circle prep)	1% SDS, 2mM EDTA, 50mM NaCl, 40mM NaOH
DNA loading buffer	0.25% Bromphenolblue, 40% (w/v) Sucrose, dissolved in H_2O
TE	10mM Tris.HCl, 1mM EDTA (pH 8.0)
LB medium	(2:1:2) Tryptone, Yeast extract, NaCl in H2O pH7.0
LB agar	15g Bacto-Agar in 1L LB mudium
4% PFA	4% Paraformaldehyde in PBS (pH 7.4)
Staining buffer (IF)	10% Heat-inactivated goat serum in PBS
Mounting buffer (IF)	90& Glycerol in PBS

2.1.13 Oligonucleotides

Oligonucleotides were synthesized by Eurofins, if not indicated otherwise. All oligonucleotides uses in this study and their sequences are listed below.

Name	Sequence	Aim
EBER1 fwd	5'-gtcttgaggagatgtagacttgtagacactgcaaaacctcaacagctatgaccatgattacgcc-3'	M81/ΔE1 cloning
EBER1 rev	5'-ggataatggatgcataaatcctaaaacaaaagtttggatcccagtcacgacgttgtaaaacgac-3'	
EBER2 fwd	5'-tttaccagcatgtatagagttacggttcgctacatcaaacaacagctatgaccatgattacgcc-3'	M81/ΔE2 cloning
EBER2 rev	5'-tttaccagcatgtatagagttacggttcgctacatcaaacaacagctatgaccatgattacgcc-3'	

EBER1+2 fwd	5'-gtcttgaggagatgtagacttgtagacactgcaaaacctcaacagctatgaccatgattacgcc-3'	M81/ΔE1+2 cloning
EBER1+2 rev	5'-tttaccagcatgtatagagttacggttcgctacatcaaacaacagctatgaccatgattacgcc-3'	
EBER1+2 fwd	5'-gtcttgaggagatgtagacttgtagacactgcaaaacctcaacagctatgaccatgattacgcc-3'	B95-8/ΔE1+2 cloning
EBER1+2 rev	5'-tttaccagcatgtatagagttacggttcgctacatcaaacaacagctatgaccatgattacgcc-3'	
EBERseq_fwd	5'-acacaccaactatagcaaacc-3'	Cloning of the M81/ΔE1+2 revertant
EBERseq_rev	5'-ttttgtgttgtaggggtagc-3'	
EBER SceI EP fwd	5'-tttcatcctcaggacctacgctgccctagaggttttgctagggaggcttcaagatccccgatctatgattccc-3'	Cloning of the ΔE1+2 revertant -put I-sceI enzyme restriction sites
EBER SceI EP rev	5'-tttcatcctgaggtagggataacagggtaatcagagcgcttttgaagctccag-3'	
EBER1 probe	5'FAM-aggacggtgtctgtggttgt-3'TAMRA	RT-qPCR for Taqman
EBER1 fwd	5'-acgctgccctagaggttttg-3'	
EBER1 rev	5'-gcagaaagcagagtctggga-3'	
EBER2 probe	5'FAM-tcccgcctagagcatttgcaa-3'TAMRA	RT-qPCR for Taqman
EBER2 fwd	5'-gttgccctagtggtttcgga-3'	
EBER2 rev	5'-gccgaataccttctcccag-3'	
M81.EBNA2 probe	5'FAM-cccaaccacaggttcaggcaaaacttt-3'TAMRA	RT-qPCR for Taqman
M81.EBNA2 fwd	5'-gcttagccagtaacccagcact-3'	
M81.EBNA2 rev	5'-tgcttagaaggttgttggcatg-3'	
M81.LMP1 probe	5'FAM-tgctgttcatctttggctgc-3'TAMRA	RT-qPCR for Taqman
M81.LMP1 fwd	5'-cacggacaggcattgtacct-3'	
M81.LMP1 rev	5'-ggatgaaggccaaaagctgc-3'	
M81.LMP2A probe	5'FAM-cagtatgcctgcctgtaattgttgcgc-3'TAMRA	RT-qPCR for Taqman
M81.LMP2A fwd	5'-cgggatgactcatctcaacacata-3'	
M81.LMP2A rev	5'-ggcgctgacaacggtactaact-3'	
M81.LMP2B probe	5'FAM-cagtatgcctgcctgtaattgttgcgc-3'TAMRA	RT-qPCR for Taqman
M81.LMP2B fwd	5'-cgggaggctgtgcttta-3'	

M81.LMP2B rev	5'-ggcgctgacaacggtactaact-3'	
B95-8.LMP1 probe	5'FAM-tccagatacctaagacaagtaagcacccgaagat-3'TAMRA	RT-qPCR for Taqman
B95-8.LMP1 fwd	5'-gcacggacaggcattgttc-3'	
B95-8.LMP1 rev	5'-aaggccaaaagctgccagat-3'	
B95-8.LMP2A probe	5'FAM-cagtatgcctgcctgtaattgttgcgc-3'TAMRA	RT-qPCR for Taqman
B95-8.LMP2A fwd	5'-cgggatgactcatctcaacacata-3'	
B95-8.LMP2A rev	5'-ggcggtcacaacggtactaact-3'	
B95-8.LMP2B probe	5'FAM-cagtatgcctgcctgtaattgttgcgc-3'TAMRA	RT-qPCR for Taqman
B95-8.LMP2B fwd	5'-cgggaggccgtgcttta-3'	
B95-8.LMP2B rev	5'-ggcggtcacaacggtactaact-3'	
RN7SK probe	5'FAM-gttgattcggctgatctggctg-3'TAMRA	RT-qPCR for Taqman
RN7SK fwd	5'-tctgtcaccccattgatcgc-3'	
RN7SK rev	5'-ttggaggttctagcagggga-3'	
EBV-pol fwd	5'-ctttggcgcggatcctc-3'	Quantification of viral titers
EBV-pol rev	5'-agtccttcttggctagtctgttgac-3'	
EBV-pol probe	5'FAM-catcaagaagctgctggcggcc-3'TAMRA	
BART 1-3p RT	5'-ctcaactggtgtcgtggagtcggcaattcagttgagagacatag-3'	Stem-loop RT-qPCR BART 1-3p Taqman PCR
BART 1-3p fwd	5'-acactccagctgggtagcaccgctatccac-3'	
BART 1-3p probe	5'FAM-ttcagttgagagacatag-3'TAMRA	
BART 1-3p rev	5'-ctcaactggtgtcgtggagtcggca-3'	
BART 7* RT	5'-ctcaactggtgtcgtggagtcggcaattcagttgagtgtttcat-3'	Stem-loop RT-qPCR BART 7* Taqman PCR
BART 7* fwd	5'-acactccagctgggcctggaccttgactat-3'	
BART 7* probe	5'FAM-ttcagttgagtgtttcat-3'TAMRA	
BART 7* rev	5'-ctcaactggtgtcgtggagtcggca-3'	
BART 2-5p RT	5'-ctcaactggtgtcgtggagtcggcaattcagttgaggcaagggc-3'	Stem-loop RT-qPCR BART 2-5p Taqman PCR
BART 2-5p fwd	5'-acactccagctgggtattttctgcattcgc-3'	
BART 2-5p probe	5'FAM-ttcagttgaggcaagggc-3'TAMRA	
BART 2-5p rev	5'-ctcaactggtgtcgtggagtcggca-3'	
BHRF 1-1 RT	5'-ctcaactggtgtcgtggagtcggcaattcagttgagaactccgg-3'	Stem-loop RT-

BHRF 1-1 fwd	5'-acactccagctgggtaacctgatcagcccc-3'	qPCR BHRF1 miR1 Taqman PCR
BHRF 1-1 probe	5'FAM-ttcagttgagaactccgg-3'TAMRA	
BHRF 1-1 rev	5'-ctcaactggtgtcgtggagtcggca-3'	
BHRF 1-2 RT	5'-ctcaactggtgtcgtggagtcggcaattcagttgagttcaattt-3'	Stem-loop RT-qPCR BHRF1 miR2 Taqman PCR
BHRF 1-2 fwd	5'-acactccagctgggtatcttttgcggcaga-3'	
BHRF 1-2 probe	5'FAM-ttcagttgagttcaattt-3'TAMRA	
BHRF 1-2 rev	5'-ctcaactggtgtcgtggagtcggca-3'	
BHRF 1-2* RT	5'-ctcaactggtgtcgtggagtcggcaattcagttgaggctatctg-3'	Stem-loop RT-qPCR BHRF1 miR2* Taqman PCR
BHRF 1-2* fwd	5'-acactccagctgggaaattctgttgcagca-3'	
BHRF 1-2* probe	5'FAM-ttcagttgaggctatctg-3'TAMRA	
BHRF 1-2* rev	5'-ctcaactggtgtcgtggagtcggca-3'	
BHRF 1-3 RT	5'-ctcaactggtgtcgtggagtcggcaattcagttgaggtgtgctt-3'	Stem-loop RT-qPCR BHRF1 miR3 Taqman PCR
BHRF 1-3 fwd	5'-acactccagctgggtaacgggaagtgtgta-3'	
BHRF 1-3 probe	5'FAM-ttcagttgaggtgtgctt-3'TAMRA	
BHRF 1-3 rev	5'-ctcaactggtgtcgtggagtcggca-3'	
M81.BZLF1 fwd	5'-acgacgtacaaggaaacc-3'	RT-qPCR for Taqman
M81.BZLF1 rev	5'-cttggcccggcattttct-3'	
M81.BZLF1 probe	5'FAM-gcattcctccagcgattctggctgta-3'TAMRA	
GADPH fwd	5'-caatgacccttcattgacc-3'	SYBR green RT-qPCR
GADPH rev	5'-tggaagatggtgatgggatt-3'	
CXCL8 fwd	5'-tctgcagctctgtgtgaagg-3'	
CXCL8 rev	5'-ttccttggggtccagacaga-3'	
T44G fwd	5'-ggacacaccgccaacgcgcagtgcggtgctaccgac-3'	EBER2 mutation in position 44
T44G G44T A46T T46A rev	5'-gaaaccactagggcaacggc-3'	
G44T fwd	5'-ggacacaccgccaacgctctgtgcggtgctgccgt-3'	
T44G G44T A46T T46A rev	5'-gaaaccactagggcaacggc-3'	
A46T fwd	5'-ggacacaccgccaacgctctgtgcggtgctaccgaccc-3'	EBER2 mutation in position 46
T44G G44T rev	5'-gaaaccactagggcaacggc-3'	
T46A fwd	5'-ggacacaccgccaacgcgcagtgcggtgctgccgtccc-3'	
T44G G44T rev	5'-gaaaccactagggcaacggc-3'	
A57G fwd	5'-caacgctcagtgcggtgctgccgacccgaggtcaagtc-3'	EBER2 mutation in position 57
A57G G57A rev	5'-gcggtgtgtccgaaaccac-3'	

G57A fwd	5'-caacgcgctgtgcggtgctaccgtcccgaggtcaagtc-3'	
A57G G57A rev	5'-gcggtgtgtccgaaaccac-3'	
A61T fwd	5'-tcagtgcggtgctaccgtcccgaggtcaagtcccg-3'	EBER2 mutation in position 61
A61T T61A rev	5'-gcgttggcggtgtgtcc-3'	
T61A fwd	5'-gctgtgcggtgctgccgacccgaggtcaagtcccg-3'	
A61T T61A rev	5'-gcgttggcggtgtgtcc-3'	
A93C fwd	5'-ccgggggaggagaagagcggcttcccgcctagagc-3'	EBER2 mutation in position 93
A93C rev	5'-gacttgacctcgggtcggtag-3'	
C93A fwd	5'-ccgggggaggagaagagaggcttcccgcctagagc-3'	
C93C rev	5'-gacttgacctcgggacggca-3'	
A168G fwd	5'-gggtattcggcttgtccgctgttttttacgcgttaagatacattgatgag-3'	EBER2 mutation in position 168
A168G G168A rev	5'-ttctcccagagggattagagaatcctg-3'	
G168A fwd	5'-gggtattcggcttgtccgctatttttacgcgttaagatacattgatgag-3'	
A168G G168A rev	5'-ttctcccagagggattagagaatcctg-3'	

2.2 Methods

2.2.1 Bacterial culture and transformation

2.2.1.1 Culture conditions

All *E.coli* strains were cultured in LB-medium by shaking or alternatively on LB-agar plates in order to obtain single colonies. Ampicillin (100 ug/ml), kanamycin (50 ug/ml) or chloramphenicol (15 ug/ml) were used to culture cells in LB-medium or LB-agar plates, depending on the antibiotic resistance genes cloned into the plasmids. Except special conditions, bacteria were cultured at 37°C. For long-term storage, 10 % glycerol was used to freeze cells at -80°C.

2.2.1.2 Transformation

The plasmids were introduced into bacteria by the heat shock method. In general, chemically competent cells (eg. DH5α) were mixed with plasmids or the ligation product on ice for 5 min. The mixture was then incubated at 42°C for 90 sec, immediately added to 900 ul of LB-medium and left in culture at 37°C for 45 min for recovery. After recovery, bacteria were spun down by centrifugation at 4800 rpm for 5 min and the pelleted cells were resuspended and cultured on LB-agar plate overnight to obtain single colony.

2.2.1.3 Electroporation

Electroporation was also used to transform plasmids into electroporation-competent bacteria that were made by a technician. In general, 25 ul of electroporation-competent DH10B cells pre-prepared in 10% glycerol were thawed slowly on ice from -80 °C. The thawed cells were mixed with DNA and this mixture was incubated

on ice for 5 min. The mixture was transferred into cuvettes and subjected to electroporation at 1.2 KV, 200 Ω, and 25 μFd. The bacteria were then immediately resuspended in 1 ml of LB-medium and cultured at 37°C for 1 h. Individual colony was obtained in the same way as the heat shock method.

2.2.2 Eukaryotic cells culture and transfection

2.2.2.1 Culture conditions

All eukaryotic cells were cultured at 37 °C in the incubator stably supplied with 100% humidity and 5% CO_2.

Cells that grow in suspension, including LCLs, were cultured in RPMI with 10% FBS. The cells were split 1 to 5 or 1 to 10 regularly, depending on their growth rate or state. 293 cells that grow adherently were cultured in RPMI with 10% FBS. Additional 100 μg/ml Hygromycin was used to culture 293 cells that stably transfected with the recombinant EBV. The 293 cells were split 1 to 10 by using 0.05% trypsin at 37°C for 2 min when they reach about 80% confluence. WI 38 feeder cells were cultured in the same condition except that 0.25% trypsin was used to split them.

2.2.2.2 293 cells transfection

The cells were seeded at a concentration of 3x 10^5 cells/well on a 6-well-plate in 2 ml RPMI with 10% FBS without any antibiotics one day before transfection. At day 2, the transfection mixture was prepared in the following procedure: 1 μg plasmid DNA was resuspended in 100 μl of RPMI w/o any additions and 3 μl of Metafectene was also resuspended with 100 μl of RPMI w/o any additions. These two mixtures were combined gently by carefully pipetting few times, and left for 25 min at room

temperature. The plasmid-Metafectene mixture was added dropwise into the cells, and the cells were incubated at 37°C overnight. At day 3**,** the medium of the transfected cells was carefully removed and replaced with 2 ml fresh medium RPMI with 10% FCS. The transfected cells can usually be analyzed 3 days post transfection.

2.2.2.3 LCLs transfection

We used Neon Transfection System to introduce plasmids into LCLs. The cells were washed with PBS without $Ca2^{+}$ and $Mg2^{+}$ three times and resuspended with buffer T, which is used for primary blood-derived suspension cells, at a final density of 2.0x 10^{7} cells/mL in a 1.5 mL tube. In parallel, an appropriate amount of plasmid DNA in deionized water at a concentration of 3-5 μg/μL was transferred into a 1.5 mL tube. The cells and plasmid DNA were combined gently by carefully pipetting few times. Then we performed the transfection following the manufacturer's instructions. The mixture was subjected to electroporation at 1.1 KV of pulse voltage, 30 ms of pulse width and 2 of pulse number. The transfected cells can usually be analyzed 3 days post transfection.

2.2.3 Construction of recombinant EBVs and related techniques

The wild type EBV strain M81 is available as a recombinant BACMID (Tsai et al., 2013). The viral genome was cloned onto a prokaryotic F-plasmid that carries the chloramphenicol (Cam) resistance gene, the gene for green fluorescent protein (GFP), and the Hygromycin resistance gene (B240). All PCR primers used for PCR cloning or chromosomal building are listed in the Table and are based on the M81 EBV sequence (GenBank accession number KF373730.1). Deletion of the EBER1 (deletion from nt 6632 to nt 6797) generated ΔE1; deletion of the EBER2 (deletion

from nt 6959 to nt 7128) gave rise to ΔE2. The double knockout EBER1 plus EBER2 (ΔE1+2) was obtained by a deletion from nt 6632 to nt 7128 including the intergenic sequences between EBER1 and EBER2. These mutations were achieved by homologous recombination of the recombinant virus with a linear DNA fragment that encodes the kanamycin resistance gene, flanked by Flp recombination sites, and short DNA regions homologous to the regions immediately outside of the deletion to be obtained, as described (Feederle et al., 2010). We applied the same strategy to the wild type B95-8 BAC to obtain a recombinant EBV that lacks EBER1 plus EBER2 (B95-8/ΔE1+2) with a deletion from nt 6630 to nt 7128 including the intergenic region between EBER1 and EBER2. We constructed a revertant of ΔE1+2 in M81 strain by using an En passant mutagenesis method. Here the complete EBER locus, from the EBER1 to EBER2, was cloned from the M81 BAC and reintroduced into the M81/ΔE1+2 BAC genome. In parallel, we applied the same En passant method to construct an exchange mutant that carries EBER locus of B95-8 in M81 strain. Here the complete EBER locus, from the EBER1 to EBER2, was cloned from the B95-8 BAC and reintroduced into the M81/ΔE1+2 BAC genome. In addition, we also applied the same En passant method to construct an exchange mutant that carries EBER locus of M81 in B95-8 EBV strain.

We introduced the rat CD2 gene under the control of an EA-D promoter into the BXLF1 gene of the M81 genome (nt 131044 to nt 133362) by homologous recombination using a linear vector that included the kanamycin resistance cassette as a selection marker. The disruption of BXLF1 gene does not interfere with the growth of LCLs (Kanda et al., 2004; Yoshiyama et al., 1995). Upon induction of the lytic replication, CD2 is expressed at the surface of replicating cells. CD2-positive cells can be pulled down with a specific monoclonal antibody (OX34) coupled with anti-

mouse IgG Dynabeads and submitted to protein or RNA extraction.

2.2.4 Generation of EBV/293 producer cells

To generate HEK293 producer cells stably transfected with EBV, 6 or 8 μg BACmid was transfected into 293 cells at a concentration of $3x10^5$ cells/well cultured in 6-well plate by using Metafectene following the manufacturer's instructions. Transfection efficiency could be checked under microscope 24 hours post transfection by observing the percentage of GFP positive cells. The cells were transferred into 15 cm culture dishes in the presence of 100 μg/ml Hygromycin B in order to select 293 cells stably transfected with the recombinant EBV. Selected single cell clones were transferred to 6 well-plate around 3 weeks post transfection. The cells were expanded and tested for virus production by transient transfection of a plasmid encoding BZLF1, a viral protein that trans-activates lytic EBV replication. The BZLF1 transfected clones were stained with antibody against gp350, the major viral glycoprotein 3,5 days post transfection. The supernatants of clones with a high signal of gp350 staining after BZLF1 transfection was measured by qPCR to determine the viral titer. The clones, which display the highest viral titer, were tested by circle preparation to determine their genome integrity in 293 producer cells (Lin et al., 2015).

2.2.5 Virus production

After establishment of viral producer cell lines, these cells were continuously maintained with 100 μg/ml Hygromycin B selection in order to keep EBV BAC inside the cells in the long term. The 293 producer cell lines were lytically induced by transfection of a BZLF1 expression plasmid together with a BALF4 expression plasmid.

The medium of the transfected cells was carefully removed 16 hours post transfection and replaced with fresh medium RPMI with 10% FCS. Virus supernatant was harvested at 3.5 days post transfection, filtered with 0.45 μm cellulose filter and stored at 4 °C (Lin et al., 2015).

2.2.6 Viral titers measurement by qPCR

The viral genome copy number was determined by qPCR measurement. 50 μl of supernatants were firstly treated with 5 unit DNAseI at 37 °C for 1 h to completely remove free viral DNA in supernatants and DNAseI was then inactivated at 70 °C for 10 min. In this way, the viral DNA inside the viral particles was not digested by DNAseI due to the protection from viral envelope. The viral envelope was then digested by proteinase K in order to release the vial genome for qPCR analysis. 5 μl of DNAseI treated supernatants were incubated with 5 μl of proteinase K (100 μg/ml) for 1 h at 50 °C. Proteinase K was destroyed at 75 °C for 20 min. The qPCR master mix with primers and probe specific for the viral DNA polymerase BALF5 gene was prepared, mixed with the proteinase K treated supernatants and amplified by real time PCR using a StepOnePlus device.

An example is given below for a 25 μl reaction containing the following components:

12.5 μL	Taqman 2x Universal Mastermix
2.5 μL	EBV Pol for primer (10 μM)
2.5 μL	EBV Pol rev primer (10 μM)
1.0 μL	FAM-labeled EBV Pol probe (20 μM)
1.5 μL	water
+5.0 μL	Proteinase K treated samples
25 μL in total	

The qPCR was run with the following settings:

50 °C for 2 min (initial denaturation)

95 °C for 10 min (denaturation)

40 cycles:
95 °C for 15 s
60 °C for 1 min

The qPCR results were analyzed to get an abosulate copy number of EBV genomes per ml of viral supernatants by using a standard curve (This protocol is modified from the shared folder from F100, DKFZ).

2.2.7 Confirmation of the genome integrity of rEBV in the stably transfected 293 cells by analyzing the rescued circular BACmid (circle prep)

20 millions of 293 cells were washed in PBS for two times and lysed with circle prep lysis buffer at room temperature for exactly 5 min. 500 µl of 1 M Tris-HCl, pH 7.1 were added into the solution dropwise to neutralize the pH of the lysate. 2 ml of 3 M NaCl were then added. Proteins in the lysate were incubated with proteinase K (10mg/ml) at 50 °C for 2 h or at 37°C overnight. In order to get a high quality circular DNA, a phenol/butanol extraction method was performed. DNA was precipated with 2.5 volume of absolute ethonal for 1 h at -20 °C or overnight. DNA was pelleted down at 5.000 rpm for 30 min at romm temperature. DNA was washed with 70% ethonal twice and was dissolved in 50 µl TE. The TE-dissolved BAC DNA was transformed into *E.coli* DH10B and the BACmid from at least 5 cam-resistant colonies were prepared and subjected to digestion with the BamHI enzyme. The genome integrity of these rEBV in the stably transfected cells was confirmed by using the parental rEBV as a control (This protocol is modified from the shared folder from F100, DKFZ).

2.2.8 Virus infections

Purified CD19+ human B cells from peripheral blood were exposed to viral supernatant with various multiplicity of infection (MOI), determined by qPCR, for two hours, then washed once with PBS and cultured with RPMI supplemented with 20% FBS in the absence of immunosuppressive drugs. For transformation assays, the percentages of EBNA2-positive cells in the infected B cells were evaluated by immunostaining with a specific antibody at 3 days post-infection (dpi). Cell numbers containing 3 or 10 EBNA2-positive cells per well were seeded into 48 wells of 96-U-well plates that contained 10^3 gamma-irradiated WI38 feeder cells. Non-infected B cells were used as a negative control. The outgrowth of LCLs was monitored at 30 dpi (Lin et al., 2015).

2.2.9 ImmunofIuorescence staining

The cells were fixed with 4% paraformaldehyde in PBS for 20 min at room temperature. Fixed cells were permeabilized in PBS 0.5% Triton X-100 for 2 min except for samples stained with an antibody specific for the viral glycoprotein gp350. Cells were incubated with the first antibody for 30 min at 37°C, washed in PBS three times, and incubated with a secondary antibody conjugated to Cy-3 for 30 min at 37°C. The stained slides were embedded in 90% glycerol and stored at 4°C. Pictures were taken with a camera attached to a fluorescence microscope (Leica) (This protocol is modified from the shared folder from F100, DKFZ).

2.2.10 RNA extraction

Total RNA was extracted from LCLs generated with multiple M81 EBV or M81 mutant or control strains. RNA extracted from HEK293 cells was used as a negative control for the data analysis.

RNA was isolated from each sample by using a TRIzol reagent. Cells pellet was lyzed with 1 ml TRIzol and extracted with 0.2 ml CHCl3. TRIzol lysate was shaked

vigorously for at least 30 s at room temperature and then was incubated for 2 mins. Samples were centrifuged at 4 °C, at 12000 g, for 15 mins (cold room). The upper colorless aqueous phase was carefully transferred into a new tube that containing 500 µl of 2-Propanol (iso-PrOH). Carefully mix by inverting the centrifuge tube and RNA was precipated at -20 °C for at least 20 mins. RNA was pelleted at 4°C, at 12000 g, for 10 mins (cold room). The supernatant was removed and the pellet was washed with 75% Ethanol (EtOH; prepared with nuclease-free water) and centrifuged at 4°C, at 8000 g, for 5 mins (cold room). The RNA pellet was resuspended in 40 µl of pre-heated nuclease-free water (95 °C). To dissolve the RNA pellet completely, the samples were incubated at 60°C for 10 mins with vortex. RNA concentration was determined at OD260 nm in a nandrop photospectrometer. RNA was stored at -80°C (This protocol is modified from the shared folder from F100, DKFZ).

2.2.11 Real-time qPCR

Total RNA isolated from LCLs were reverse transcribed with AMV-reverse transcriptase (Roche) using a mix of random hexamers. 200 ng total RNA was used for reverse transcription.

An example is given below for a 20 µl reaction containing the following components:

4 µl	5x RT buffer
2 µl	**2**mM dNTPs
2 µl	random hexamers
4 µl	MgCl2
0.8 µl	AMV reverse transcriptase
1 µl	RNA inhibitor
1.2 µl	water
15 µl in total	Mix

5 µl of RNA sample was added to the master mix and incubated on ice for 5 minutes.

The RT reaction was running following program:

25 ˚C	10 min
42 ˚C	60 min
90˚C	5 min
4˚C	hold

Store final cDNA at –20 ˚C until required. Add 80 ul water and use 5ul per RT-PCR reaction.

An example is given below for a 25 µl reaction containing the following components:

12.5 µL	Taqman 2x Universal Mastermix
6 µL	Primer/Probe mix
0.5 µL	hGAPDH
1 µL	water
+5.0 µL	cDNA sample
25 µL in total	

The qPCR was run with the following settings:

50 °C for 2 min (initial denaturation)
95 °C for 10 min (denaturation)
40 cycles:
95 °C for 15 s
60 °C for 1 min

The qPCR results were analyzed by using $2^{-\Delta\Delta Ct}$ method to get a relative expression levels (This protocol is modified from the shared folder from F100, DKFZ).

2.2.12 Real-time RT-qPCR to quantify EBV transcripts

RNA extracted with Trizol from LCLs was reverse transcribed with AMV-reverse transcriptase (Roche) using a mix of random primers. The primers and probes used to detect EBER, BZLF1, EBNA2, LMP1, LMP2A, and LMP2B are listed in the table. The PCR and data analysis was carried out using the universal thermal cycling protocol on an ABI STEP ONE PLUS Sequence Detection System (Applied Biosystems). All samples were run in duplicates, together with primers specific to the human GAPDH gene to normalize for variations in cDNA recovery (This protocol is modified from the shared folder from F100, DKFZ).

2.2.13 Determination of EBER half-time

We treated LCLs transformed by M81 or B95-8 wild type by adding RNA polymerase III inhibitor ML-60218 (100 μM, Sigma Aldrich) to the culture medium. Cells were collected at different treatment time and submitted to RT-qPCR (Wu et al., 2003).

2.2.14 Complementation experiments

B1460 is a plasmid that contains a bi-directional tetracycline-inducible CMV promoter that encodes a truncated nerve growth factor receptor (NGFR) on one site, and the EBER1 and EBER2 in 4 copies on the other. B1249 contains only NGFR and was used as a negative control. M81/ΔEBER1+2 LCLs were transfected with either

B1249 or B1460 (contains M81 EBER1 and EBER2 in 4 copies) or B1510 (contains B95-8 EBER1 and EBER2 in 4 copies) and cultured with 1 μg/ml doxycycline for 21 days. NGFR-positive cells were isolated with specific antibodies and used for protein and RNA analyses.

2.2.15 Western blots

Proteins were extracted with a standard RIPA buffer (150 mM NaCl, 0.5% NP-40, 1% Sodium deoxycholat, 0.1% SDS, 5 mM EDTA, 20 mM Tris-HCl pH7.5, proteinase inhibitor cocktail (Roche)) for 15 min on ice followed by sonication to shear the genomic DNA. Up to 20 μg of proteins denatured in loading buffer for 10 min at 95 degree were separated on SDS-polyacryl-amide gels and electroblotted onto a nitrocellulose membrane (Hybond C, Amersham). After pre-incubation of the blot in 3% milk dry powder in PBST (PBS with 0.1% Tween-20), the antibody against the target protein was added and incubated at 4 degree overnight. After extensive washings in PBST, the blot was incubated for 1 hr with suitable secondary antibodies coupled to horseradish peroxidase (goat anti-mouse (Promega), goat anti-rabbit (Life technologies), or rabbit anti-goat (Santa Cruz) IgG). Bound antibodies were revealed using the ECL detection reagent (Pierce) (This protocol is modified from the shared folder from F100, DKFZ).

2.2.16 Measurement of CXCL8 production

Cell culture supernatants were collected and analyzed for CXCL8 production by using a Human IL-8 (CXCL8) ELISA development kit (Mabtech) according to the manufacturer's protocol.

2.2.17 Human cytokine array

We seeded LCLs transformed by M81 or M81/ΔE1+2 at 30 dpi at a density of $3*10^5$ per milliliter in a 24-well-plate. Cell culture supernatants were collected after 3 days seeding and filtered through a 0.22 μm filter. The filtered supernatants were analyzed for cytokine production by using a Human Cytokine Array kit (R&D Systems) according to the manufacturer's protocol.

2.2.18 SYBR Green real-time PCR

Total RNA isolated from LCLs were reverse transcribed with AMV-reverse transcriptase (Roche) using a mix of random hexamers. 200 ng total RNA was used for reverse transcription.

An example is given below for a 20 μl reaction containing the following components:

4 μl	5x RT buffer
2 μl	2mM dNTPs
2 μl	random hexamers
4 μl	MgCl2
0.8 μl	AMV reverse transcriptase
1 μl	RNA inhibitor
1.2 μl	water
15 μl in total	Mix

5 μl of RNA sample was added to the master mix and incubated on ice for 5 minutes.

The RT reaction was running following program:

25 ˚C	10 min
42 ˚C	60 min
90˚C	5 min
4˚C	hold

Store final cDNA at –20 ˚C until required. Add 80 ul water and use 5ul per RT-PCR reaction.

An example is given below for a 20 µl reaction containing the following components:

10 µL	2x Power SYBR green PCR Mix
1 µL	Forward primer (target gene)
1 µL	Reverse primer (target gene)
3 µL	water
+5.0 µL	cDNA sample
20 µL in total	

And remember to do **Internal Reference** PCR (eg. GAPDH)

10 µL	2x Power SYBR green PCR Mix
1 µL	forward primer GAPDH (10µM)
1 µL	reverse primer GAPDH (10µM)
3 µL	water
+5.0 µL	cDNA sample
20 µL in total	

The qPCR was run with the following settings:

50 °C for 2 min (initial denaturation)
95 °C for 10 min (denaturation)
40 cycles:
95 °C for 15 s
60 °C for 1 min

The qPCR results were analyzed by using $2^{-\Delta\Delta Ct}$ method to get a relative expression levels (This protocol is modified from the shared folder from F100, DKFZ).

2.2.19 Apoptosis assay

Apoptosis was induced in LCLs generated with different wild types and mutants at 40-60 days after infection. Cells were treated with Etoposide (4µg/ml, Sigma),

Staurosporine (4µg/ml, Sigma) or a DMSO solvent control for 20 hrs. Cells were also treated with Ionomycin (4µg/ml, Sigma Aldrich) for 48 hrs or Simvastatin (2µM, Calbiochem) for 5 days.

Cells were then washed twice with ice-cold PBS, dried on glass slides and fixed with 4% paraformaldehyde in PBS to perform a TUNEL assay that labels apoptotic cells with DNA breaks (Cell Death Detection Kit, TMR red, Roche) following the instruction of manufacturer. Cells were also stained with a rabbit antibody specific for cleaved caspase 3 (Cell signal technology).

2.2.20 Exosomes isolation

Exosomes were isolated from multiple EBV positive LCLs transformed with M81, M81ΔE1+2, M81ΔZR, M81ΔE1+2ΔZR, B95-8 viruses and RPMI1640 supplemented with 10% Exosomes Free FBS used as a negative control by differential ultra-centrifugation as previously described. Briefly, $2x10^7$cells in late log phase were used for exosomes extraction. Cell viability was checked by trypan blue and cultures with viabilities above 95% were used. For each cell line, culture supernatant was centrifuged at 1,000xg at 4 °C for 20 minutes to pellet down cells. The supernatant was carefully removed, and centrifuged at 2,000xg at 4 °C for 20 min to pellet down apoptotic bodies (ABs). The supernatant was then carefully removed, and centrifuged at 10,000xg at 4 °C for 30 min using SW32 Ti rotor (Beckman, Fullerton, USA) to pellet down microvesicles (MVs) and EBV particles. To further remove microvesicles and EBV particles, 0,22 µm filter was used. The supernatant was collected and centrifuged at 100,000xg at 4 °C for 70 minutes. The supernatant was carefully aspirated off and the exosome containing pellets were resuspended in PBS or RIPA buffer for further experiments (Ahmed et al., 2014).

2.2.21 Infection experiments in NSG mice

We isolated human CD19+ B cells from buffy coats and exposed them to virus supernatants for 2 hours at room temperature under constant agitation at a MOI sufficient to generate 20% of EBNA2-positive cells. The infected cells were collected by centrifugation and washed twice with PBS. $2x10^5$ infected primary B cells, equivalent to $4x10^4$ EBNA2-positive cells, were injected intraperitoneally into NSG mice (*NOD.Cg-Prkdc^{scid}Il2rg^{tm1Wjl}/SzJ*; NSG). The pre-established inclusion criteria in this study were healthy male NSG mice aged between 6 and 8 weeks. The mice were euthanized as soon as any clinical symptoms appeared (apathy, food refusal, ruffled hair, weight loss, palpable tumor). After careful autopsy, the organs were subjected to macroscopic and microscopic investigation, including hematoxylin and eosin (H&E) staining and immunohistochemistry (Tsai et al., 2017).

2.2.22 Immunohistochemistry

The organs from the studied mice were fixed in 10% formalin overnight and embedded in paraffin blocks. 3-µm-thin continuous sections were prepared and submitted to antigen retrieval at 98°C for 40 min in a 10 mM sodium citrate, 0.05% Tween 20 pH 6.0 solution. Bound antibodies were visualized with the Envision+ Dual link system-HRP (Dako). In parallel, adjacent sections were stained with H&E. The presence of EBV was detected by *in situ* hybridization with an EBER-specific PNA probe, in conjunction with a PNA detection kit (Dako) following the manufacturer's protocol. Pictures were taken with a camera attached to a light microscope (Axioplan, Zeiss) (Tsai et al., 2017).

2.2.23 Statistical analysis

All results obtained in *in vitro* studies with LCLs generated by EBV wild type or mutants with B cells from the same blood donor were paired and analyzed by paired student t-test. Unpaired student t-test was applied for analyzing the grouped NSG mice infected by either M81 or M81/ΔE1+2 virus. All p-values were analyzed as 2-tailed and the values equal to 0.05 or less were considered significant unless indicated. The statistical analyses were performed with the GraphPad Prism 5 software.

2.2.24 Microarray analysis

Three independent samples for each of the M81/ΔE1+2 mutant and revertant were used for the RNA microarray analysis. RNA was isolated from each sample by using a TRIzol reagent and treated with DNase to remove genome DNA. RNA samples must be provided in a 1.5ml-tube and put on dry ice. The minimal concentration and volume for each sample is 50 ng/µl and 10 µl in total respectively. After preparing our RNA samples, we send them to Core Facility in DKFZ for further analysis. They preform experimental design, incoming QC for quality and concentration of all samples, labeling and hybridization to the microarrays, monitoring the quality at all steps, and basic data analysis. IIIumina HT12 platform was used to analyze our RNA samples.

2.2.25 TLR7 experiments

We used LCLs generated with M81ΔE1+2 mutant for the agonist experiments. Cells were treated with Imiquimod (10 µg/ml, Santa Cruz), which is specific for TLR7

MyD88-dependent and NF-κB pathways or a DMSO solvent control for 36 hs. After 36 hs post treatment, cell culture supernatants were collected and analyzed for CXCL8 production by using a Human IL-8 (CXCL8) ELISA development kit (Mabtech) according to the manufacturer's protocol.

We used LCLs generated with M81 wild type for the antagonist experiments. Cells were treated with synthetic oligonucleotides (4 μM), which is specific inhibitor for TLR7. After 3 days post treatment, cell culture supernatants were collected and analyzed for IL-8 production by using a Human IL-8 (CXCL8) ELISA development kit (Mabtech) according to the manufacturer's protocol.

Synthetic oligonucleotides with phosphorothioate backbones IRS 661 (5-TGC TTGCAAGCTTGCAAGCA-3) and a control oligonucleotide (5-TCCTGCAGGTTAAGT-3) were synthesized by Eurofins (Dominguez-Villar et al., 2015).

2.2.26 EBER alignment

We completed sequence alignments with 173 EBV EBER1 and EBER2 sequences published online. The identified polymorphisms were mostly located in the EBER2 gene.

3 Results

3.1 EBER expression varies after infection with different EBV strains

3.1.1 EBER expression pattern in B cells infected with different EBV strains

The EBERs have been implicated in transformation and lytic replication (Lee et al., 2015; Swaminathan et al., 1991; Wu et al., 2007). Because these properties have been reported to be heterogeneous among different viral strains, we assessed EBER expression in the same B cells infected by different EBV strains by qPCR. We found that EBER2 was expressed 4 times more in cells infected with M81 than in the same cells infected with B95-8 (Fig. 3.1). Interestingly, the EBER2 expression levels mirrored the lytic replication levels previously recorded in these cells, with cells infected with M81 showing the highest levels of replication, followed by the viruses identified in gastric carcinomas SNU719, YCCEL1, GP202 and finally Akata and B95-8 (Tsai et al., 2017). There was some variation in EBER1 expression levels among cells infected by the different strains, but it was much milder than with EBER2.

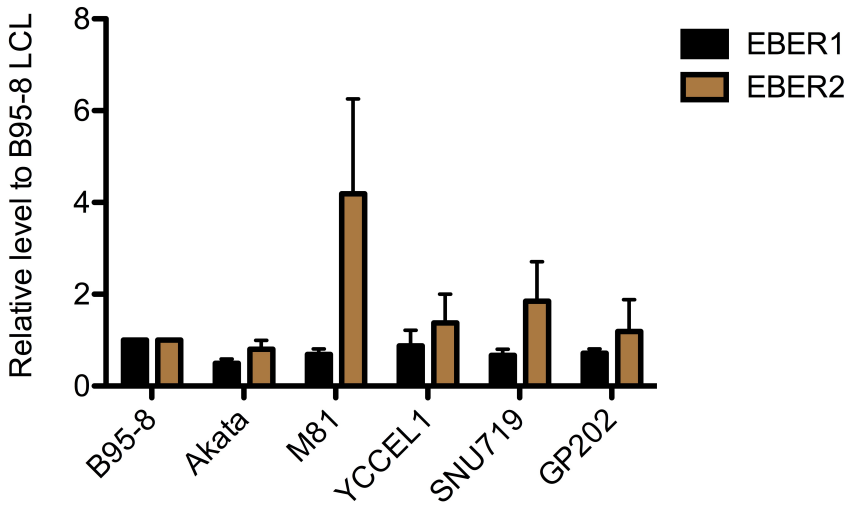

Fig. 3.1 EBER expression levels in B cells infected with different EBV strains. We assessed EBER expression in B cells infected by different EBV strains by qPCR. The data are given relative to values obtained in LCLs generated with B95-8. The data represents the mean of three independent experiments ± SD.

3.1.2 M81 EBER2 is more stable than its homolog in the B95-8 EBV genome

The variable EBER2 expression levels could be potentially explained by a different half-life of the different EBERs. Therefore, we treated an LCL pair generated by M81 or B95-8 infection with the drug (CAS 577784-91-9), an inhibitor of the RNA polymerase III and recorded EBER1 and EBER2 levels over time (Wu et al., 2003) (Fig. 3.2). This analysis showed marginal differences in the half-life of EBER1 between the species. In contrast, EBER2's half-life was 50% higher in cells infected with M81, relative to cells infected with B95-8. Thus, the higher EBER levels recorded in M81-infected cells can be at least in part ascribed to a longer half-life.

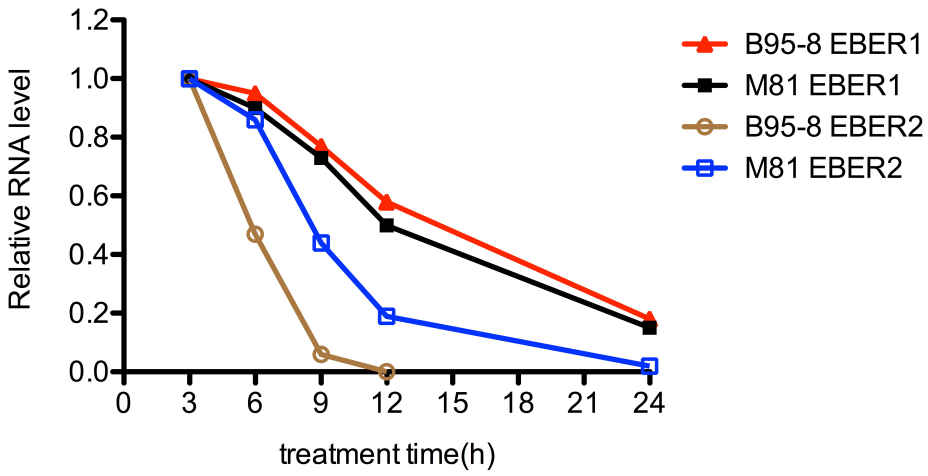

Fig. 3.2 Half-life of EBER1 and EBER2 from two different strains. We measured EBER expression in B cells infected by M81 and B95-8 strains by qPCR after treatment with a drug that specifically inhibits RNA polymerase III activity to determine the EBER half time. Result from one representative experiment is presented.

3.1.3 EBV strains from NPC carry a unique EBER2 sequence

To explain the differences between B95-8 and M81 EBER2, we completed this analysis by performing sequence alignments with all EBER sequences. We identified multiple polymorphisms that were mostly located in the EBER2 gene. These polymorphisms were not located in the sequences recognized by the primers and probes used for the analysis described in Fig. 3.1, except YCCEL1 that carries a polymorphism at position 26 (Table. 3.1).

We found that the distribution of the different EBER2 polymorphisms in lymphoma, post-transplant lymphoproliferative disorder (PTLD), infectious mononucleosis (IM), and in EBV-associated gastric carcinoma (EBVaGC) was nearly identical. However, there are some polymorphisms that are seen more frequently in nasopharyngeal

carcinoma (NPC), as described in the introduction section, suggesting that NPCs carry a specific type of EBER2 that might have unique functions. Table. 3.1 displays the EBER2 polymorphisms in the multiple EBV strains analyzed in Fig. 3.1.

The B95-8 EBER2 structure is reproduced from Lee *et al* (Fig. 3.3). The red positions display polymorphisms between B95-8 and M81 strains. In M81, position 44 is a G, position 46 is a U, position 57 is a G, position 61 is a U, position 93 is a C and position 168 is a G.

Table. 3.1 EBER2 polymorphisms in multiple EBV strains

EBV strains	26	44	46	57	61	93	168
B95-8	C	T	A	A	A	A	A
Akata	C	T	A	A	A	A	G
YCCEL1	A	T	A	A	A	A	G
SUN719	C	T	A	A	A	A	G
GP202	C	T	A	A	A	A	A
P3HR1	C	T	A	A	A	A	G
M81	C	G	T	G	T	C	G

The B95-8 strain was isolated from a patient with infectious mononucleosis (IM). Akata and P3HR1 were derived from Burkitt's lymphoma cells. YCCEL1, SNU719, and GP202 were derived from gastric carcinomas cells. M81 was derived from a patient with nasopharyngeal carcinoma (NPC).

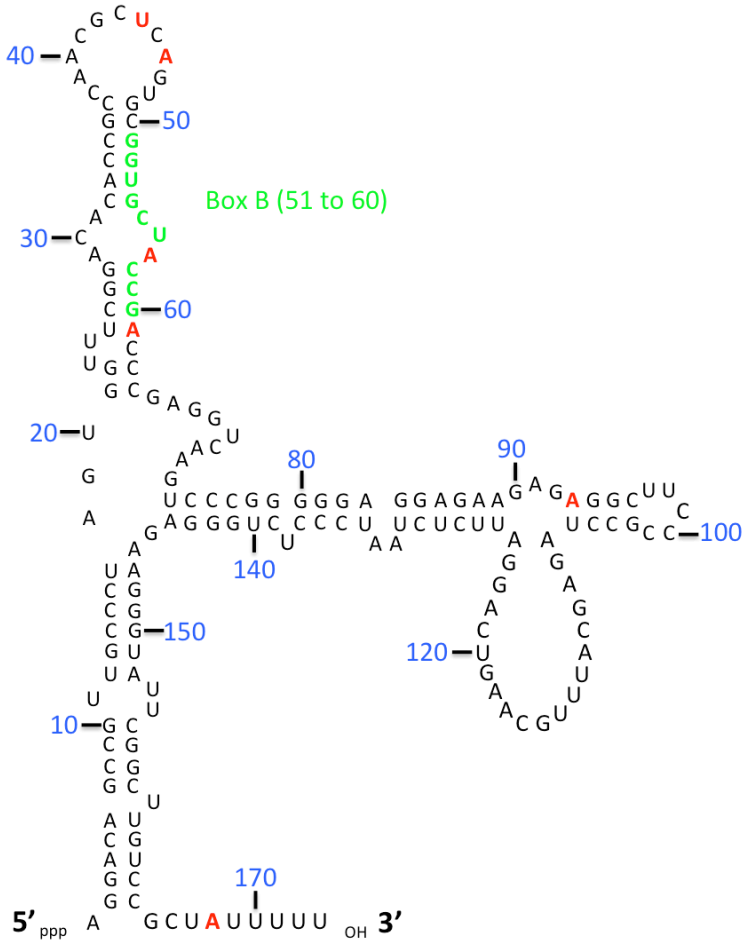

Fig. 3.3 The B95-8 EBER2 structure. The B95-8 EBER2 structure is reproduced from Lee *et al*. The green region (+51 to +60) shows a typical Box B pol III promoter sequence in the B95-8 EBV genome (Howe and Shu, 1989). The red positions display polymorphisms between the B95-8 and M81 strains. In M81, position 44 is a G, position 46 is a U, position 57 is a G, position 61 is a U, position 93 is a C and position 168 is a G.

3.1.4 EBER2 polymorphisms contribute to its expression

To assess the impact of the 6 polymorphisms located in B95-8 and M81 EBER2, we introduced each of the mutations present in B95-8 EBER2 in the M81 EBER2 and reciprocally those mutations present in M81 EBER2 in the B95-8 EBER2. This

analysis showed that the ribonucleotides located at position 44, 46 and 61 had a strong influence on EBER2 expression, with M81-type mutations conferring higher expression levels than B95-8-type ones (Fig. 3.4). We conclude from this set of assays that strain-specific mutations influence the EBER2 expression levels. Alignments with available sequences showed that the sequence pattern displayed by the Akata EBER2 is the most common one and are shared with 68.6% of all EBV genomes. The B95-8 EBER2 is found in 7% of all 172 EBV genomes, and the M81 EBER2 is common to 16.3% of all 172 EBV genomes, including the majority of strains isolated in NPCs.

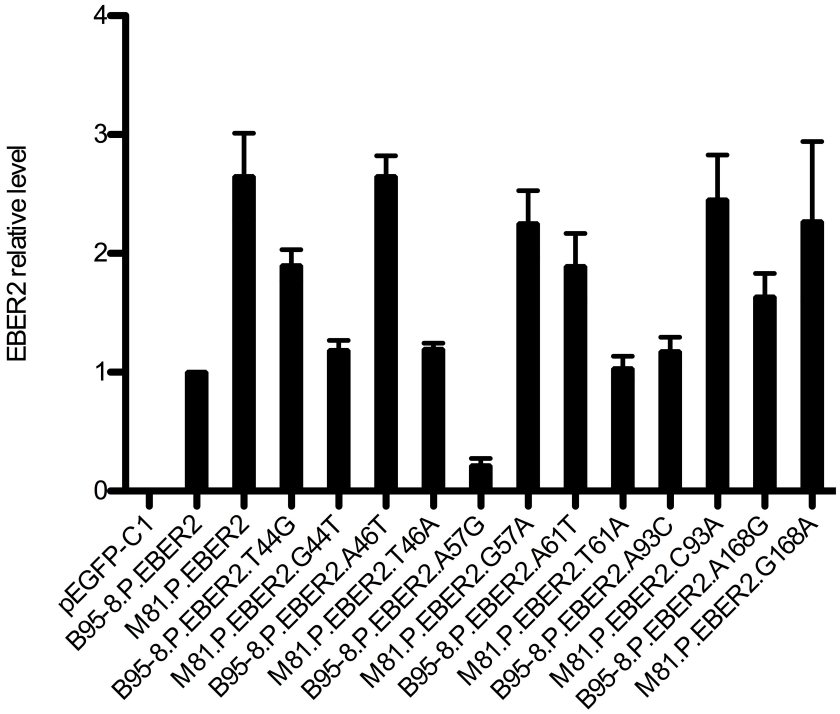

Fig. 3.4 EBER2 polymorphisms influence their expression levels. We assessed EBER expression in 293 cells transiently transfected with multiple EBER2 mutation plasmids by qPCR. pEGFP-C1 is an empty plasmid. B95-8.P.EBER2 means native B95-8 EBER2 in pEGFP-C1 plasmid. M81.P.EBER2 means native M81 EBER2 in

pEGFP-C1 plasmid. B95-8.P.EBER2.T44G means B95-8 native EBER2 that carries a mutation at position 44, T to G. M81.P.EBER2.G44T means M81 native EBER2 that carries a mutation at position 44, G to T. The data are given relative to values obtained in 293 cells transfected with B95-8.P.EBER2. The data represent the mean of three independent experiments ± SD.

3.2 Lytically replicating cells contain more EBERs than latently infected B cells.

3.2.1 Purification of BZLF1-positive cells in LCLs infected with wild type M81

The apparent link between viral lytic replication and EBER2 expression levels led us to analyze the expression levels of this non-coding RNA in spontaneously replicating cells. To this end, we infected B cells with a recombinant M81 EBV that carries an inactive form of the rat CD2 gene driven by an early antigen promoter that is responsive to the BZLF1 protein that drives the onset of lytic replication. Thus, infected B cells undergoing lytic replication express CD2 at their cell surface and can be immunocaptured by a specific antibody (Lin et al., 2015). We quantified BZLF1 expression in the CD2-positive and CD2-negative populations using quantitative RT-PCR and western blot (Fig. 3.5). As expected, we found that only CD2-positive cells produced BZLF1 at the mRNA and protein levels. This implies that cells that express the BZLF1 mRNA also express the BZLF1 protein. This also suggests that these mRNAs are not subjected to massive miRNA interference.

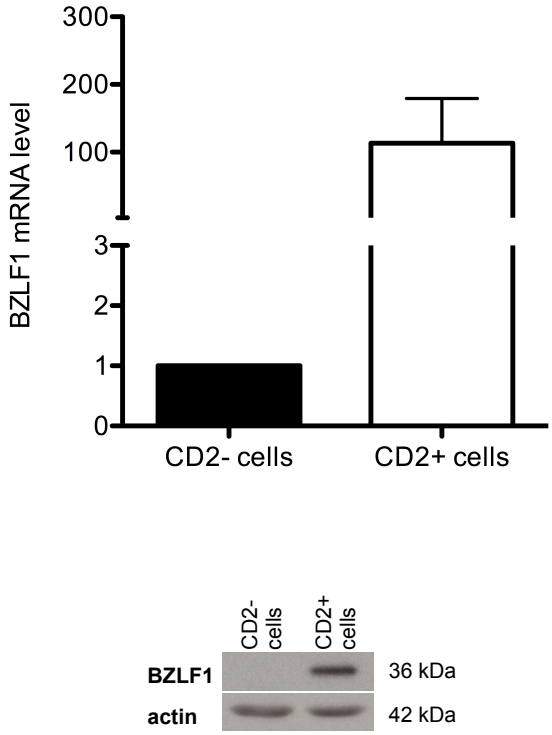

Fig. 3.5 Purification of CD2-positive cells and CD2-negative cells. CD2-positive cells were isolated from LCLs generated with a M81 mutant that expresses a truncated form of rat CD2 behind an EA-D-responsive promoter. The CD2-positive cells were purified with a specific antibody. CD2-positive or CD2-negative cell populations were submitted to RT-qPCR to assess BZLF1 mRNA expression (top graph) and to a western blot analysis with a BZLF1-specific antibody (bottom picture).

3.2.2 Lytically replicating cells express more EBERs than non-replicating B cells

We assessed EBER expression levels in the CD2-positive and CD2-negative populations by qPCR. We found that EBER1 and EBER2 are, on average, expressed 5 and 10 times fold higher in lytically replicating B cells than in non-replicating ones,

respectively (Fig. 3.6). Thus, there is a positive relationship between EBV EBER RNAs and BZLF1 expression. Replicating B cells expressed 40 times more EBER2 than B cells latently infected with B95-8.

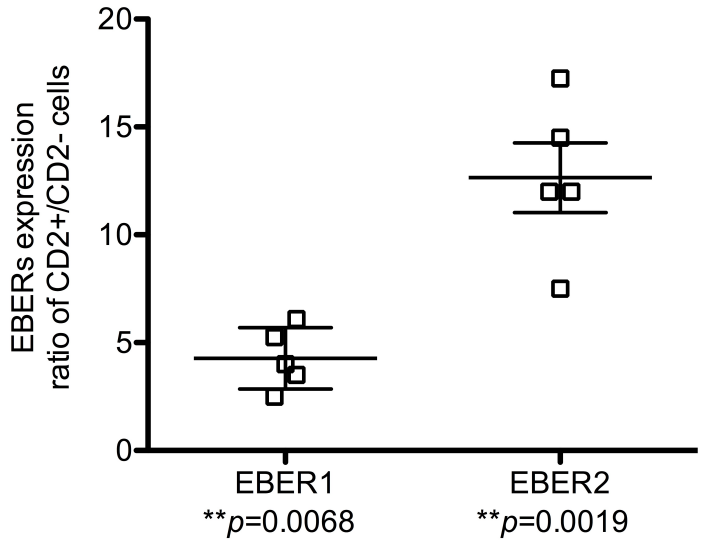

Fig. 3.6 EBER expression pattern in CD2-positive cells and CD2-negative cells. The scatter plot shows the expression of viral EBER1 and EBER2 extracted from CD2-positive or CD2-negative cell populations obtained from 5 different LCLs generated with the CD2-expressing virus. A result from one LCL is indicated by a square. All the p values were obtained from paired student t tests.

3.2.3 Lytic replication enhances EBER production

Although replicating cells represent only a minority among infected cells, the very high EBER expression levels found in these cells are likely to influence total EBER levels. Therefore, we assessed the expression of these non-coding RNAs in LCLs generated with wild type M81 or its replication-defective M81/ΔZR version that lacks the BZLF1 and BRLF1 transactivators. While EBER1 was produced approximately at the same level in both types of LCLs, cells infected with M81 produced nearly twice

as much EBER2, relative to cells infected with the M81/ΔZR mutant (Fig. 3.7). Considering that only 5% of the cells undergo lytic replication, this suggests that replicating cells generate considerable amounts of EBER2 and to a lesser extent of EBER1. To confirm that lytic replication enhances EBER production, we transfected BZLF1 into LCLs generated with M81/ΔZ. Forced expression of BZLF1 led to an increase in EBER1 and EBER2 expression that was comparable in intensity to the changes observed in spontaneously replicating cells (Fig. 3.7). Thus, EBERs, and in particular EBER2, are amplified in replicating cells. These data also suggest that the expression of EBER1 and 2 is independent from one another, with EBER2 being preferentially transcribed in replicating cells.

(A) (B)

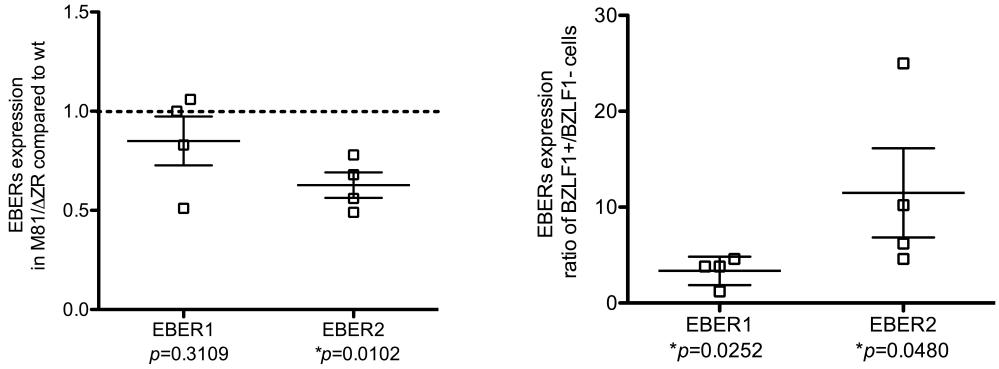

Fig. 3.7 EBERs are amplified in replicating cells. (A) We determined the EBER expression by qPCR in 4 different LCLs generated with M81/ΔZR virus. This scatter plot shows the ratio of EBER expression between M81/ΔZR-infected LCLs verse M81 wild type-infected LCLs. A result from one LCL is indicated by a square. Paired t-student tests were performed to analyze the data. (B) A LCL transformed by M81/ΔZ was stably transfected with a plasmid that encodes a truncated form of NGFR and BZLF1 or with a plasmid that encodes NGFR only (empty). The NGFR-

positive cells were purified with a specific antibody. We determined the EBER expression extracted from BZLF1-positive or BZLF1-negative cell populations obtained from 4 different LCLs generated with the M81/ΔZ virus. A result from one LCL is indicated by a square. Paired t-student tests were performed to analyze the data.

3.2.4 EBV latent genes mRNA expression profile in replicating cells relative to non-replicating cells

We then extended our analysis to quantify the expression level of some viral mRNAs in these 2 cell populations using quantitative RT-PCR. We found that EBNA2 and LMP1 transcripts, but not LMP2A are expressed at higher levels in replicating cells than in non-replicating cells (Fig. 3.8).

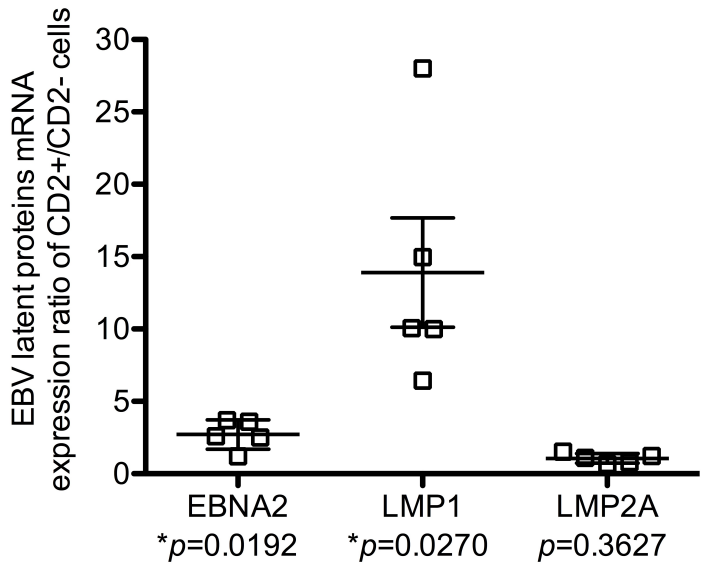

Fig. 3.8 EBV viral mRNA expression profile in replicating cells and in non-replicating cells. The scatter plot shows expression of viral EBNA2, LMP1, and LMP2A mRNAs extracted from CD2-positive or CD2-negative cell populations obtained from 5 different LCLs generated with the CD2-expressing virus. A result

from one LCL is indicated by a square. All the p values were obtained from paired student t tests.

3.3 M81 EBER2 stimulates spontaneous lytic replication in B cells

3.3.1 B cells infected with a M81 virus devoid of the EBER RNAs display decreased spontaneous lytic replication in B cells

The EBERs have been implicated in the control of virus production, but different groups reported contradictory results (Lee et al., 2015; Swaminathan et al., 1991). To delineate the contribution of the EBERs to viral functions, we generated a set of triplets that included the wild type M81 virus, an EBER1 and 2 M81 double knockout and a revertant thereof (Fig. 3.9).

We used these viruses to generate a panel of LCLs and assessed lytic replication in the infected cells. To this end, we monitored the expression of the BZLF1 protein in infected cells using western blot. The Epstein-Barr virus (EBV) immediate-early protein BZLF1 is a transcriptional activator that mediates the initiation of lytic replication (Mauser et al., 2002). This assay showed a 2 to 5 decrease in BZLF1 expression at 35 days post infection (dpi) in B cells infected with the M81/ΔE1+2 virus, relative to wild type controls, in three investigated sample sets (Fig. 3.10).

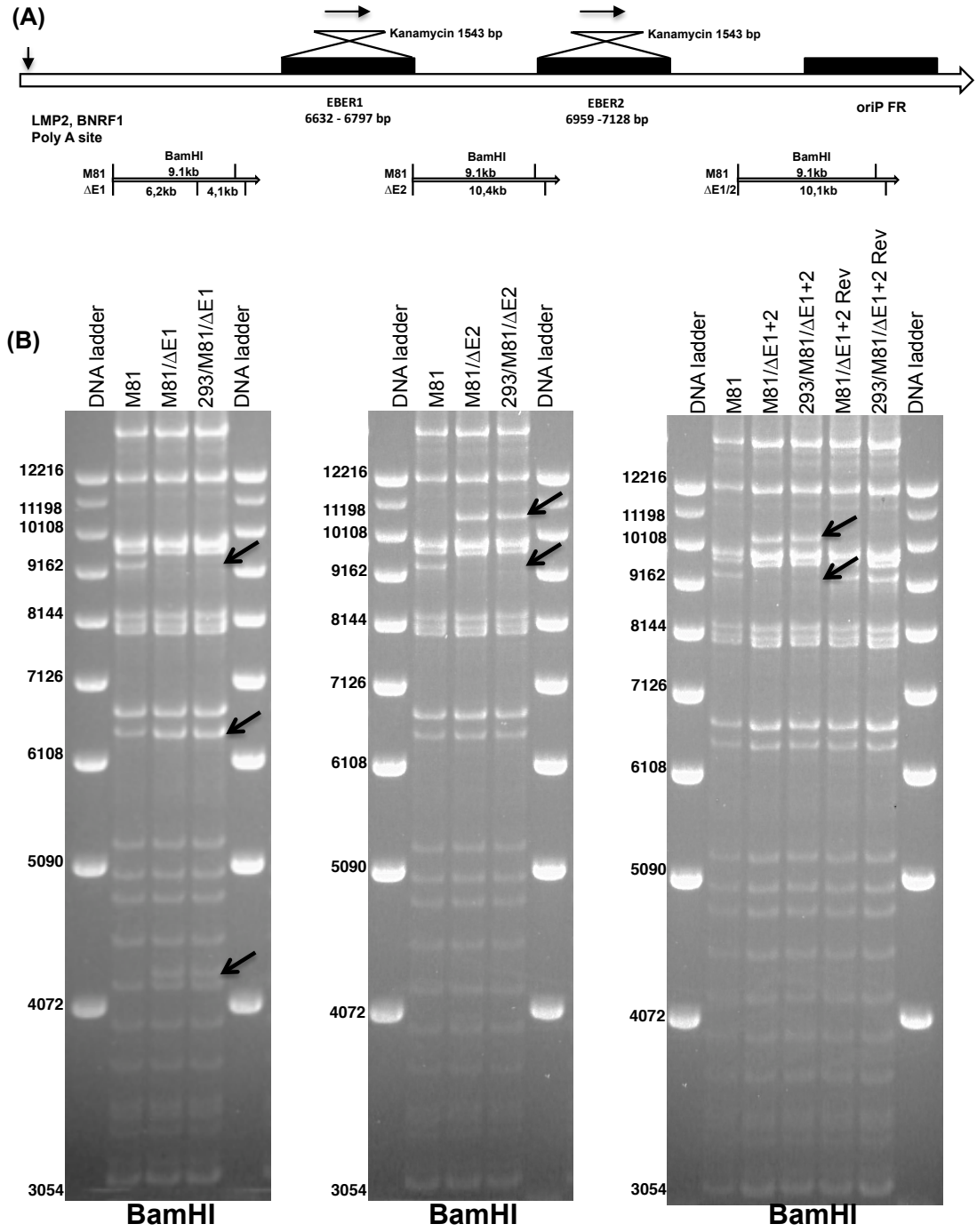

Fig. 3.9 Construction of the M81 EBER non-coding RNAs mutants. (A) Schematic map of a segment from the rM81 genome that encompasses the EBER genes region. The deletion mutants were obtained by replacing the EBER1 and EBER2 with a kanamycin resistance cassette. (B) These restriction analyses from DNA Bacmid minipreparations show the restriction pattern of the M81/ΔE1, M81/ΔE2, M81/ΔE1+2 and M81/ΔE1+2 revertant mutants. The investigated samples

include rM81 bacmids after construction in *E.coli* or after rescue from the producer cell lines. The viral DNAs were cleaved with BamHI and separated on an agarose gel. The parental rM81 recombinant EBV plasmid was loaded as a control. The arrows indicate the viral DNA fragments whose sizes differ between the wild type rM81 and the mutants as illustrated in the schematic shown in (A).

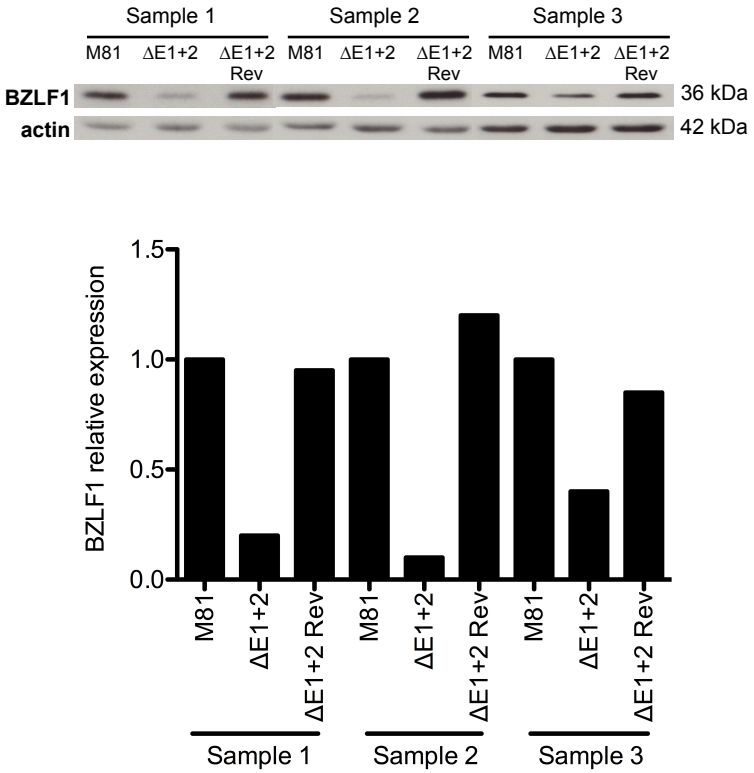

Fig. 3.10 The deletion of the EBER RNAs decreases lytic replication. We performed immunoblot analyses on LCLs transformed with M81, M81/ΔE1+2 and M81/ΔE1+2 Rev with antibodies specific for BZLF1 and actin. The graph of bars shows the relative intensity of the signals quantified by the ImageJ software.

3.3.2 M81 EBER could affect the initiation of BZLF1 in EBV-infected B cells

We confirmed these results with immunofluorescence stains performed at three different time points after transformation using antibodies specific to BZLF1. At all investigated time points, the M81/ΔE1+2 mutant displayed a lower percentage of replicating cells than wild type M81 virus (Fig. 3.11).

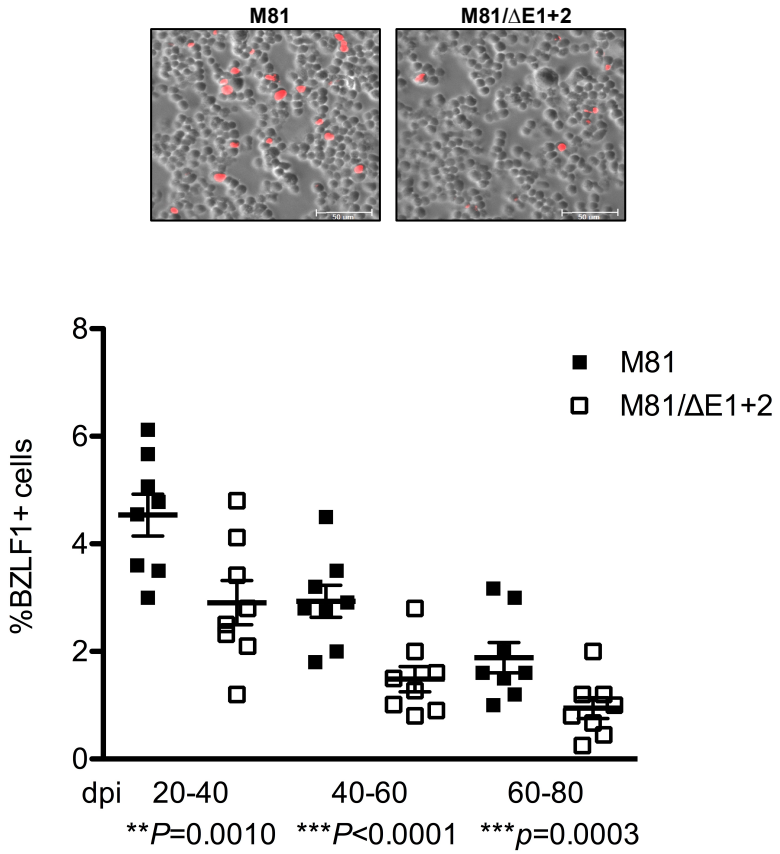

Fig. 3.11 The deletion of the EBER RNAs decreases lytic replication. This picture shows the BZLF1 expression pattern in 8 different LCLs transformed by M81 or M81/ΔE1+2, as determined by BZLF1 immunofluorescence staining. The percentage of BZLF1-positive cells in LCLs from multiple B-cell donors at different days post infection (dpi) is given in the scatter plot. All the p values were obtained from paired t tests performed with the two types of LCLs.

3.3.3 Deletion of M81 EBER also affects viral late lytic production

We further confirmed these results with immunofluorescence stains performed at three different time points after transformation using antibodies specific to gp350. Gp350 is expressed during the late phase of the lytic cycle and is a major component of the mature virion. At all investigated time points, the M81/ΔE1+2 mutant displayed a lower percentage of replicating cells than wild type M81 virus (Fig. 3.12).

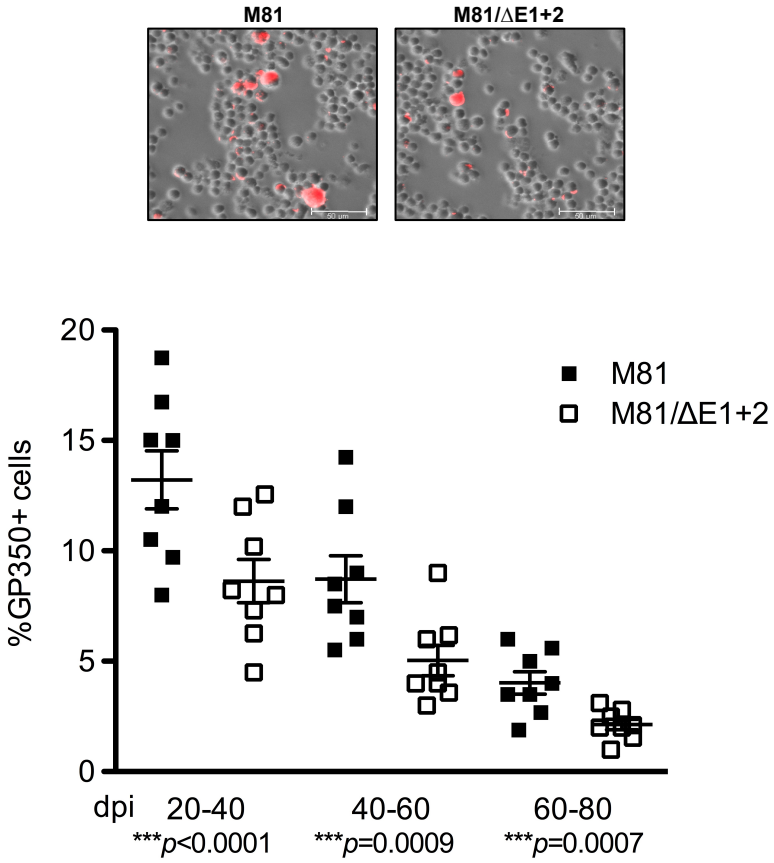

Fig. 3.12 The deletion of the EBER RNAs decreases virus production. This picture shows the gp350 expression pattern in 8 different LCLs transformed by M81 or M81/ΔE1+2 as determined by gp350 immunofluorescence staining. The percentage of gp350-positive cells in LCLs from multiple B-cell donors at different days post infection (dpi) is given in the scatter plot. All the p values were obtained from paired t tests performed with the two types of LCLs.

3.3.4 M81 EBER2 plays an important role in spontaneous lytic replication, but EBER1 is also involved in the control of this process.

We then wished to determine which of the EBERs was responsible for the increased replication levels. To this end, we constructed M81 knock out viruses that lacked either EBER1 or EBER2 and repeated the aforementioned replication experiments. These results showed that the deletion of EBER2 but not of EBER1 reduces lytic replication. However, deletion of both EBERs has a stronger impact on lytic replication than deletion of EBER2 only, suggesting that both molecules contribute to this process, although EBER2 plays a much more important role than EBER1 (Fig. 3.13).

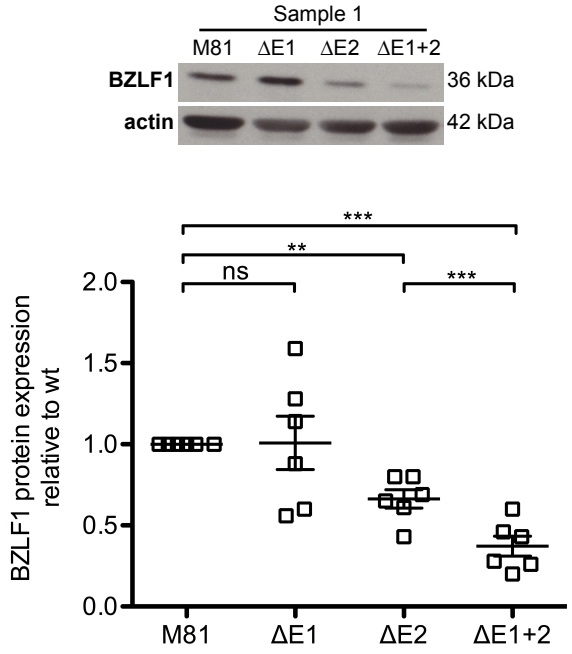

Fig. 3.13 M81 EBER2 plays a predominant role in lytic replication in B cells. We showed one immunoblot analysis performed on LCLs transformed with M81, M81/ΔE1, M81/ΔE2, and M81/ΔE1+2 with antibodies specific for BZLF1 and actin. The scatter plot shows the relative intensity of the signals quantified by the ImageJ

software from 6 independent samples. The data are given relative to values obtained in LCLs generated with M81. All the p values were obtained from paired t tests performed with the two types of LCLs.

3.4 The EBER2 homolog on the B95-8 EBV genome does not influence spontaneous virus lytic replication in B cells

3.4.1 Complementation of M81/ΔE1+2 LCLs with M81 EBERs, but not with B95-8 EBERs increases spontaneous lytic replication

Similar experiments were performed with the B95-8 derived virus but neither the cell samples infected with wild type virus nor those infected by the EBER1+2 null mutant showed evidence of lytic replication (Data not shown). Thus, the B95-8 EBERs are not responsible for the absence of virus production in B cells after infection with B95-8.

We continued the characterization of B95-8 EBERs by performing complementation experiments and by constructing hybrid EBV viruses in which the EBER genes are exchanged between the viruses. To this end, we introduced multiples copies of the EBERs from B95-8 or M81 cloned in tandem (Komano et al., 1999) under the control of a tetracycline-inducible promoter that also drives the expression of a truncated rat CD2 protein. After transfection, the CD2-positive cells were purified to obtain a homogeneous cell population that we found to express the different EBERs at 40 to 60% of the levels seen in cells infected with wild type virus (Fig. 3.14).

Transfection of the M81 EBERs but not of the B95-8 EBERs restored BZLF1 expression in B cells infected with the M81/ΔE1+2 mutant (Fig. 3.14). As complementation of both M81 and B95-8 EBERs cloned under a tet-inducible promoter led to nearly similar expression levels, this suggested that polymorphisms between both types of EBER explain the differences between the viral isolates.

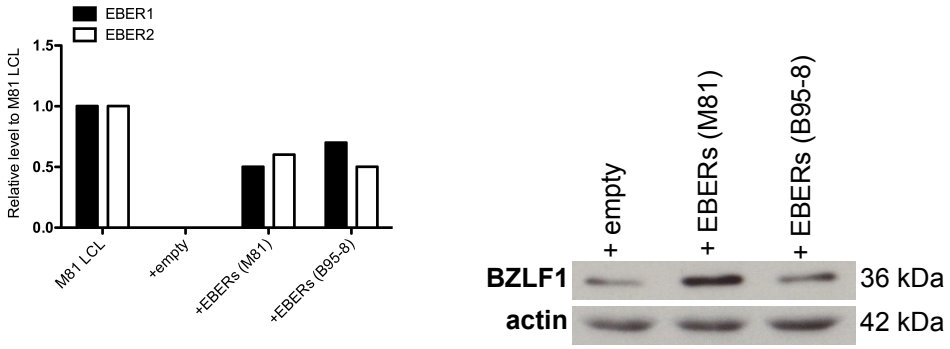

Fig. 3.14 M81 EBER2, but not B95-8 EBER2 influences lytic replication. A LCL transformed by M81/ΔE1+2 was stably transfected with a plasmid that encodes a truncated form of NGFR and both EBER1 and EBER2 from M81 or from B95-8 strain or with a plasmid that encodes NGFR only (empty). The NGFR-positive cells were purified with a specific antibody. We determined the EBERs expression in these cells relative to M81 LCL (left panel) and their BZLF1 protein expression (right panel). These data represent three independent experiments.

3.4.2 A M81 virus that carries B95-8's EBERs displays reduced spontaneous lytic replication in B cells

Analysis of the hybrid viruses yielded similar results. The M81 virus that carries B95-8 EBERs expressed EBERs at levels comparable to those seen in cells infected with B95-8 and lower than in cells infected with M81 (Fig. 3.15). This exchange virus

produced BZLF1 at levels similar to those observed in cells infected with M81/ΔE1+2, confirming that the M81 EBER have specific properties (Fig. 3.15). Introduction of the M81 EBERs into the B95-8 genome did not lead to lytic replication, suggesting that the EBERs only amplify spontaneous lytic replication but do not initiate it, a finding in line with the observation that cells infected with M81/ΔE1+2 still show some degree of lytic replication.

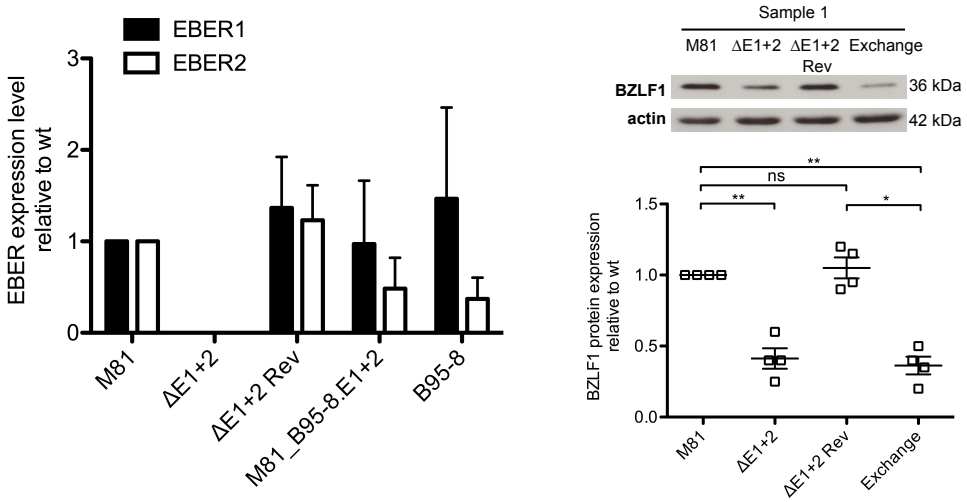

Fig. 3.15 A M81 virus that carries B95-8's EBERs displays reduced lytic replication in B cells. We determined EBERs expression levels in these LCLs relative to M81 LCL by qPCR. The data represents the mean of three independent experiments ± SD. We showed one immunoblot analysis performed on LCLs transformed with M81, ΔE1+2, ΔE1+2 Rev, and Exchange viruses (M81_B95-8.E1+2) with antibodies specific for BZLF1 and actin. The scatter plot shows the relative intensity of the signals quantified by the ImageJ software from 4 independent samples. A result from one LCL is indicated by a square. The data are given relative to valuse obtained in LCLs generated with M81. All the p values were obtained from paired t tests performed with the two types of LCLs.

3.5 M81 EBERs control lytic replication *in vivo*

We wished to confirm our data using an *in vivo* model of EBV infection and injected resting B cells exposed to M81/ΔE1+2 or M81/ΔE1+2 Rev into immuno-suppressed NSG mice. We terminated the experiment at 6 weeks post injection. We analyzed the tumor tissues for EBER, BZLF1, gp350, and EBNA2 expression. EBNA2 is a latent EBV protein expressed in proliferating cells. Continuous tissue sections were stained with hematoxylin and eosin (H&E), immunostained with antibodies specific for BZLF1, gp350, EBNA2, or subjected to an in situ hybridization with an EBER-specific probe. As expected, the mice infected with the M81/ΔE1+2 virus did not express the EBER molecules and showed reduction in the expression of the early marker (BZLF1) and late marker (gp350) of lytic replication as shown in Fig. 3.16A. However, the percentage of infected cells that expressed EBNA2 among the EBV-infected population showed no difference between wild type- and ΔE1+2-infected mice (Fig. 3.16B). Therefore, we used EBNA2 expression to normalize the percentage of BZLF1 positive cells between wild type- and ΔE1+2-infected mice. All infected tissues contained cells expressing the early marker of lytic replication (BZLF1), but the ratio between BZLF1 and EBNA2 proved to be globally lower in the mice infected with the virus devoid of the EBER RNAs (Fig. 3.16D). We conclude that M81 EBERs control lytic replication *in vivo*.

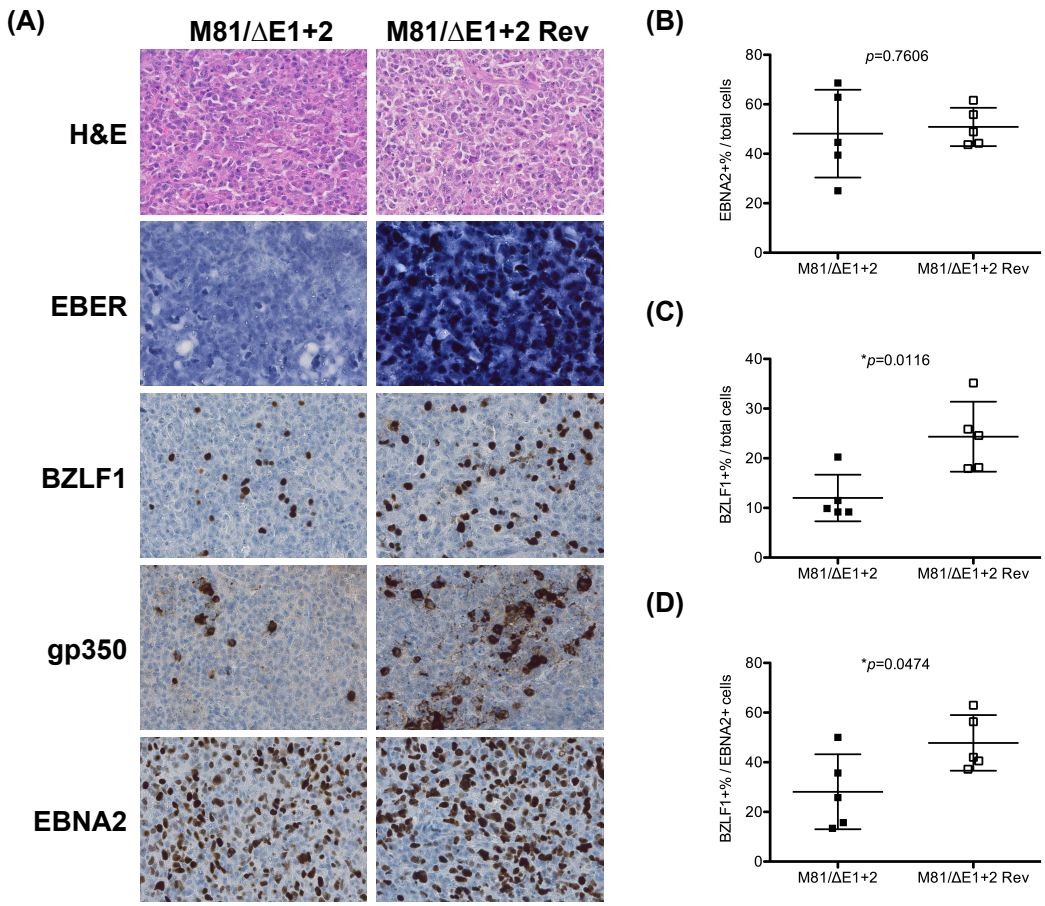

Fig. 3.16 M81 EBERs control lytic replication *in vivo.* (A) These pictures show immunohistochemistry in the tumors that developed in the gut. Continuous tissue sections were stained with hematoxylin and eosin (H&E), immunostained with antibodies specific for BZLF1, gp350, EBNA2, or subjected to an *in situ* hybridization with an EBER-specific probe. Among 5 M81/ΔE1+2 infected mice, they all exhibited a lower percentage of BZLF1-positive cells. (B-C) The number of total cells per 0.04μm^2 (surface of the field at high magnification) is given. The boxplots display the ratio between (B) EBNA2- or (C) BZLF1-positive cells versus total cells. (D) This boxplot display the ratio between BZLF1-positive cells versus EBNA2-positive cells. A result from one mouse is indicated by a square. We used two-tailed unpaired student t test for all the results.

3.6 Latent membrane proteins (LMPs) expression profile in B cells infected with EBER knockout in M81 and B95-8 strain

3.6.1 mRNAs expression profile in B cells infected with EBER knockout in M81 and B95-8 strain

EBER2 was recently shown to bind PAX5 and to promote PAX5 binding to the terminal repeat region of the EBV genome (Lee et al., 2015). Knockdown of EBER2 by small interfering RNA (siRNA) caused a 50% increase in LMP1 and LMP2 RNA levels in this study (Lee et al., 2015). Using quantitative TaqMan PCR (qPCR), we did not observe any significant difference between the M81 EBER deletion LCLs and wild-type EBV LCLs in the levels of LMP2A and LMP2B RNA (Fig. 3.17B and C), but LMP1 RNA levels were slightly lower at early days post infection (30-50dpi) when M81 EBER2 was deleted (Fig. 3.17A). The same experiments were performed in the B95-8 EBV strain. Using quantitative TaqMan PCR (qPCR), we also did not observe any significant difference between the B95-8 EBER deletion LCLs and wild-type EBV LCLs in the levels of LMP2A and LMP2B RNA (Fig. 3.17B and C), but LMP1 RNA levels were 2-fold higher at early time day post infection (30-50dpi) when B95-8 EBERs were deleted (Fig. 3.17A).

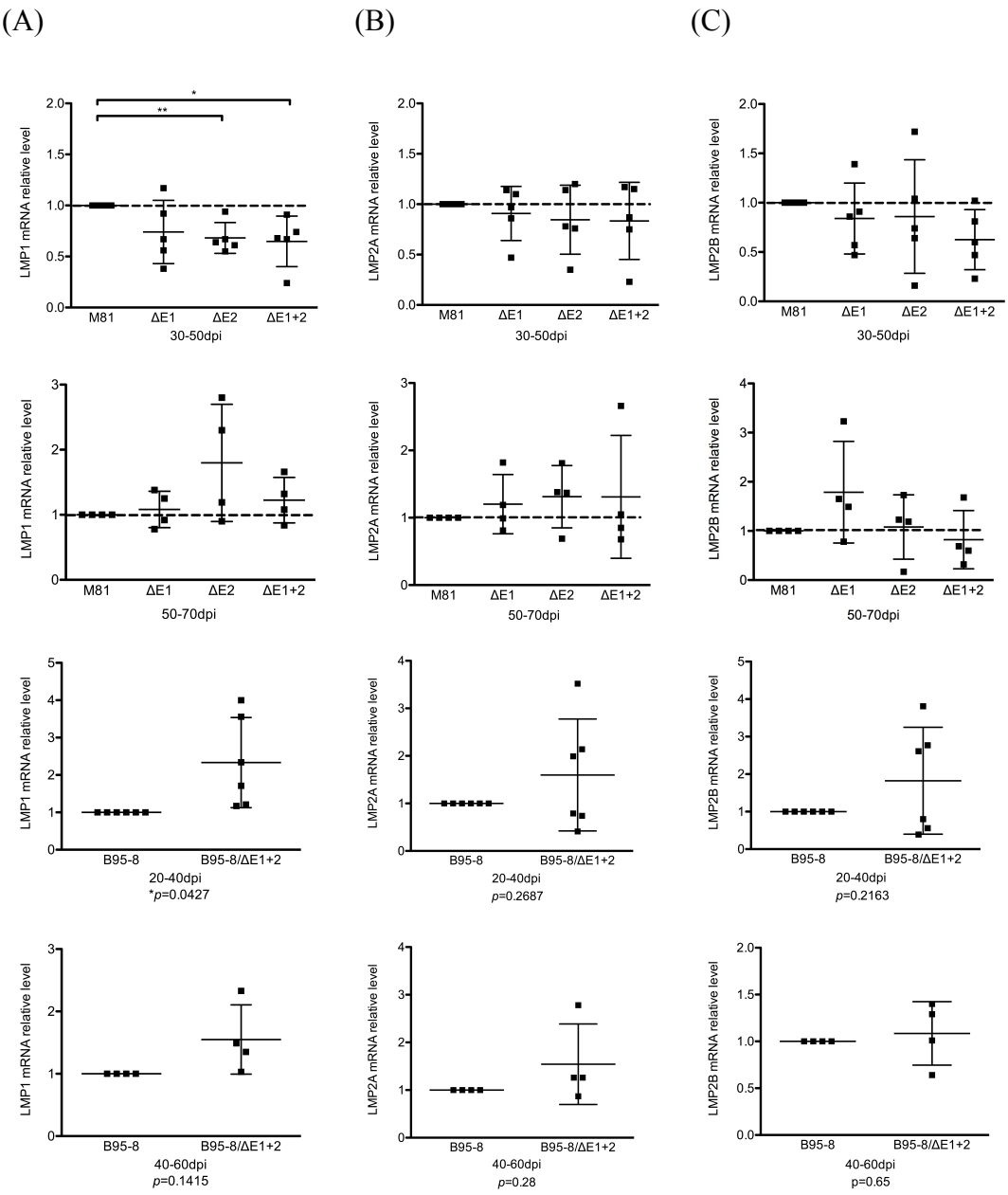

Fig. 3.17 mRNAs expression profile in B cels infected with the EBER deletion mutants in M81 and B95-8 strains. (A) We determined the LMP1 expression by qPCR in LCLs generated with multiple EBER mutants at different days post infection (dpi) in M81 and B95-8 EBV strains. (B) We determined the LMP2A expression by qPCR in LCLs generated with multiple EBER mutants at different days post infection (dpi) in M81 and B95-8 EBV strains. (C) We determined the LMP2B expression by qPCR in LCLs generated with multiple EBER mutants at different days post infection

(dpi) in M81 and B95-8 EBV strains. The data are given relative to values obtained in LCLs generated with M81 or B95-8. A result from one LCL is indicated by a square. All the p values were obtained from paired t tests performed with the two types of LCLs.

3.6.2 protein expression profile in B cells infected with EBER knockout in M81 and B95-8 strain

The LMP1 and LMP2A protein levels were comparable in EBER KO and WT generated LCLs on the basis of both M81 and B95-8 EBV strains (Fig. 3.18), and there was no apparent correlation with EBER expression. Our results thus provide some support for the earlier proposed model that B95-8 EBER2 reduces the level of LMP1 RNA, but find instead that M81 EBER2 increases the level of LMP1 RNA. These discrepancies could be explained by different properties of different EBV strains and that could probably result from polymorphic EBER2 sequences.

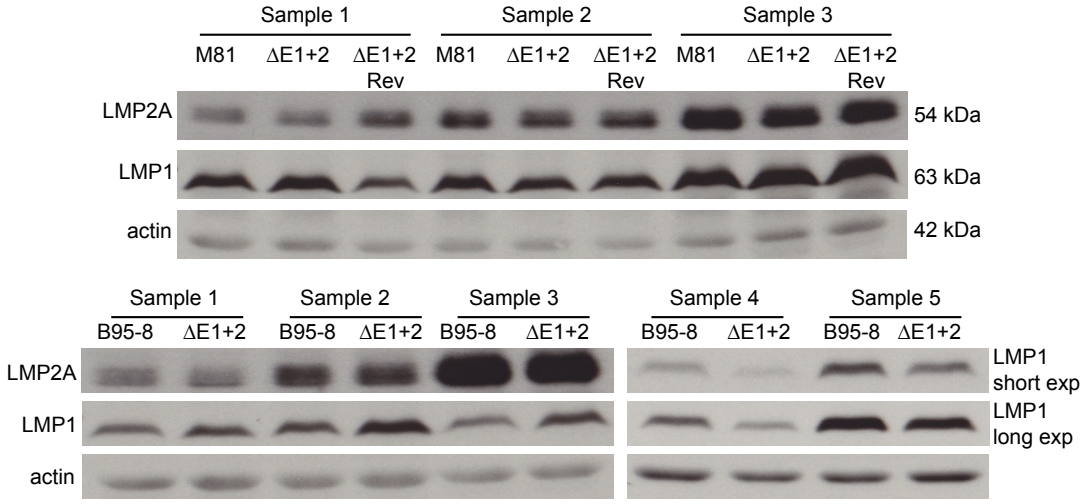

Fig. 3.18 Proteins expression profile in B cells infected with EBER mutant in M81 and B95-8 strains. We performed immunoblot analyses on LCLs transformed

with M81 or B95-8 wild type strains, and corresponding EBER mutants with antibodies specific for LMP1, LMP2A, and actin. Top pictures show immunoblots in M81 strain and below pictures show immunoblots in B95-8 strain.

3.7 M81 EBER modulates lytic replication by inducing CXCL8

3.7.1 RNA microarray analysis

The data gathered so far led us to conclude that M81 EBERs play an important role in stimulating spontaneous virus lytic replication in B cells. We wished to understand the mechanistic link between EBER expression and lytic replication in B cells. To this end, we generated three panels of LCLs infected with M81 wild type and M81/ΔE1+2 mutant and subjected them to a RNA microarray analysis. Table 3.2 shows the top 10 up-regulated and down-regulated genes following EBER expression. We found that CXCL8 mRNA was significantly down regulated in B cells infected with the M81/ΔE1+2 virus.

Table 3.2 Top 10 genes in up-regulation and down-regulation

Symbol	Fold Change (ΔE1+2/Rev)
FXYD2	12,67
HLA-DRB5	3,51
UGT2B17	3,22
ATP1B1	3,19
DBNDD2	3,02
UGT2B7	2,82
BHLHE22	2,80
LINCR	2,72
LAD1	2,58
C1orf106	2,56
LOC401845	0,18
CXCL8	0,35
COL5A1	0,41
LOC649923	0,41
LOC100134331	0,42
LOC647450	0,45
SGK	0,46
ADM	0,46
LOC652694	0,45
RN7SK	0,49

Previous studies have also demonstrated that EBERs can induce the transcription of various cytokines, such as interleukin-10 (IL-10) in BL cells, insulin-like growth factor-1 (IGF1) in epithelial cells and IL-9 in T cells (Iwakiri et al., 2005; Samanta et al., 2008; Yang et al., 2004). Thus, we also subjected two pairs of LCLs to a Human Cytokine Array screening. We found that CXCL8 protein expression level was slightly lower in B cells infected with the M81/ΔE1+2 virus than in B cells infected

with the M81 WT. However, we could not identify any difference in IL-10 expression between M81/ΔE1+2 and M81 WT LCLs (Fig. 3.19).

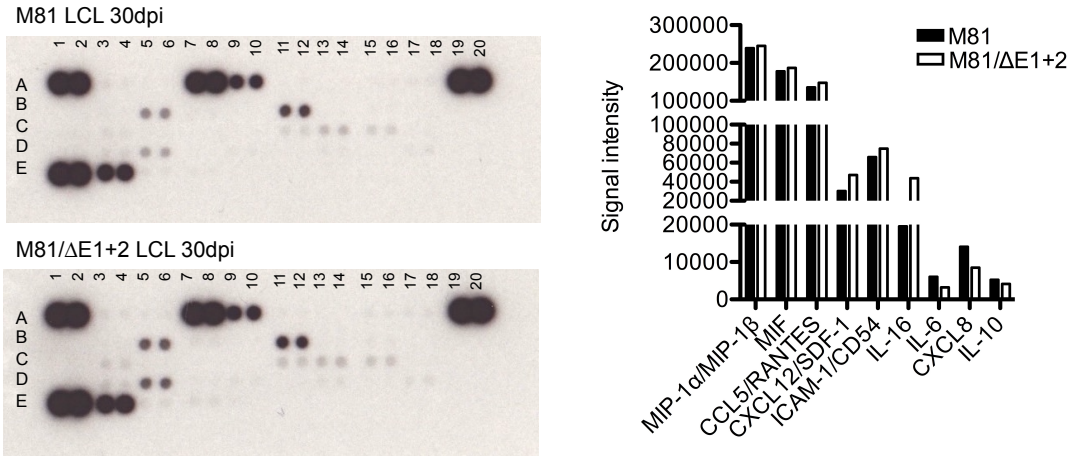

Cytokines expression levels in M81 LCLs

	Coordinate	Target/Control	Signal intensity
High	A7,A8	MIP-1α/MIP-1β	Very high
	E3,E4	MIF	High
	A9,A10	CCL5/RANTES	High
	B5,B6	CXCL12/SDF-1	Medium
	B11,B12	ICAM-1/CD54	Medium
	D5,D6	IL-16	Medium
	C11,C12	IL-6	Low
	C13,C14	CXCL8	Low
Low	C15,C16	IL-10	Low

Note: A1,A2, A19,A20, E1,E2 are positive controls; E19,E20 is a negative control. The positive control spots are standardized amounts of biotinylated IgG. They are used for signal normalization, monitoring of the detection step, and to help orient the array image. The negative control spots are printed with buffer only, and thus are not expected to give signals. Negative control spots are used for background subtraction.

Fig. 3.19 Human Cytokine Array screening. We seeded LCLs transformed by M81 WT or M81/ΔE1+2 at 30 dpi at a density of $3*10^5$ per milliliter in a 24-well-plate. Cell culture supernatants were collected after 3 days seeding and filtered through a 0.22 μm filter. The filtered supernatants were analyzed for cytokine production by

using a Human Cytokine Array kit (R&D Systems) according to the manufacturer's protocol.

3.7.2 CXCL8 expression in LCLs infected with multiple viruses

We concentrated on CXCL8 and confirmed its regulation by EBERs using qPCR and ELISA in LCLs generated with multiple viruses. These assays showed that CXCL8 is clearly down regulated at both the mRNA and the protein levels in M81/ΔE1+2 infected B cells, relative to wild type controls, including M81 WT and M81/ΔE1+2 Rev (Fig. 3.20).

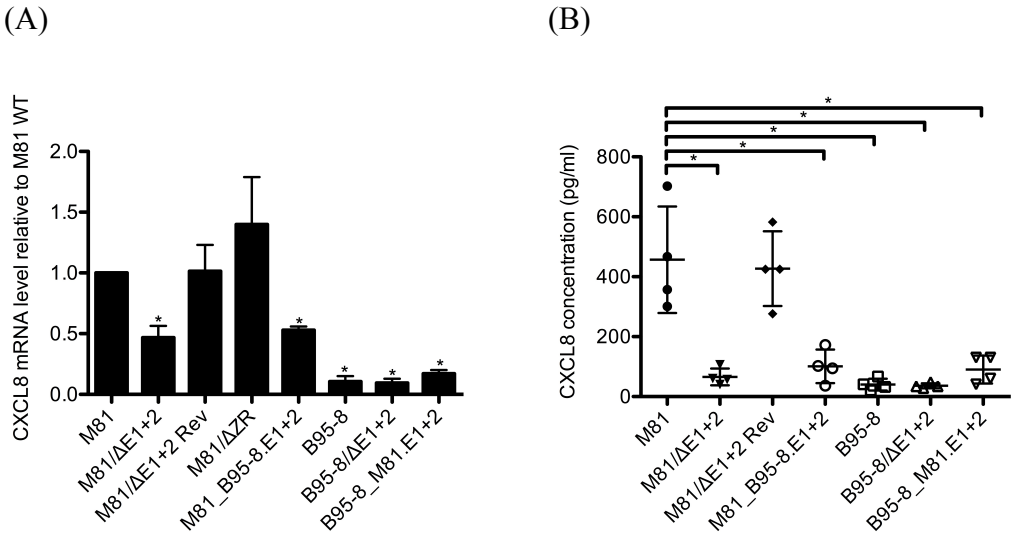

Fig. 3.20 CXCL8 expression in B cells infected with multiple viruses. (A) We determined CXCL8 mRNA expression in the same B cells infected by multiple EBV viruses by qPCR. The data are given relative to values in LCLs generated with M81. The data represents the mean of three independent infection experiments ± SD. (B) We assessed CXCL8 expression in the different 4 LCLs generated with multiple EBV viruses by ELISA. We used two-tailed paired student t test for all the results.

3.7.3 CXCL8 can compensate the absence of EBER RNA in the role of lytic replication

In order to understand why CXCL8 down-regulation in LCLs infected with the M81/ΔE1+2 virus results in decreased lytic replication in B cells, we performed complementation assays by continuously adding recombinant CXCL8 to LCLs infected with the M81/ΔE1+2 virus for 7 days. We quantified BZLF1 expression in LCLs with or without CXCL8 supplementation, relative to wild type controls. We found that BZLF1 expression is increased in M81/ΔE1+2 LCLs with CXCL8, relative to LCLs without CXCL8 (Fig. 3.21). Importantly, CXCL8 supplementation can completely compensate the absence of EBER RNA in the role of virus lytic replication, suggesting that CXCL8 represents the main target of this EBER molecule. We conclude that M81 EBERs stimulate the expression of CXCL8, and that this cytokine increases lytic replication in infected B cells.

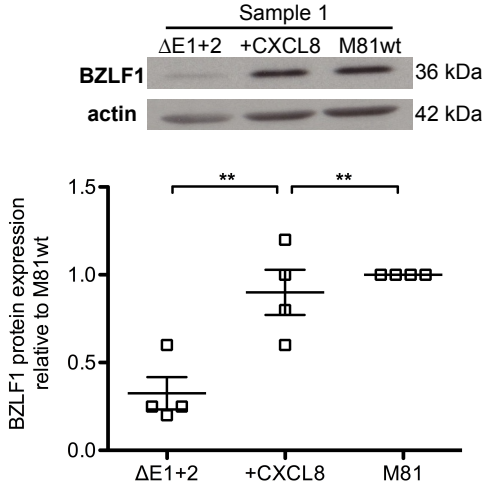

Fig. 3.21 CXCL8 can compensate the absence of EBER RNA in the role of lytic replication. We assessed BZLF1 expression by a BZLF1-specific antibody by western blot in the CXCL8 complementation assay (top picture) and bottom graph

shows 4 independent experiments. A result fron one LCL is indicated by a square. We used two-tailed paired student t test for all the results.

3.7.4 The EBER2 homolog on the B95-8 EBV genome cannot induce CXCL8 production

After performing the aforementioned experiments, we concluded that M81 EBER2 stimulates spontaneous virus lytic replication in B cells. However, its homolog in the B95-8 genome loses this property in the control of spontaneous virus lytic replication. We also concluded that M81 EBER2 could induce CXCL8 production and that CXCL8 was able to compensate the absence of M81 EBER2 in the role of virus lytic replication. Next, we wished to understand the role of B95-8 EBER2 in the stimulation of CXCL8 production in B cells. We infected B cells with the M81 virus that carries B95-8's EBER2 and performed qPCR and ELISA analysis in these LCLs. We found that the expression of CXCL8 in B cells infected with the M81 hybrid virus is lower than the expression in wild type controls, including M81 WT and M81/ΔZR **(**Fig. 3.20**)**. In addition, we performed EBER complementation assays. We transfected M81/ΔE1+2 infected LCLs with a plasmid that encodes multiple copies of the M81 EBERs or B95-8 cloned in tandem under the control of a tetracycline-inducible promoter that also drives the expression of a truncated nerve growth factor receptor (NGFR) or with a control vector. After transfection, the NGFR-positive cells were purified to obtain a homogeneous cell population that expresses EBERs at approximately 50% of the levels seen in cells infected with wild type virus (Fig. 3.22). We quantified CXCL8 expression in these cell populations and found that only M81 EBER could increase CXCL8 expression, however, B95-8 EBER could not (Fig. 3.22).

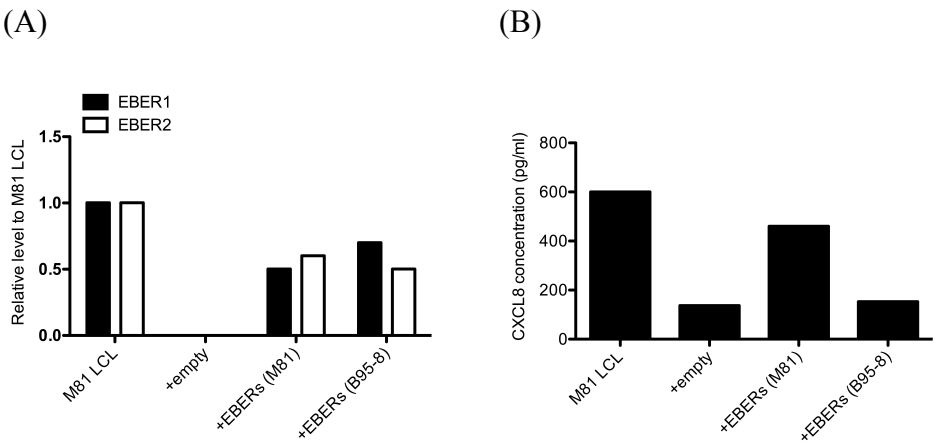

Fig. 3.22 M81 but not B95-8 EBER2 can induce CXCL8 production. A LCL transformed by M81/ΔE1+2 was stably transfected with a plasmid that encodes a truncated form of NGFR and both EBER1 and EBER2 from M81 or from B95-8 strain or with a plasmid that encodes NGFR only (empty). The NGFR-positive cells were purified with a specific antibody. We determined the EBERs expression by qPCR in these cells relative to M81 LCL (left panel) and their CXCL8 protein production by ELISA (right panel). This data represents three independent experiments.

In this chapter, we conclude that M81 EBER2 enhances CXCL8 and BZLF1 production, but its homolog in the B95-8 genome is compromised in these processes.

3.8 Exosomal fractions of B cells infected with wild type M81 that carries the EBER molecules are able to increase CXCL8 and BZLF1 production

3.8.1 EBER is able to increase CXCL8 and BZLF1 production after exposure to exosomes from infected cells

The data accumulated so far led us to conclude that M81 but not B95-8 EBER2 enhances CXCL8 production and spontaneous virus lytic replication.

CXCL8 is a chemokine that is secreted as a result of an activation of the immune system, including its innate branch. We searched for mechanisms that could link EBER and CXCL8 production. Because lytic replication takes place in infected B cells in the absence of T cells or other members of the adaptive immune response, we deemed it more likely that CXCL8 was activated in M81-infected B cells by the innate immune response. However, EBER is mainly located in the nucleus of infected cells and cannot a priori access restriction factors that are mainly located in the cytoplasm or in the endosome compartments. EBER has been reported to be incorporated in exosomes produced by infected cells (Ahmed et al., 2014). These subcellular organelles could access dendritic cells and activate TLR3 in the endosome (Iwakiri et al., 2009). We tested whether such a mechanism could also act in a paracrine manner. However, TLR3 is not expressed in B cells (Hanten et al., 2008). We canvassed a transcriptome of EBV-infected B cells and looked at the expression of TLR members expressed in the endosome. This analysis confirmed that while

TLR3 and TLR8 are hardly expressed in infected B cells, TLR7 is expressed in these cells, as previously reported (Hanten et al., 2008).

We performed immunoblot analyses on exosomal fractions isolated from multiple LCLs supernatants with antibodies specific for CD63, an exosome marker (Wang et al., 2017). We found that the isolates indeed contained CD63 proteins and thus confirmed that the isolates contain exosomes (Fig. 3.23A). We also performed immunoblot analyses on exosomal fractions with antibodies specific for LMP1, and we found that LMP1 proteins can be detected in the exosomal fractions, as previously reported (Flanagan et al., 2003) (Fig. 3.23A). We measured EBER2 expression by qPCR in the exosomal preparations isolated form the same cell numbers and we found that EBER2 expression is 4 times lower in exosomes generated from cells infected with B95-8 compared to the cells infected with M81 (Fig. 3.23B). These results suggested that we successfully isolated exosomal fractions of B cells and these exosomes carry the EBER molecules. To learn whether EBER increases CXCL8 and BZLF1 production via exosomes, we assessed CXCL8 expression by ELISA in M81/ΔE1+2 LCLs treated with exosomes isolated from multiple LCLs. We found that exosomal fractions of B cells infected with wild type M81 or M81/ΔZR that carry the EBER molecules are able to increase CXCL8 and BZLF1 production. However, exosomal fractions of B cells infected with M81/ΔE1+2 or M81/ΔE1+2/ΔZR that do not carry the EBER molecules are unable to do it.

Exosomes from cells infected with B95-8 contained much less EBER than cells infected with M81 (Fig. 3.23B). However, the inability of B95-8 EBER2 to potentiate lytic replication could not be ascribed to a low production of EBER2, as incubation of a null EBER1+2 M81 LCL with large amounts of B95-8 exosomes had no influence on replication. On the other hand, exposure of cells with M81 exosomes at the level

found in B95-8 exosomes led to a weak potentiation of BZLF1 production. Thus, the inability of B95-8 exosomes to stimulate lytic replication can be ascribed to EBER2 polymorphisms.

We conclude that the M81 EBER molecules located in exosomes enhance CXCL8 and BZLF1 production.

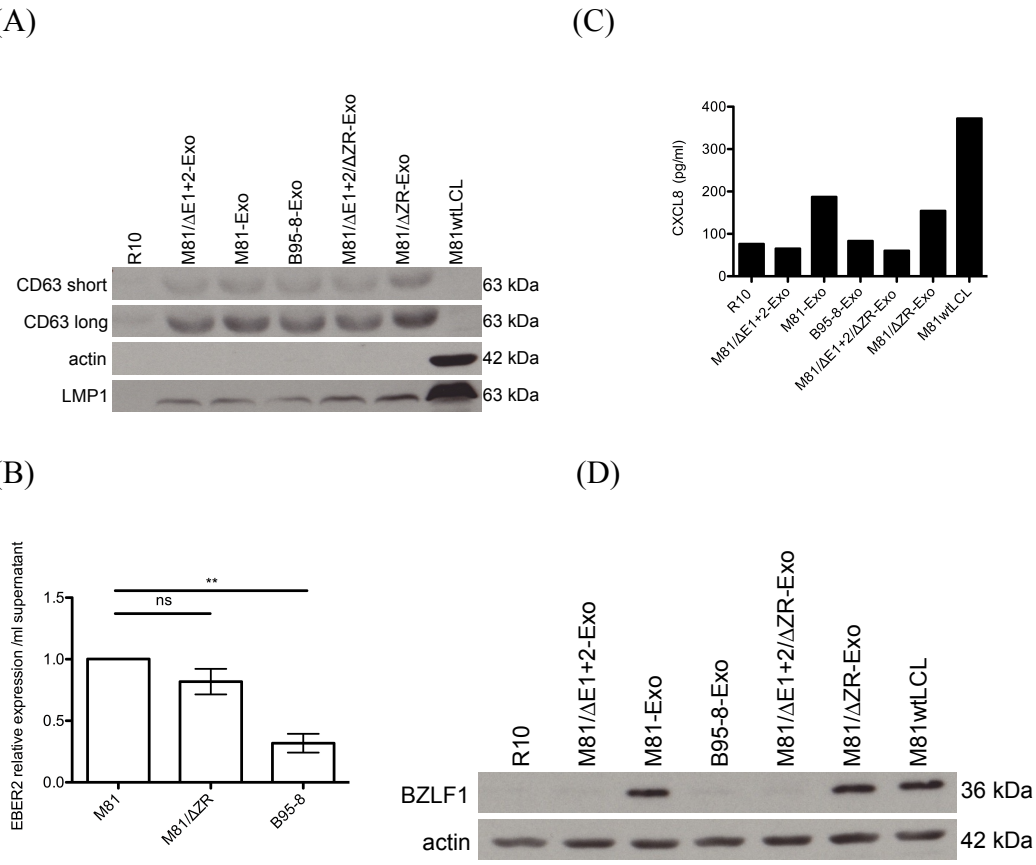

Fig. 3.23 M81 EBER molecules located in exosomes enhance CXCL8 and BZLF1 production. (A) We performed immunoblot analyses on exosomal fractions isolated from R10 (medium only), M81/ΔE1+2, M81 WT, B95-8 WT, M81/ΔE1+2/ΔZR and M81/ΔZR LCLs supernatants with antibodies specific for CD63, LMP1, and actin. (B) We assessed EBER2 expression by qPCR in the exosomal fractions of B cells infected with M81, M81/ΔZR, and B95-8. The data are given relative to values obtained in LCLs generated with M81. Data is the mean of

three independent experiments ± SD. (C) We assessed CXCL8 expression by ELISA in M81/ΔE1+2 LCLs after treatment with exosomes isolated from multiple LCLs. (D) We performed immunoblot analyses on these exosomes-treated-LCLs with antibodies specific for BZLF1 and actin. Fig. C and Fig. D represent three independent experiments.

3.8.2 The EBER molecules can be visualized after exosome uptake by B cells

The data gathered suggested that exosomes transferred the EBERs into the cells transformed by M81/ΔE1+2. Exosomes are thought to be incorporated into their target cells via endocytosis (Mulcahy et al., 2014). Therefore, we exposed M81/ΔE1+2 LCLs to exosomes from wild type M81 under conditions that inhibited (incubation at + 4°C), or stimulated endocytosis (incubation at + 37°C, inclusion of polybrene combined to centrifugation) and performed an *in situ* hybridization on the treated LCLs with an EBER-specific probe. This assay unequivocally revealed that EBER are incorporated into cells from exosomes and that the incorporation of EBER into cells increased in parallel with the conditions that enhance endocytosis (Fig. 3.24). After cytocentrifugation in the presence of polybrene at 37°C at one hour, 40% of the treated cells had incorporated EBER to a level very close to wild type levels. Why some LCL cells are resistant to this type of endocytosis remains to be determined. This treatment also restored wild type levels of replication (Fig. 3.24). We also incubated a ΔEBER1+2 LCL with exosomes from wild type M81 LCLs without enhancers of endocytosis ether at 37°C or at 4°C. Only cells incubated at 37°C with the exosomes showed accumulation of EBER molecules, albeit at much

lower levels that in the presence of endocytosis enhancers. Cells incubated at 4°C with the exosomes did not show any evidence of endocytosis.

(A)

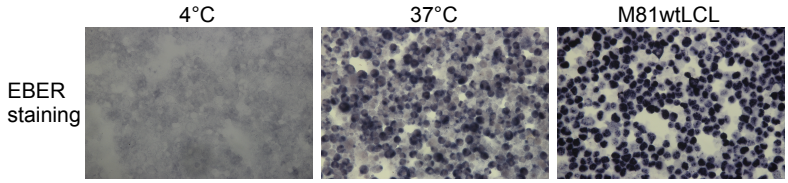

(B)

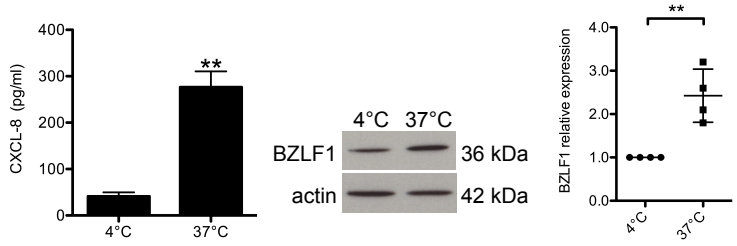

(C)

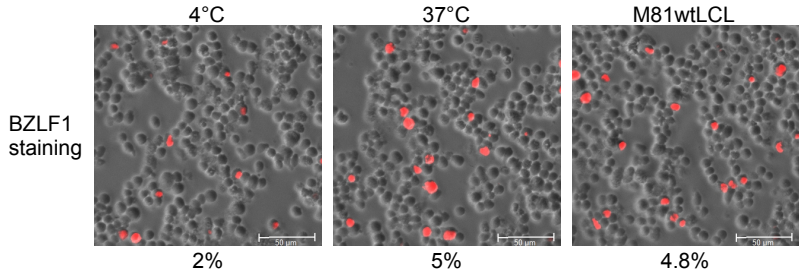

Fig. 3.24 The EBER molecules can be visulized after exosome uptake by B cells. (A) We performed EBER staining in M81/ΔE1+2 LCLs treated with exosomal fractions isolated from M81 WT LCLs supernatants in the presence of polybrene (6 µg/ml) and spinoculation at 300 g for 1 h at 24°C. The cells were returned to the incubator for 3 h at 37°C. These pictures show an example of EBER staining. (B) We assessed CXCL8 expression by ELISA in M81/ΔE1+2 LCLs after treatment with exosomes isolated from LCLs for 2 days and we performed immunoblot analyses on these exosomes-treated-LCLs with antibodies specific for BZLF1 and actin. Fig. B

represents three independent experiments. (C) This picture shows an example of BZLF1 immunofluorescence staining in M81/ΔE1+2 LCLs after treatment with exosomes.

3.8.3 Exosomes uptake is dose-dependent in B cells

We then repeated the experiments with increasing amounts of exosomes and observed a clear dose-dependent relationship, although the maximum enhancement of lytic replication was reached at exosome concentrations lower than those observed in cells infected with wild type virus. We then compared EBER production in infected cells and in exosomes. Interestingly, there was a clear parallel between the level of EBER production in these two types of structures (Fig. 3.25A). Also there was a positive relationship between the quantity of exsomes applied to M81/ΔE1+2 LCLs and the CXCL8 production levels (Fig. 3.25B).

(A) (B)

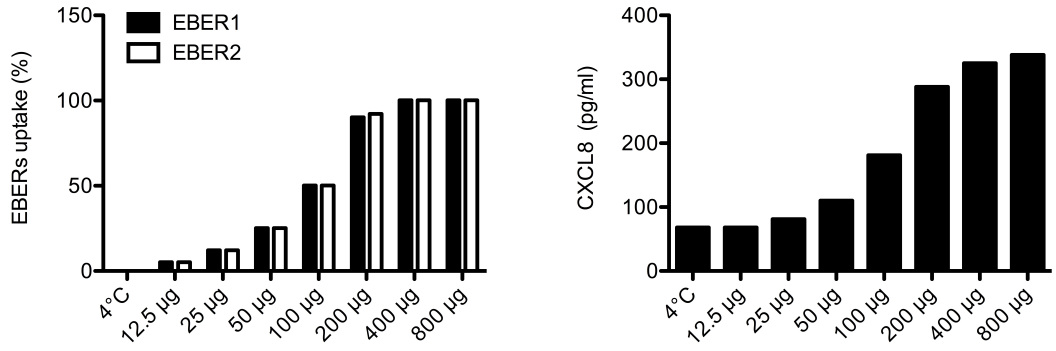

Fig. 3.25 Exosomes uptake is dose-dependent in B cells. (A) We assessed EBER expression in M81/ΔE1+2 LCLs treated with different dose of exosomal fractions isolated from M81 WT LCLs. (B) We assessed CXCL8 expression by ELISA in exosome treated LCLs. This represents three independent experiments.

3.9 The impact of EBER2 on EBV lytic replication required a functional TLR7, a sensor of viral single-stranded RNA (ssRNA)

3.9.1 Transcriptome data in EBV-infected B cells

We concluded that exosomal fractions of B cells infected with wild type M81 that carries the EBER molecules are able to increase CXCL8 and BZLF1 production. The molecular mechanism by which M81 EBER2 induces CXCL8 expression needed to be clarified. Toll-like receptors (TLRs) are a class of proteins that play a key role in the innate immune system. TLR3, TLR7, and TLR8 can sense double-stranded RNA or single-stranded RNAs. According to our transcriptome data generated in M81 WT and B95-8 WT transformed LCLs, TLR7, a sensor of single-stranded RNA, is highly expressed after EBV infection. However, TLR3 and TLR8 are hardly expressed in these two types of EBV-transformed LCLs (Table 3.3), although TLR3 is expressed in T and NK cells. It is known that TLR7 is located in the endosome (Heil et al., 2003; Lee et al., 2003; Nishiya and DeFranco, 2004). Those observations indicate that in principle EBER might be able to activate signaling through TLR7 via exosomes and induce the production of cytokine CXCL8.

Table 3.3 Transcriptome data in M81 and B95-8 LCLs

	M81wtLCL	B95-8wtLCL	Sensor of
TLR3	19	28	dsRNA
TLR7	14990	25958	ssRNA
TLR8	26	55	ssRNA

3.9.2 CXCL8 production is increased after TLR7 agonist treatment

In an attempt to demonstrate that TLR7 is involved in the induction of CXCL8, we treated LCLs transformed by M81/ΔE1+2 at 30-40 dpi by adding the TLR7 agonist Imiquimod to the culture medium for 36 hrs. We included DMSO-treated cells as controls. Cell culture supernatants were collected and analyzed for CXCL8 production by ELISA. Cells were then washed twice with ice-cold PBS and submitted to protein analysis. We found that Imiquimod treatment can enhance CXCL8 production and BZLF1 expression in M81/ΔE1+2 LCLs (Fig. 3.26).

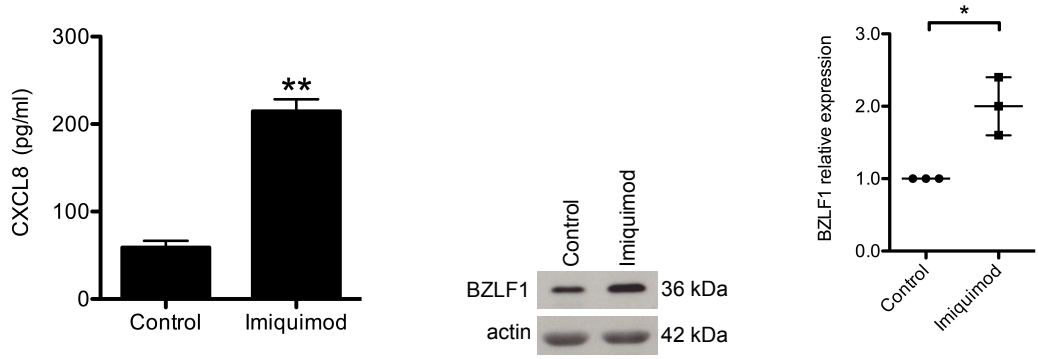

Fig. 3.26 CXCL8 production is increased after treatment with the TLR7 agonist. We assessed CXCL8 production by ELISA on LCLs transformed by M81/ΔE1+2

after treating with the TLR7 agonist Imiquimod (5µg/ml) (left graph). The data shows the mean of three independent experiments ± SD. We performed immunoblot analyses on the LCLs with antibodies specific for BZLF1 and actin (middle picture). The middle picture shows one sample and the right graph represents three independent experiments.

3.9.3 CXCL8 production is decreased after TRL7 antagonist treatment

We then treated LCLs transformed by M81 WT by adding the TLR7 antagonist IRS 661 to the culture medium for 72 hrs. IRS 661 consists of synthetic oligonucleotides with phosphorothioate backbones and it specifically targets TLR7 (Dominguez-Villar et al., 2015). We included Control-Oligos-treated cells as controls. Cell culture supernatants were collected and analyzed for CXCL8 production by ELISA. Cells were then washed twice with ice-cold PBS and submitted to protein analysis. We found that IRS 661 treatment can suppress CXCL8 production and BZLF1 expression in M81 WT LCLs (Fig. 3.27).

From this series of results, we conclude that the impact of EBER2 on EBV lytic replication required a functional TLR7, a sensor of viral single-stranded RNA (ssRNA).

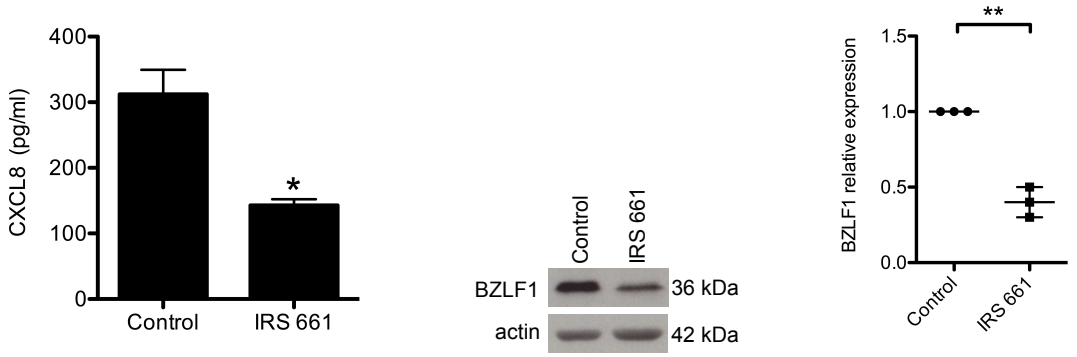

Fig. 3.27 CXCL8 production is decreased after treatment with the TLR7 antagonist. We assessed CXCL8 expression by ELISA on LCLs transformed by M81 wild type after treating with TLR7 antagonist IRS 661 (10 μM) (left graph). The data shows the mean of three independent experiments ± SD. We performed immunoblot analyses on IRS 661-treated-LCLs with antibodies specific for BZLF1 and actin (middle picture). The middle picture shows one sample and the right graph represents three independent experiments.

3.9.4 Proposed Model

In summary, we found that the number of cells in which lytic replication takes place is increased both *in vitro* and *in vivo* by the non-coding RNA EBER2, but not by its homolog on the B95-8 genome. These two EBER2 RNAs display a limited number of polymorphisms, some of which influence their half-life and expression levels. M81 EBER2 modified the expression of a large number of cellular genes including CXCL8. This chemokine was able to compensate the absence of EBER2, suggesting that it represents the main target of this non-coding RNA. We found that the exosomal fraction of B cells infected with wild type M81 that carries the EBER molecules, are able to increase CXCL8 and BZLF1 production and thus partly complement the phenotype of B cells infected with a virus that lacks the EBER RNAs. The effect of EBER2 on EBV lytic replication required a functional TLR7, a sensor of viral single-stranded RNA (ssRNA). Therefore, we propose a model in which EBERs are vehicled into the exosomal fraction of infected B cells to initiate lytic replication in a paracrine manner through CXCL8 secretion induced by TLR7 stimulation (Fig. 3.28). These results indicate that EBERs from a NPC-derived virus variant contribute to lytic

replication in B cells and activate production of a chemokine involved in carcinogenesis.

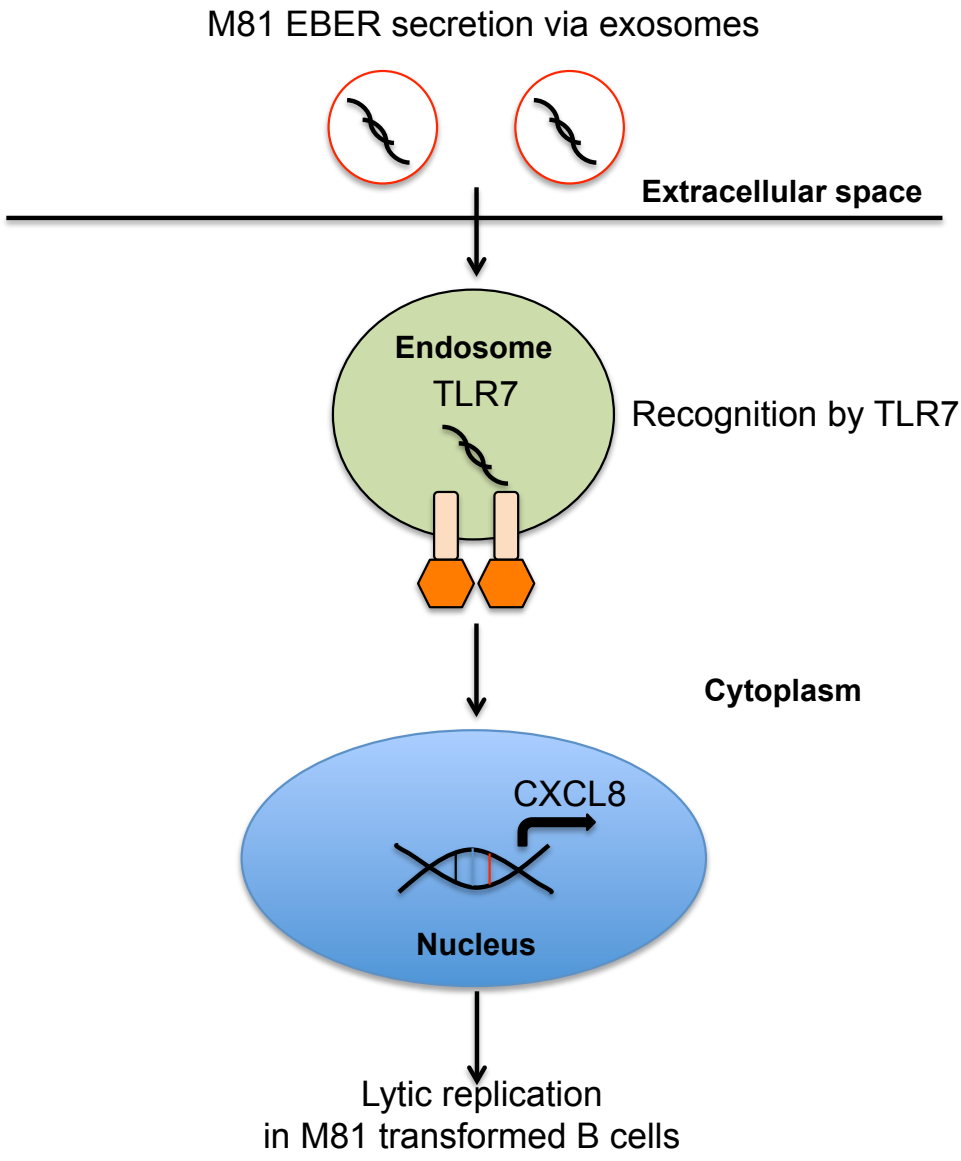

Fig. 3.28 Working model. We propose a model in which EBERs are vehicled into the exosomal fraction of infected B cells to initiate lytic replication in a paracrine manner through CXCL8 secretion induced by TLR7 stimulation.

4 Discussion

The Epstein-Barr virus (EBV) M81 strain was isolated from a carcinoma and induces potent spontaneous virus production in infected B cells. M81 lytic replication was found to induce chromosome instability, offering a direct link between both events. Thus, the study of the mechanisms that mediate M81's ability to replicate is also important to study its oncogenic properties. We found that the non-coding RNA EBER2 potentiated lytic replication both *in vitro* and *in vivo*, but that this property was not shared by its homolog from the B95-8 EBV strain. M81 and B95-8 EBER2 homologs displayed a limited number of polymorphisms, some of which influence their half-life and expression levels. M81 EBER2 modified the expression of a large number of cellular genes including CXCL8. This chemokine was able to compensate the absence of EBER2, suggesting that it represents the main target of this non-coding RNA. We found that the exosomal fraction of B cells infected with wild type M81 carries the EBER molecules and is able to increase CXCL8 and to launch virus production but that this effect required a functional TLR7, a sensor of viral single-stranded RNA (ssRNA). Therefore, we propose a model in which EBERs are vehicled into the exosomal fraction of infected B cells to initiate lytic replication in a paracrine manner through CXCL8 secretion induced by TLR7 stimulation. These results indicate that M81 EBERs contribute to lytic replication in B cells and activate production of a chemokine involved in inflammation and carcinogenesis.

4.1 EBV strains derived from NPC carry a unique EBER2 sequence

The pathogenesis of NPC remains unclear. Biopsies of NPC show expression of the EBERs, EBNA1, and BART miRNAs, that is accompanied by weak and patchy expression of LMP1 and LMP2A/B. This form of EBV latency, also known as latency II, was subsequently found in cases of EBV-associated Hodgkin lymphoma (HL) (Young and Dawson, 2014). However, the expression of these viral products remains unsufficient to transform epithelial cells.

EBV lytic replication is a major risk factor for the development of EBV-positive nasopharyngeal carcinoma (NPC). The geographical distribution of NPC is mainly but not entirely restricted to South East Asia (Busson et al., 2004). What causes this distribution in disease incidence is unclear, although the age at which EBV infection takes place, environmental factors such as food contaminations with nitrosamines and phorbol esters or smoking, are all known to play an important role (Hsu and Glaser, 2000; Hsu et al., 2009; Jia and Qin, 2012; Yu and Yuan, 2002). The genetic background of the affected individuals has also been invoked to explain this puzzling phenomenon (Hildesheim et al., 1997; Li et al., 2009; Lu et al., 1990; Ung et al., 1999). Another nonexclusive hypothesis is that the occurrence of these diseases reflects the existence of multiple virus subtypes that are endowed with different properties but are found only in restricted geographic areas. Strong evidence for genetic polymorphisms between EBV isolates has been garnered from partial or total sequencing of multiple viruses from all over the world (Feederle et al., 2015).

By performing alignments in 172 EBV genomes, we found that EBV strains from NPC, frequently carry EBER2 polymorphisms that differs from the EBV strains derived from benign and tumor lesions such as Burkitt's lymphomas (BL) and gastric

carcinomas (GC). This suggests that NPC strains carry unique EBER2 sequences. EBER recombinants have been engineered and introduced into host B-lymphocytes. All these observations indicate that M81 EBER2 derived from NPC might have unique functions. M81 EBER2 polymorphisms influenced multiple parameters including half-life and expression levels. Therefore, we think that the EBER2 RNA might play an important role in the development of NPC through its role on lytic replication.

4.2 Functional analysis of EBERs in lytic replication *in vitro* and *in vivo*

The functions served by the EBERs in the infected cells have been controversially discussed since their identification. Early papers found that deletion of the EBERs does not influence lytic replication in a model of replication induced by TPA (Swaminathan et al., 1991). More recently, EBER2 has been proposed to increase lytic replication. Lee et al reported that knockdown of EBER2 decreases EBV lytic replication in replication-permissive EBV-positive cell line HH514-16 with sodium butyrate. Interestingly, EBER2 knockdown did not affect the expression of BZLF1 that is important for the initiation of lytic replication (Lee et al., 2015). Thus, the effects described in this paper are not related to our own results.

We used a model of spontaneous lytic replication combined to knockout viruses from two viral strains lacking the EBERs in primary B cells to analyze their impact on lytic replication. We concluded that M81 EBER2, but not B95-8 EBER2, increases the frequency of lytic replication initiation in infected B cells, although some degree of lytic replication remained visible in cells infected with the mutant virus. It is

important to note that the EBERs only amplify spontaneous lytic replication but do not initiate it, a finding in line with the observation that cells infected with M81/ΔE1+2 still show some degree of lytic replication. The positive contribution of EBER2 to M81 replication could be confirmed by complementation assays. Here we found that transfection of the M81 EBERs, but not of the B95-8 EBERs, restored BZLF1 expression in B cells infected with the M81/ΔE1+2 mutant.

M81 EBER2 possesses unique polymorphisms but M81-infected cells also express this non-coding RNA at much higher levels than cells infected with other virus strains. Thus, both the quantity and the sequence of the M81 EBER2 might explain its ability to boost replication. However, complementation of the M81/ΔE1+2 mutant with either M81 and B95-8 EBERs cloned under an inducible promoter led to nearly similar expression levels. Because the B95-8 EBER2 did not complement M81/ΔE1+2 efficiently despite being expressed at the same levels as M81 EBER2, this suggests that polymorphisms between both types of EBERs rather than differences in expression levels explain the differences between the viral isolates. However, this does not mean that the high levels of EBER expression in M81 plays no role in the amplification of replication. Indeed, the increase in lytic replication induced by the M81 EBER2 is dose-dependent. We also evaluated the role played by EBER in the control of lytic replication using an *in vivo* model of EBV infection and injected resting B cells exposed to M81/ΔE1+2 or M81/ΔE1+2 Rev viruses to into immuno-suppressed NSG mice. We found that mice infected with the M81/ΔE1+2 mutant also showed a reduction in expression of the lytic proteins as reported *in vitro*. We conclude that the non-coding RNA EBER2 potentiated lytic replication both *in vitro* and *in vivo* in a mice model.

The larger amounts of EBER present in M81-infected cells could partly be ascribed to an increased half life of the M81, relative to B95-8 EBER2. Four of the M81-specific polymophisms explain this differential behavior and mutation of any of these sites clearly modifies the abundance of the non-coding RNA. However, we also found that the replicating cells themselves produce very large amounts of EBERs. Indeed, induction of lytic replication through transfection of BZLF1 massively increases the amount of EBER2, and to a lower extent of EBER1, produced in the cells. A previous paper reported that EBER-1 and EBER-2 were downregulated during the switch to lytic viral replication (Greifenegger et al., 1998). In contrast, another paper reported that EBER1 and EBER2 were upregulated in Akata cell line following IgG cross-linking-induced replication (Yuan et al., 2006). These discrepancies could be explained by the different experimental systems used in the different studies.

It remains unclear at this point whether the BZLF1 protein directly transactivates the promoter elements of the EBER RNAs or indirectly incluence some viral or cellular proteins that play a role in the EBER expression. Although only few cells undergo lytic replication, the massive production of EBER by these cells is likely to influence the global EBER production of the infected cell population. Thus, multiple mechanisms converge to explain the high levels of EBER2 production in M81-infected cells.

We currently do not know how the M81 EBER2 polymorphisms render the molecule active. We know that they influence the half-life and thus the global production of EBER2. Furthermore, they might influence the global structure of the EBER2 RNA or modify the multiple RNA-protein interactions of EBER2 that were presented in the introduction. It is interesting to note that the EBER2 polymorphisms are located in a

region of the molecule that has previously been found to interact with the terminal repeats of the viral DNA molecule (Please see paragraph 4.4).

4.3 M81 EBER2 amplifies CXCL8 through TLR7 to promote lytic replication

Using a RNA microarray analysis and a Human Cytokine Array, we found that M81 EBER2 induces the expression of CXCL8 in infected cells, a chemokine that stimulates the intensity of replication in infected cells. This effect was specific to the M81 EBER2 molecule and not shared with its B95-8 homolog and this probably explains why only M81 EBER2 potentiated lytic replication but not by B95-8 EBER2. CXCL8 is a chemokine that is secreted as a result of an activation of the immune system, including its innate branch. We searched for mechanisms that could link EBER and CXCL8 production. Because lytic replication takes place in infected B cells in the absence of T cells or other members of the adaptive immune response, we deemed it more likely that CXCL8 was activated in M81-infected B cells by the innate immune response. However, EBER is mainly located in the nucleus of infected cells and cannot a priori access restriction factors that are mainly located in the cytoplasm or in the endosome compartments. EBER has been reported to be incorporated in exosomes produced by infected cells (Ahmed et al., 2014). These subcellular organelles could access dendritic cells and activate TLR3 in the endosome (Iwakiri et al., 2009).

We tested whether such a mechanism could also act in a paracrine manner. However, TLR3 is not expressed in B cells. We canvassed a transcriptome of EBV-infected B cells and looked at the expression of TLR members expressed in the endosome. This

analysis confirmed that while TLR3 and TLR8 are hardly expressed in infected B cells, TLR7 is expressed in these cells, as previously reported (Hanten et al., 2008).

We found that the effect of EBER2 on lytic replication via CXCL8 stimulation could be reproduced by exposing infected cells to exosomes from LCLs infected with wild type M81 virus, a subcellular structure that was previously identified by several authors to contain EBERs in association with the La protein (Iwakiri et al., 2009). Extracellular EBERs were previously found to activate TLR3 in NK cells and in T cells, leading to the release of IFN beta and gamma, together with TNF alpha (Iwakiri et al., 2009). We could not identify such an effect in M81-infected B cells that neither express TLR3, nor secrete these latter cytokines. A major difference between the present and the published experimental systems is that the latter used transfected EBER molecules that are likely to reach cytoplasmic structures where they could induce signaling, e.g. after recognition by RIG-I, although EBERs are typically nuclear in location. Instead we found a link between EBER, CXCL8 expression and TLR7 activation. TLR7 is located in the cellular endosome and its expression is up regulated by the EBV infection (Martin et al., 2007). The results of the cytokine array and of the transcriptome analysis make us confident that the positive impact of EBERs on cytokines in LCLs infected by M81 is limited to CXCL8 and that TLR7 is implicated in that process. We could show that the EBER complex contained in the exosomes is sufficient to include CXCL8 expression and lytic replication, although it remains possible that EBER2 also accesses infected cells through another route. Similarly, M81 EBER2 might also interact with cellular PAMPs other than TLR7. It is interesting to note that lytic replication itself strongly enhances EBER production within replicating cells. This increased production might enhance the total concentration of EBER in exosomes of the extracellular milieu and contribute to the

induction of lytic replication in neighboring cells, thereby building a self-reinforcing positive loop.

Interestingly, we found that the effect of EBER2 on lytic replication via CXCL8 stimulation could not be reproduced by exposing infected cells to exosomes from LCLs infected with wild type B95-8 virus.

Researchers reported that guanosine (G)- and uridine (U)-rich ssRNA oligonucleotides derived from human immunodeficiency virus-1 (HIV-1) stimulate dendritic cells (DC) and macrophages to secrete interferon-α and proinflammatory, as well as regulatory cytokines. These data suggest that ssRNA represents a physiological ligand for TLR7 and TLR8 (Heil et al., 2004). Forsbach et al then identified GU-rich Oligoribonucleotides (ORNs) as TLR7/8 RNA ligands that stimulate human TLR7 and TLR8 immune responses (Forsbach et al., 2008).

We reported that M81 carries EBER2 polymorphisms that generate a GU-rich sequence. Whether these EBER2 polymorphisms influence the TLR7 recognization is currently under investigation.

We conclude from this set of data that the non-coding RNA M81 EBER2 induced inflammation in a paracrine manner to enhance virus production. However, it is important to note that cells undergoing lytic replication remain a minority, although all cells are in contact with exosomes, demonstrating that additional mechanisms that negatively control lytic replication exist. We found one of these mechanisms, as only 40% of cells incorporate EBERs, presumably because they actively block endocytosis of EBER-containing exosomes. These observations have important consequences for the pathogenesis of EBV-associated tumors. Elevated chronic CXCL8 production is a well-established cancer risk. Furthermore, carcinoma cells from nasopharyngeal carcinoma cells that are infected with the Epstein-Barr virus frequently express high

levels of CXCL8. This identifies a second M81-specific oncogenic trait after the ability of the M81 particles to induce centrosome overduplication.

4.4 Interplay between LMP1/2 and the EBER RNAs

EBER2 has previously been implicated in the lytic replication induced by sodium butyrate in the Burkitt's lymphoma cell line HH514, although the precise role of EBER2 in this process is not clear from this study. The authors found that EBER2 facilitates recruitment of PAX5 to the LMP1 and LMP2 transcripts through RNA-RNA association between EBER2 and the terminal repeats sequences found in the 5'UTR of the viral latent proteins. This interaction was suggested to facilitate DNA replication, although the precise mechanism that underlies this function remains unknown (Lee et al., 2015). There are many differences between this study and the currently presented. First, we could not gather any evidence that EBER2 influences transcription of M81 LMP1 and LMP2. These transcripts varied in amplitude over a period of 3 months and were actually expressed slightly more in cells infected with the ΔEBER knockout. However, it is interesting to note that we observed such an effect in cells infected with B95-8, suggesting another difference between B95-8 and M81. It is noteworthy that the four polymorphisms that characterize M81 EBER2 are located in the EBER region that were found to interact with the terminal repeats, thereby possibly explaining the absence of modification of LMP1 and 2 transcription in cells infected with M81/ΔEBER1+2. Although LMP1 and LMP2 transcription is mildly up regulated in cells infected with B95-8/ΔEBER, this deletion had no effect on the rate of lytic replication in infected cells as cells remained non-permissive to lytic replication. Thus, the effects of EBER2 on lytic replication described in the study by Lee et al. are distinct from those reported in the present study. The cellular

background might also play a role in the effect served by EBER2. Earlier studies found that the deletion of EBER2 had no influence on the lytic replication of primary B cells transformed with an EBER-null virus constructed on the basis of P3HR1 and induced with TPA (Swaminathan et al., 1991). Therefore, the EBER deletion has a different effect in transformed B cells and in Burkitt's lymphoma B cells.

4.5 The relationship between CXCL8 and NPC

Nasopharyngeal carcinoma (NPC) has a high incidence rate in southern China and southeast Asia. Among head and neck cancers, NPC has the highest metastasis rate (Ahmad and Stefani, 1986; Lee et al., 1993): at the time of diagnosis: 74.5% of patients present with regional lymph node metastasis and 19.9% present with distant metastasis (Huang et al., 1996; Wei and Mok, 2007). Distant metastasis is therefore the major cause of treatment failure, although NPC is sensitive to radio-therapy.

Epstein-Barr virus infection has been closely linked to NPC (Dong et al., 2012; Ji et al., 2011; Liang et al., 2012). It has been observed that CXCL8 expression in NPC cells can also be induced by Epstein–Barr virus proteins (Hsu et al., 2008; Ren et al., 2004; Yoshizaki et al., 2001). Here, we have identified that CXCL8 expression in B cells can be enhanced by EBV-encoded RNAs.

Previous papers report that CXCL8 serves as an independent prognostic indicator of overall survival, disease-free survival, and metastasis-free survival for patients with NPC. CXCL8 promotes NPC metastasis via autocrine and paracrine means, involving activation of AKT signaling and inducing EMT in NPC cells (Liu et al., 2012).

Our study suggests that drugs against CXCL8 receptor could be firstly tested in mice model and in case of success could possibly be tested in clinical trials.

5 References

Adamson, A.L., D. Darr, E. Holley-Guthrie, R.A. Johnson, A. Mauser, J. Swenson, and S. Kenney. 2000. Epstein-Barr virus immediate-early proteins BZLF1 and BRLF1 activate the ATF2 transcription factor by increasing the levels of phosphorylated p38 and c-Jun N-terminal kinases. *Journal of virology* 74:1224-1233.

Ahmad, A., and S. Stefani. 1986. Distant metastases of nasopharyngeal carcinoma: a study of 256 male patients. *Journal of surgical oncology* 33:194-197.

Ahmed, W., P.S. Philip, S. Tariq, and G. Khan. 2014. Epstein-Barr virus-encoded small RNAs (EBERs) are present in fractions related to exosomes released by EBV-transformed cells. *PloS one* 9:e99163.

Akira, S., and K. Takeda. 2004. Toll-like receptor signalling. *Nature reviews. Immunology* 4:499-511.

Akusjarvi, G., M.B. Mathews, P. Andersson, B. Vennstrom, and U. Pettersson. 1980. Structure of genes for virus-associated RNAI and RNAII of adenovirus type 2. *Proceedings of the National Academy of Sciences of the United States of America* 77:2424-2428.

Alexopoulou, L., A.C. Holt, R. Medzhitov, and R.A. Flavell. 2001. Recognition of double-stranded RNA and activation of NF-kappaB by Toll-like receptor 3. *Nature* 413:732-738.

Amelio, A.L., L.J. Miraglia, J.J. Conkright, B.A. Mercer, S. Batalov, V. Cavett, A.P. Orth, J. Busby, J.B. Hogenesch, and M.D. Conkright. 2007. A coactivator trap identifies NONO (p54nrb) as a component of the cAMP-signaling pathway. *Proceedings of the National Academy of Sciences of the United States of America* 104:20314-20319.

Arrand, J.R., and L. Rymo. 1982. Characterization of the major Epstein-Barr virus-specific RNA in Burkitt lymphoma-derived cells. *Journal of virology* 41:376-389.

Bachmann, M., K. Pfeifer, H.C. Schroder, and W.E. Muller. 1989. The La antigen shuttles between the nucleus and the cytoplasm in CV-1 cells. *Molecular and cellular biochemistry* 85:103-114.

Baer, R., A.T. Bankier, M.D. Biggin, P.L. Deininger, P.J. Farrell, T.J. Gibson, G. Hatfull, G.S. Hudson, S.C. Satchwell, C. Seguin, and et al. 1984. DNA sequence and expression of the B95-8 Epstein-Barr virus genome. *Nature* 310:207-211.

Balfour, H.H., Jr., O.A. Odumade, D.O. Schmeling, B.D. Mullan, J.A. Ed, J.A. Knight, H.E. Vezina, W. Thomas, and K.A. Hogquist. 2013. Behavioral, virologic, and immunologic factors associated with acquisition and severity of primary Epstein-Barr virus infection in university students. *The Journal of infectious diseases* 207:80-88.

Bhat, R.A., and B. Thimmappaya. 1983. Two small RNAs encoded by Epstein-Barr virus can functionally substitute for the virus-associated RNAs in the lytic growth of adenovirus 5. *Proceedings of the National Academy of Sciences of the United States of America* 80:4789-4793.

Budhiraja, S., H. Liu, J. Couturier, A. Malovannaya, J. Qin, D.E. Lewis, and A.P. Rice. 2015. Mining the human complexome database identifies RBM14 as an XPO1-associated protein involved in HIV-1 Rev function. *Journal of virology* 89:3557-3567.

Busson, P., C. Keryer, T. Ooka, and M. Corbex. 2004. EBV-associated nasopharyngeal carcinomas: from epidemiology to virus-targeting strategies. *Trends in microbiology* 12:356-360.

Calderwood, M.A., A.M. Holthaus, and E. Johannsen. 2008. The Epstein-Barr virus LF2 protein inhibits viral replication. *Journal of virology* 82:8509-8519.

Cesarman, E. 2011. Gammaherpesvirus and lymphoproliferative disorders in immunocompromised patients. *Cancer letters* 305:163-174.

Chang, K.L., Y.Y. Chen, D. Shibata, and L.M. Weiss. 1992. Description of an in situ hybridization methodology for detection of Epstein-Barr virus RNA in paraffin-embedded tissues, with a survey of normal and neoplastic tissues. *Diagnostic molecular pathology : the American journal of surgical pathology, part B* 1:246-255.

Clarke, P.A., N.A. Sharp, and M.J. Clemens. 1992. Expression of genes for the Epstein-Barr virus small RNAs EBER-1 and EBER-2 in Daudi Burkitt's lymphoma cells: effects of interferon treatment. *The Journal of general virology* 73 (Pt 12):3169-3175.

Daikoku, T., A. Kudoh, M. Fujita, Y. Sugaya, H. Isomura, N. Shirata, and T. Tsurumi. 2005. Architecture of replication compartments formed during Epstein-Barr virus lytic replication. *Journal of virology* 79:3409-3418.

Darr, C.D., A. Mauser, and S. Kenney. 2001. Epstein-Barr virus immediate-early protein BRLF1 induces the lytic form of viral replication through a mechanism involving phosphatidylinositol-3 kinase activation. *Journal of virology* 75:6135-6142.

Dobbelstein, M., and T. Shenk. 1995. In vitro selection of RNA ligands for the ribosomal L22 protein associated with Epstein-Barr virus-expressed RNA by using randomized and cDNA-derived RNA libraries. *Journal of virology* 69:8027-8034.

Dominguez-Villar, M., A.S. Gautron, M. de Marcken, M.J. Keller, and D.A. Hafler. 2015. TLR7 induces anergy in human CD4(+) T cells. *Nature immunology* 16:118-128.

Dong, J.Q., M.Z. Li, Z.G. Liu, Q. Zhong, D. Xiong, L.H. Xu, Y. Du, Y.F. Xia, and M.S. Zeng. 2012. Establishment and characterization of a novel nasopharyngeal carcinoma cell line (SUNE2) from a Cantonese patient. *Chinese journal of cancer* 31:36-44.

Elia, A., J. Vyas, K.G. Laing, and M.J. Clemens. 2004. Ribosomal protein L22 inhibits regulation of cellular activities by the Epstein-Barr virus small RNA EBER-1. *European journal of biochemistry* 271:1895-1905.

Epstein, M.A., B.G. Achong, and Y.M. Barr. 1964. Virus particles in cultured lymphoblasts from Burkitt's lymphomas. *Lancet (London, England)* 1:702-703.

Feederle, R., E.J. Bartlett, and H.J. Delecluse. 2010. Epstein-Barr virus genetics: talking about the BAC generation. *Herpesviridae* 1:6.

Feederle, R., O. Klinke, A. Kutikhin, R. Poirey, M.H. Tsai, and H.J. Delecluse. 2015. Epstein-Barr Virus: From the Detection of Sequence Polymorphisms to the Recognition of Viral Types. *Current topics in microbiology and immunology* 390:119-148.

Feederle, R., M. Kost, M. Baumann, A. Janz, E. Drouet, W. Hammerschmidt, and H.J. Delecluse. 2000. The Epstein-Barr virus lytic program is controlled by the co-operative functions of two transactivators. *The EMBO journal* 19:3080-3089.

Flanagan, J., J. Middeldorp, and T. Sculley. 2003. Localization of the Epstein-Barr virus protein LMP 1 to exosomes. *The Journal of general virology* 84:1871-1879.

Fok, V., K. Friend, and J.A. Steitz. 2006. Epstein-Barr virus noncoding RNAs are confined to the nucleus, whereas their partner, the human La protein, undergoes nucleocytoplasmic shuttling. *The Journal of cell biology* 173:319-325.

Forsbach, A., J.G. Nemorin, C. Montino, C. Muller, U. Samulowitz, A.P. Vicari, M. Jurk, G.K. Mutwiri, A.M. Krieg, G.B. Lipford, and J. Vollmer. 2008. Identification of RNA sequence motifs stimulating sequence-specific TLR8-dependent immune responses. *Journal of immunology (Baltimore, Md. : 1950)* 180:3729-3738.

Glickman, J.N., J.G. Howe, and J.A. Steitz. 1988. Structural analyses of EBER1 and EBER2 ribonucleoprotein particles present in Epstein-Barr virus-infected cells. *Journal of virology* 62:902-911.

Gottlieb, E., and J.A. Steitz. 1989. The RNA binding protein La influences both the accuracy and the efficiency of RNA polymerase III transcription in vitro. *The EMBO journal* 8:841-850.

Gratacos, F.M., and G. Brewer. 2010. The role of AUF1 in regulated mRNA decay. *Wiley interdisciplinary reviews. RNA* 1:457-473.

Gregorovic, G., R. Bosshard, C.E. Karstegl, R.E. White, S. Pattle, A.K. Chiang, O. Dittrich-Breiholz, M. Kracht, R. Russ, and P.J. Farrell. 2011. Cellular gene expression that correlates with EBER expression in Epstein-Barr Virus-infected lymphoblastoid cell lines. *Journal of virology* 85:3535-3545.

Greifenegger, N., M. Jager, L.A. Kunz-Schughart, H. Wolf, and F. Schwarzmann. 1998. Epstein-Barr virus small RNA (EBER) genes: differential regulation during lytic viral replication. *Journal of virology* 72:9323-9328.

Hagemeier, S.R., E.A. Barlow, A.A. Kleman, and S.C. Kenney. 2011. The Epstein-Barr virus BRRF1 protein, Na, induces lytic infection in a TRAF2- and p53-dependent manner. *Journal of virology* 85:4318-4329.

Hanten, J.A., J.P. Vasilakos, C.L. Riter, L. Neys, K.E. Lipson, S.S. Alkan, and W. Birmachu. 2008. Comparison of human B cell activation by TLR7 and TLR9 agonists. *BMC immunology* 9:39.

Heil, F., P. Ahmad-Nejad, H. Hemmi, H. Hochrein, F. Ampenberger, T. Gellert, H. Dietrich, G. Lipford, K. Takeda, S. Akira, H. Wagner, and S. Bauer. 2003. The Toll-like receptor 7 (TLR7)-specific stimulus loxoribine uncovers a strong relationship within the TLR7, 8 and 9 subfamily. *European journal of immunology* 33:2987-2997.

Heil, F., H. Hemmi, H. Hochrein, F. Ampenberger, C. Kirschning, S. Akira, G. Lipford, H. Wagner, and S. Bauer. 2004. Species-specific recognition of single-stranded RNA via toll-like receptor 7 and 8. *Science (New York, N.Y.)* 303:1526-1529.

Heilmann, A.M., M.A. Calderwood, D. Portal, Y. Lu, and E. Johannsen. 2012. Genome-wide analysis of Epstein-Barr virus Rta DNA binding. *Journal of virology* 86:5151-5164.

Henson, B.W., E.M. Perkins, J.E. Cothran, and P. Desai. 2009. Self-assembly of Epstein-Barr virus capsids. *Journal of virology* 83:3877-3890.

Hildesheim, A., L.M. Anderson, C.J. Chen, Y.J. Cheng, L.A. Brinton, A.K. Daly, C.D. Reed, I.H. Chen, N.E. Caporaso, M.M. Hsu, J.Y. Chen, J.R. Idle, R.N. Hoover, C.S. Yang, and S.K. Chhabra. 1997. CYP2E1 genetic polymorphisms and risk of nasopharyngeal carcinoma in Taiwan. *Journal of the National Cancer Institute* 89:1207-1212.

Hong, G.K., H.J. Delecluse, H. Gruffat, T.E. Morrison, W.H. Feng, A. Sergeant, and S.C. Kenney. 2004. The BRRF1 early gene of Epstein-Barr virus encodes a transcription factor that enhances induction of lytic infection by BRLF1. *Journal of virology* 78:4983-4992.

Hong, G.K., M.L. Gulley, W.H. Feng, H.J. Delecluse, E. Holley-Guthrie, and S.C. Kenney. 2005. Epstein-Barr virus lytic infection contributes to lymphoproliferative disease in a SCID mouse model. *Journal of virology* 79:13993-14003.

Hornung, V., J. Ellegast, S. Kim, K. Brzozka, A. Jung, H. Kato, H. Poeck, S. Akira, K.K. Conzelmann, M. Schlee, S. Endres, and G. Hartmann. 2006. 5'-Triphosphate RNA is the ligand for RIG-I. *Science (New York, N.Y.)* 314:994-997.

Houmani, J.L., C.I. Davis, and I.K. Ruf. 2009. Growth-promoting properties of Epstein-Barr virus EBER-1 RNA correlate with ribosomal protein L22 binding. *Journal of virology* 83:9844-9853.

Howe, J.G., and M.D. Shu. 1988. Isolation and characterization of the genes for two small RNAs of herpesvirus papio and their comparison with Epstein-Barr virus-encoded EBER RNAs. *Journal of virology* 62:2790-2798.

Howe, J.G., and M.D. Shu. 1989. Epstein-Barr virus small RNA (EBER) genes: unique transcription units that combine RNA polymerase II and III promoter elements. *Cell* 57:825-834.

Howe, J.G., and J.A. Steitz. 1986. Localization of Epstein-Barr virus-encoded small RNAs by in situ hybridization. *Proceedings of the National Academy of Sciences of the United States of America* 83:9006-9010.

Hsu, J.L., and S.L. Glaser. 2000. Epstein-barr virus-associated malignancies: epidemiologic patterns and etiologic implications. *Critical reviews in oncology/hematology* 34:27-53.

Hsu, M., S.Y. Wu, S.S. Chang, I.J. Su, C.H. Tsai, S.J. Lai, A.L. Shiau, K. Takada, and Y. Chang. 2008. Epstein-Barr virus lytic transactivator Zta enhances chemotactic activity through induction of interleukin-8 in nasopharyngeal carcinoma cells. *Journal of virology* 82:3679-3688.

Hsu, W.L., J.Y. Chen, Y.C. Chien, M.Y. Liu, S.L. You, M.M. Hsu, C.S. Yang, and C.J. Chen. 2009. Independent effect of EBV and cigarette smoking on nasopharyngeal carcinoma: a 20-year follow-up study on 9,622 males without family history in Taiwan. *Cancer epidemiology, biomarkers & prevention : a publication of the American Association for Cancer Research, cosponsored by the American Society of Preventive Oncology* 18:1218-1226.

Huang, C.J., S.W. Leung, S.L. Lian, C.J. Wang, F.M. Fang, and Y.H. Ho. 1996. Patterns of distant metastases in nasopharyngeal carcinoma. *The Kaohsiung journal of medical sciences* 12:229-234.

Iwakiri, D., Y. Eizuru, M. Tokunaga, and K. Takada. 2003. Autocrine growth of Epstein-Barr virus-positive gastric carcinoma cells mediated by an Epstein-Barr virus-encoded small RNA. *Cancer research* 63:7062-7067.

Iwakiri, D., T.S. Sheen, J.Y. Chen, D.P. Huang, and K. Takada. 2005. Epstein-Barr virus-encoded small RNA induces insulin-like growth factor 1 and supports growth of nasopharyngeal carcinoma-derived cell lines. *Oncogene* 24:1767-1773.

Iwakiri, D., and K. Takada. 2010. Role of EBERs in the pathogenesis of EBV infection. *Advances in cancer research* 107:119-136.

Iwakiri, D., L. Zhou, M. Samanta, M. Matsumoto, T. Ebihara, T. Seya, S. Imai, M. Fujieda, K. Kawa, and K. Takada. 2009. Epstein-Barr virus (EBV)-encoded small RNA is released from EBV-infected cells and activates signaling from Toll-like receptor 3. *The Journal of experimental medicine* 206:2091-2099.

Ji, M.F., Y.L. Yu, W.M. Cheng, Y.S. Zong, P.S. Ng, D.T. Chua, and M.H. Ng. 2011. Detection of Stage I nasopharyngeal carcinoma by serologic screening and clinical examination. *Chinese journal of cancer* 30:120-123.

Jia, W.H., and H.D. Qin. 2012. Non-viral environmental risk factors for nasopharyngeal carcinoma: a systematic review. *Seminars in cancer biology* 22:117-126.

Jochum, S., A. Moosmann, S. Lang, W. Hammerschmidt, and R. Zeidler. 2012. The EBV immunoevasins vIL-10 and BNLF2a protect newly infected B cells from immune recognition and elimination. *PLoS pathogens* 8:e1002704.

Kalejta, R.F. 2008. Tegument proteins of human cytomegalovirus. *Microbiology and molecular biology reviews : MMBR* 72:249-265, table of contents.

Kanda, T., M. Yajima, N. Ahsan, M. Tanaka, and K. Takada. 2004. Production of high-titer Epstein-Barr virus recombinants derived from Akata cells by using a bacterial artificial chromosome system. *Journal of virology* 78:7004-7015.

Kang, D.C., R.V. Gopalkrishnan, Q. Wu, E. Jankowsky, A.M. Pyle, and P.B. Fisher. 2002. mda-5: An interferon-inducible putative RNA helicase with double-stranded RNA-dependent ATPase activity and melanoma growth-suppressive properties. *Proceedings of the National Academy of Sciences of the United States of America* 99:637-642.

Kasahara, Y., A. Yachie, K. Takei, C. Kanegane, K. Okada, K. Ohta, H. Seki, N. Igarashi, K. Maruhashi, K. Katayama, E. Katoh, G. Terao, Y. Sakiyama, and S. Koizumi. 2001. Differential cellular targets of Epstein-Barr virus (EBV) infection between acute EBV-associated hemophagocytic lymphohistiocytosis and chronic active EBV infection. *Blood* 98:1882-1888.

Katze, M.G., M. Wambach, M.L. Wong, M. Garfinkel, E. Meurs, K. Chong, B.R. Williams, A.G. Hovanessian, and G.N. Barber. 1991. Functional expression and RNA binding analysis of the interferon-induced, double-stranded RNA-activated, 68,000-Mr protein kinase in a cell-free system. *Molecular and cellular biology* 11:5497-5505.

Kawai, T., K. Takahashi, S. Sato, C. Coban, H. Kumar, H. Kato, K.J. Ishii, O. Takeuchi, and S. Akira. 2005. IPS-1, an adaptor triggering RIG-I- and Mda5-mediated type I interferon induction. *Nature immunology* 6:981-988.

Kieff, E., T. Dambaugh, M. Heller, W. King, A. Cheung, V. van Santen, M. Hummel, C. Beisel, S. Fennewald, K. Hennessy, and T. Heineman. 1982. The biology and chemistry of Epstein-Barr virus. *The Journal of infectious diseases* 146:506-517.

Kieff, E., and A.B. Rickinson. 2007. Epstein-Barr virus and its replication. Field Virology. Philadelphia : Wolters Kluwer Health/Lippincott Williams & Wilkins, 2603-2654 pp.

Kikuta, H., Y. Sakiyama, S. Matsumoto, T. Oh-Ishi, T. Nakano, T. Nagashima, T. Oka, T. Hironaka, and K. Hirai. 1993. Fatal Epstein-Barr virus-associated hemophagocytic syndrome. *Blood* 82:3259-3264.

Kirschner, A.N., J. Omerovic, B. Popov, R. Longnecker, and T.S. Jardetzky. 2006. Soluble Epstein-Barr virus glycoproteins gH, gL, and gp42 form a 1:1:1 stable complex that acts like soluble gp42 in B-cell fusion but not in epithelial cell fusion. *Journal of virology* 80:9444-9454.

Kitagawa, N., M. Goto, K. Kurozumi, S. Maruo, M. Fukayama, T. Naoe, M. Yasukawa, K. Hino, T. Suzuki, S. Todo, and K. Takada. 2000. Epstein-Barr virus-encoded poly(A)(-) RNA supports Burkitt's lymphoma growth through interleukin-10 induction. *The EMBO journal* 19:6742-6750.

Klein, G., and I. Ernberg. 2007. Effects on apoptosis, cell cycle and transformation, and comparative aspects of EBV with other known DNA tumor viruses. In Human Herpesviruses: Biology, Therapy, and Immunoprophylaxis. A. Arvin, G. Campadelli-Fiume, E. Mocarski, P.S. Moore, B. Roizman, R. Whitley, and K. Yamanishi, editors. Cambridge University Press, Cambridge.

Komano, J., S. Maruo, K. Kurozumi, T. Oda, and K. Takada. 1999. Oncogenic role of Epstein-Barr virus-encoded RNAs in Burkitt's lymphoma cell line Akata. *Journal of virology* 73:9827-9831.

Kula, A., L. Gharu, and A. Marcello. 2013. HIV-1 pre-mRNA commitment to Rev mediated export through PSF and Matrin 3. *Virology* 435:329-340.

Lal, A., K. Mazan-Mamczarz, T. Kawai, X. Yang, J.L. Martindale, and M. Gorospe. 2004. Concurrent versus individual binding of HuR and AUF1 to common labile target mRNAs. *The EMBO journal* 23:3092-3102.

Le, S., R. Sternglanz, and C.W. Greider. 2000. Identification of two RNA-binding proteins associated with human telomerase RNA. *Molecular biology of the cell* 11:999-1010.

Lee, A.W., S.C. Law, W. Foo, Y.F. Poon, F.K. Cheung, D.K. Chan, S.Y. Tung, M. Thaw, and J.H. Ho. 1993. Retrospective analysis of patients with nasopharyngeal carcinoma treated during 1976-1985: survival after local recurrence. *International journal of radiation oncology, biology, physics* 26:773-782.

Lee, J., T.H. Chuang, V. Redecke, L. She, P.M. Pitha, D.A. Carson, E. Raz, and H.B. Cottam. 2003. Molecular basis for the immunostimulatory activity of guanine nucleoside analogs: activation of Toll-like receptor 7. *Proceedings of the National Academy of Sciences of the United States of America* 100:6646-6651.

Lee, N., W.N. Moss, T.A. Yario, and J.A. Steitz. 2015. EBV noncoding RNA binds nascent RNA to drive host PAX5 to viral DNA. *Cell* 160:607-618.

Lee, N., G. Pimienta, and J.A. Steitz. 2012. AUF1/hnRNP D is a novel protein partner of the EBER1 noncoding RNA of Epstein-Barr virus. *RNA (New York, N.Y.)* 18:2073-2082.

Lee, N., T.A. Yario, J.S. Gao, and J.A. Steitz. 2016. EBV noncoding RNA EBER2 interacts with host RNA-binding proteins to regulate viral gene expression. *Proceedings of the National Academy of Sciences of the United States of America* 113:3221-3226.

Leopardi, R., C. Van Sant, and B. Roizman. 1997. The herpes simplex virus 1 protein kinase US3 is required for protection from apoptosis induced by the virus. *Proceedings of the National Academy of Sciences of the United States of America* 94:7891-7896.

Lerner, M.R., N.C. Andrews, G. Miller, and J.A. Steitz. 1981. Two small RNAs encoded by Epstein-Barr virus and complexed with protein are precipitated by antibodies from patients with systemic lupus erythematosus. *Proceedings of the National Academy of Sciences of the United States of America* 78:805-809.

Li, X., R. Fasano, E. Wang, K.T. Yao, and F.M. Marincola. 2009. HLA associations with nasopharyngeal carcinoma. *Current molecular medicine* 9:751-765.

Liang, F.Y., W. Sun, P. Han, X. Lu, Y.N. Lian, and X.M. Huang. 2012. Detecting plasma Epstein-Barr virus DNA to diagnose postradiation nasopharyngeal

skull base lesions in nasopharyngeal carcinoma patients: a prospective study. *Chinese journal of cancer* 31:142-149.

Liebowitz D, K.E. 1993. Epstein-Barr virus. In: The Human Herpesvirus (Roizman B, Whitley RJ, Lopez C, editors). *New York.* 107–172.:

Lin, X., M.H. Tsai, A. Shumilov, R. Poirey, H. Bannert, J.M. Middeldorp, R. Feederle, and H.J. Delecluse. 2015. The Epstein-Barr Virus BART miRNA Cluster of the M81 Strain Modulates Multiple Functions in Primary B Cells. *PLoS pathogens* 11:e1005344.

Liu, Y., L.H. Chen, Y.W. Yuan, Q.S. Li, A.M. Sun, and J. Guan. 2012. Activation of AKT is associated with metastasis of nasopharyngeal carcinoma. *Tumour biology : the journal of the International Society for Oncodevelopmental Biology and Medicine* 33:241-245.

Lu, J.Y., N. Sadri, and R.J. Schneider. 2006. Endotoxic shock in AUF1 knockout mice mediated by failure to degrade proinflammatory cytokine mRNAs. *Genes & development* 20:3174-3184.

Lu, S.J., N.E. Day, L. Degos, V. Lepage, P.C. Wang, S.H. Chan, M. Simons, B. McKnight, D. Easton, Y. Zeng, and et al. 1990. Linkage of a nasopharyngeal carcinoma susceptibility locus to the HLA region. *Nature* 346:470-471.

Mahiet, C., A. Ergani, N. Huot, N. Alende, A. Azough, F. Salvaire, A. Bensimon, E. Conseiller, S. Wain-Hobson, M. Labetoulle, and S. Barradeau. 2012. Structural variability of the herpes simplex virus 1 genome in vitro and in vivo. *Journal of virology* 86:8592-8601.

Martin, H.J., J.M. Lee, D. Walls, and S.D. Hayward. 2007. Manipulation of the toll-like receptor 7 signaling pathway by Epstein-Barr virus. *Journal of virology* 81:9748-9758.

Mauser, A., S. Saito, E. Appella, C.W. Anderson, W.T. Seaman, and S. Kenney. 2002. The Epstein-Barr virus immediate-early protein BZLF1 regulates p53 function through multiple mechanisms. *Journal of virology* 76:12503-12512.

McKenna, S.A., D.A. Lindhout, T. Shimoike, C.E. Aitken, and J.D. Puglisi. 2007. Viral dsRNA inhibitors prevent self-association and autophosphorylation of PKR. *Journal of molecular biology* 372:103-113.

Meerovitch, K., Y.V. Svitkin, H.S. Lee, F. Lejbkowicz, D.J. Kenan, E.K. Chan, V.I. Agol, J.D. Keene, and N. Sonenberg. 1993. La autoantigen enhances and

corrects aberrant translation of poliovirus RNA in reticulocyte lysate. *Journal of virology* 67:3798-3807.

Meylan, E., and J. Tschopp. 2006. Toll-like receptors and RNA helicases: two parallel ways to trigger antiviral responses. *Molecular cell* 22:561-569.

Mulcahy, L.A., R.C. Pink, and D.R. Carter. 2014. Routes and mechanisms of extracellular vesicle uptake. *Journal of extracellular vesicles* 3:

Naganuma, T., S. Nakagawa, A. Tanigawa, Y.F. Sasaki, N. Goshima, and T. Hirose. 2012. Alternative 3'-end processing of long noncoding RNA initiates construction of nuclear paraspeckles. *The EMBO journal* 31:4020-4034.

Nanbo, A., K. Inoue, K. Adachi-Takasawa, and K. Takada. 2002. Epstein-Barr virus RNA confers resistance to interferon-alpha-induced apoptosis in Burkitt's lymphoma. *The EMBO journal* 21:954-965.

Nanbo, A., and K. Takada. 2002. The role of Epstein-Barr virus-encoded small RNAs (EBERs) in oncogenesis. *Reviews in medical virology* 12:321-326.

Nemerow, G.R., C. Mold, V.K. Schwend, V. Tollefson, and N.R. Cooper. 1987. Identification of gp350 as the viral glycoprotein mediating attachment of Epstein-Barr virus (EBV) to the EBV/C3d receptor of B cells: sequence homology of gp350 and C3 complement fragment C3d. *Journal of virology* 61:1416-1420.

Nishiya, T., and A.L. DeFranco. 2004. Ligand-regulated chimeric receptor approach reveals distinctive subcellular localization and signaling properties of the Toll-like receptors. *The Journal of biological chemistry* 279:19008-19017.

Nucifora, G., C.R. Begy, P. Erickson, H.A. Drabkin, and J.D. Rowley. 1993. The 3;21 translocation in myelodysplasia results in a fusion transcript between the AML1 gene and the gene for EAP, a highly conserved protein associated with the Epstein-Barr virus small RNA EBER 1. *Proceedings of the National Academy of Sciences of the United States of America* 90:7784-7788.

Odumade, O.A., K.A. Hogquist, and H.H. Balfour, Jr. 2011. Progress and problems in understanding and managing primary Epstein-Barr virus infections. *Clinical microbiology reviews* 24:193-209.

Parkin, D.M. 2006. The global health burden of infection-associated cancers in the year 2002. *International journal of cancer* 118:3030-3044.

Ragoczy, T., and G. Miller. 2001. Autostimulation of the Epstein-Barr virus BRLF1 promoter is mediated through consensus Sp1 and Sp3 binding sites. *Journal of virology* 75:5240-5251.

Ren, Q., H. Sato, S. Murono, M. Furukawa, and T. Yoshizaki. 2004. Epstein-Barr virus (EBV) latent membrane protein 1 induces interleukin-8 through the nuclear factor-kappa B signaling pathway in EBV-infected nasopharyngeal carcinoma cell line. *The Laryngoscope* 114:855-859.

Rickinson, A.B., H.M. Long, U. Palendira, C. Munz, and A.D. Hislop. 2014. Cellular immune controls over Epstein-Barr virus infection: new lessons from the clinic and the laboratory. *Trends in immunology* 35:159-169.

Rickinson, A.B.K., E. . 2007. Epstein-Barr virus. Walters Kluwer/Lippincott: Philadelphia, PA, USA, 2007; pp. 2655–2700. ,

Robinson, A.R., S.S. Kwek, S.R. Hagemeier, C.K. Wille, and S.C. Kenney. 2011. Cellular transcription factor Oct-1 interacts with the Epstein-Barr virus BRLF1 protein to promote disruption of viral latency. *Journal of virology* 85:8940-8953.

Rooney, C., J.G. Howe, S.H. Speck, and G. Miller. 1989. Influence of Burkitt's lymphoma and primary B cells on latent gene expression by the nonimmortalizing P3J-HR-1 strain of Epstein-Barr virus. *Journal of virology* 63:1531-1539.

Rosa, M.D., E. Gottlieb, M.R. Lerner, and J.A. Steitz. 1981. Striking similarities are exhibited by two small Epstein-Barr virus-encoded ribonucleic acids and the adenovirus-associated ribonucleic acids VAI and VAII. *Molecular and cellular biology* 1:785-796.

Rosonina, E., J.Y. Ip, J.A. Calarco, M.A. Bakowski, A. Emili, S. McCracken, P. Tucker, C.J. Ingles, and B.J. Blencowe. 2005. Role for PSF in mediating transcriptional activator-dependent stimulation of pre-mRNA processing in vivo. *Molecular and cellular biology* 25:6734-6746.

Ruf, I.K., K.A. Lackey, S. Warudkar, and J.T. Sample. 2005. Protection from interferon-induced apoptosis by Epstein-Barr virus small RNAs is not mediated by inhibition of PKR. *Journal of virology* 79:14562-14569.

Ruf, I.K., P.W. Rhyne, C. Yang, J.L. Cleveland, and J.T. Sample. 2000. Epstein-Barr virus small RNAs potentiate tumorigenicity of Burkitt lymphoma cells independently of an effect on apoptosis. *Journal of virology* 74:10223-10228.

Samanta, M., D. Iwakiri, T. Kanda, T. Imaizumi, and K. Takada. 2006. EB virus-encoded RNAs are recognized by RIG-I and activate signaling to induce type I IFN. *The EMBO journal* 25:4207-4214.

Samanta, M., D. Iwakiri, and K. Takada. 2008. Epstein-Barr virus-encoded small RNA induces IL-10 through RIG-I-mediated IRF-3 signaling. *Oncogene* 27:4150-4160.

Sato, K., N. Misawa, C. Nie, Y. Satou, D. Iwakiri, M. Matsuoka, R. Takahashi, K. Kuzushima, M. Ito, K. Takada, and Y. Koyanagi. 2011. A novel animal model of Epstein-Barr virus-associated hemophagocytic lymphohistiocytosis in humanized mice. *Blood* 117:5663-5673.

Schmidt, K.N., B. Leung, M. Kwong, K.A. Zarember, S. Satyal, T.A. Navas, F. Wang, and P.J. Godowski. 2004. APC-independent activation of NK cells by the Toll-like receptor 3 agonist double-stranded RNA. *Journal of immunology (Baltimore, Md. : 1950)* 172:138-143.

Schwemmle, M., M.J. Clemens, K. Hilse, K. Pfeifer, H. Troster, W.E. Muller, and M. Bachmann. 1992. Localization of Epstein-Barr virus-encoded RNAs EBER-1 and EBER-2 in interphase and mitotic Burkitt lymphoma cells. *Proceedings of the National Academy of Sciences of the United States of America* 89:10292-10296.

Sharp, T.V., M. Schwemmle, I. Jeffrey, K. Laing, H. Mellor, C.G. Proud, K. Hilse, and M.J. Clemens. 1993. Comparative analysis of the regulation of the interferon-inducible protein kinase PKR by Epstein-Barr virus RNAs EBER-1 and EBER-2 and adenovirus VAI RNA. *Nucleic acids research* 21:4483-4490.

Shiroki, K., T. Isoyama, S. Kuge, T. Ishii, S. Ohmi, S. Hata, K. Suzuki, Y. Takasaki, and A. Nomoto. 1999. Intracellular redistribution of truncated La protein produced by poliovirus 3Cpro-mediated cleavage. *Journal of virology* 73:2193-2200.

Steven, N.M., N.E. Annels, A. Kumar, A.M. Leese, M.G. Kurilla, and A.B. Rickinson. 1997. Immediate early and early lytic cycle proteins are frequent targets of the Epstein-Barr virus-induced cytotoxic T cell response. *The Journal of experimental medicine* 185:1605-1617.

Swaminathan, S., B. Tomkinson, and E. Kieff. 1991. Recombinant Epstein-Barr virus with small RNA (EBER) genes deleted transforms lymphocytes and replicates in vitro. *Proceedings of the National Academy of Sciences of the United States of America* 88:1546-1550.

Swaminathan S., K.S. 2009. The Epstein–Barr Virus Lytic Life Cycle. DNA Tumor Viruses. Springer, New York, NY,

Tabiasco, J., E. Devevre, N. Rufer, B. Salaun, J.C. Cerottini, D. Speiser, and P. Romero. 2006. Human effector CD8+ T lymphocytes express TLR3 as a functional coreceptor. *Journal of immunology (Baltimore, Md. : 1950)* 177:8708-8713.

Taylor, G.S., H.M. Long, J.M. Brooks, A.B. Rickinson, and A.D. Hislop. 2015. The immunology of Epstein-Barr virus-induced disease. *Annual review of immunology* 33:787-821.

Toczyski, D.P., A.G. Matera, D.C. Ward, and J.A. Steitz. 1994. The Epstein-Barr virus (EBV) small RNA EBER1 binds and relocalizes ribosomal protein L22 in EBV-infected human B lymphocytes. *Proceedings of the National Academy of Sciences of the United States of America* 91:3463-3467.

Toczyski, D.P., and J.A. Steitz. 1991. EAP, a highly conserved cellular protein associated with Epstein-Barr virus small RNAs (EBERs). *The EMBO journal* 10:459-466.

Toczyski, D.P., and J.A. Steitz. 1993. The cellular RNA-binding protein EAP recognizes a conserved stem-loop in the Epstein-Barr virus small RNA EBER 1. *Molecular and cellular biology* 13:703-710.

Tsai, M.H., X. Lin, A. Shumilov, K. Bernhardt, R. Feederle, R. Poirey, A. Kopp-Schneider, B. Pereira, R. Almeida, and H.J. Delecluse. 2017. The biological properties of different Epstein-Barr virus strains explain their association with various types of cancers. *Oncotarget* 8:10238-10254.

Tsai, M.H., A. Raykova, O. Klinke, K. Bernhardt, K. Gartner, C.S. Leung, K. Geletneky, S. Sertel, C. Munz, R. Feederle, and H.J. Delecluse. 2013. Spontaneous lytic replication and epitheliotropism define an Epstein-Barr virus strain found in carcinomas. *Cell reports* 5:458-470.

Ung, A., C.J. Chen, P.H. Levine, Y.J. Cheng, L.A. Brinton, I.H. Chen, A.M. Goldstein, M.M. Hsu, S.K. Chhabra, J.Y. Chen, R.J. Apple, C.S. Yang, and A. Hildesheim. 1999. Familial and sporadic cases of nasopharyngeal carcinoma in Taiwan. *Anticancer research* 19:661-665.

Vuyisich, M., R.J. Spanggord, and P.A. Beal. 2002. The binding site of the RNA-dependent protein kinase (PKR) on EBER1 RNA from Epstein-Barr virus. *EMBO reports* 3:622-627.

Wang, F., Y. Yuan, P. Yang, and X. Li. 2017. Extracellular vesicles-mediated transfer of miR-208a/b exaggerate hypoxia/reoxygenation injury in cardiomyocytes by reducing QKI expression. *Molecular and cellular biochemistry* 431:187-195.

Wei, W.I., and V.W. Mok. 2007. The management of neck metastases in nasopharyngeal cancer. *Current opinion in otolaryngology & head and neck surgery* 15:99-102.

Wille, C.K., D.M. Nawandar, A.R. Panfil, M.M. Ko, S.R. Hagemeier, and S.C. Kenney. 2013. Viral genome methylation differentially affects the ability of BZLF1 versus BRLF1 to activate Epstein-Barr virus lytic gene expression and viral replication. *Journal of virology* 87:935-950.

Wood, J., R.M. Frederickson, S. Fields, and A.H. Patel. 2001. Hepatitis C virus 3'X region interacts with human ribosomal proteins. *Journal of virology* 75:1348-1358.

Wu, L., J. Pan, V. Thoroddsen, D.R. Wysong, R.K. Blackman, C.E. Bulawa, A.E. Gould, T.D. Ocain, L.R. Dick, P. Errada, P.K. Dorr, T. Parkinson, T. Wood, D. Kornitzer, Z. Weissman, I.M. Willis, and K. McGovern. 2003. Novel small-molecule inhibitors of RNA polymerase III. *Eukaryotic cell* 2:256-264.

Wu, Y., S. Maruo, M. Yajima, T. Kanda, and K. Takada. 2007. Epstein-Barr virus (EBV)-encoded RNA 2 (EBER2) but not EBER1 plays a critical role in EBV-induced B-cell growth transformation. *Journal of virology* 81:11236-11245.

Yajima, M., T. Kanda, and K. Takada. 2005. Critical role of Epstein-Barr Virus (EBV)-encoded RNA in efficient EBV-induced B-lymphocyte growth transformation. *Journal of virology* 79:4298-4307.

Yang, L., K. Aozasa, K. Oshimi, and K. Takada. 2004. Epstein-Barr virus (EBV)-encoded RNA promotes growth of EBV-infected T cells through interleukin-9 induction. *Cancer research* 64:5332-5337.

Yoneyama, M., and T. Fujita. 2007. Function of RIG-I-like receptors in antiviral innate immunity. *The Journal of biological chemistry* 282:15315-15318.

Yoneyama, M., M. Kikuchi, T. Natsukawa, N. Shinobu, T. Imaizumi, M. Miyagishi, K. Taira, S. Akira, and T. Fujita. 2004. The RNA helicase RIG-I has an essential function in double-stranded RNA-induced innate antiviral responses. *Nature immunology* 5:730-737.

Yoshiyama, H., N. Shimizu, and K. Takada. 1995. Persistent Epstein-Barr virus infection in a human T-cell line: unique program of latent virus expression. *The EMBO journal* 14:3706-3711.

Yoshizaki, T., T. Horikawa, R. Qing-Chun, N. Wakisaka, H. Takeshita, T.S. Sheen, S.Y. Lee, H. Sato, and M. Furukawa. 2001. Induction of interleukin-8 by Epstein-Barr virus latent membrane protein-1 and its correlation to angiogenesis in nasopharyngeal carcinoma. *Clinical cancer research : an official journal of the American Association for Cancer Research* 7:1946-1951.

Young, L.S., and C.W. Dawson. 2014. Epstein-Barr virus and nasopharyngeal carcinoma. *Chinese journal of cancer* 33:581-590.

Young, L.S., and A.B. Rickinson. 2004. Epstein-Barr virus: 40 years on. *Nature reviews. Cancer* 4:757-768.

Yu, M.C., and J.M. Yuan. 2002. Epidemiology of nasopharyngeal carcinoma. *Seminars in cancer biology* 12:421-429.

Yuan, J., E. Cahir-McFarland, B. Zhao, and E. Kieff. 2006. Virus and cell RNAs expressed during Epstein-Barr virus replication. *Journal of virology* 80:2548-2565.

Zhao, Z., L. Sun, S. Liu, J. Shu, and B. Luo. 2017. Characterization of Epstein-Barr virus-encoded small RNA gene variations in virus associated lymphomas in Northern China. *Archives of virology*

Zolotukhin, A.S., D. Michalowski, J. Bear, S.V. Smulevitch, A.M. Traish, R. Peng, J. Patton, I.N. Shatsky, and B.K. Felber. 2003. PSF acts through the human immunodeficiency virus type 1 mRNA instability elements to regulate virus expression. *Molecular and cellular biology* 23:6618-6630.

6 Acknowledgments

First of all, I would like to express my sincere gratitude to my doctor father Prof. Henri-Jacques Delecluse for the continuous support of my Ph.D studies and related research, for his patience, motivation, and immense knowledge. His guidance helped me in all the time of research and writing of this thesis. I could not have imagined having a better advisor and mentor for my Ph.D studies.

Besides my advisor, I would like to thank the rest of my TAC committee: Prof. Martin Müller, Dr. Florence Baudin, and Dr. Grant Hansman, for their helpful comments and encouragement, but also for the helpful question which incented me to widen my research from various perspectives.

My sincere thanks also go to Dr. Ming-Han Tsai, Dr. Rémy Poirey, and Dr. Xiaochen Lin, who gave me great advice and many critical evaluations of my projects. I would like to thank all my dear colleagues and the previous members in F100, DKFZ. I enjoyed my research and leisure time with you in Germany.

I also want to thank DKFZ and Chinese Scholarship Council (CSC) for offering the outstanding scientific environment and supporting my expenses in the past 4 years in Germany.

Last but not the least, I would like to thank my parents for supporting me spiritually throughout my Ph.D study and writing this thesis. In particular, my wife Xueer Zhao strongly supported me both materially and spiritually during my Ph.D study.